Splitting Defect Correction

Harald Hofstätter
Othmar Koch

AURORA TR2003-23

Institute for Applied Mathematics and Numerical Analysis
Vienna University of Technology
Wiedner Hauptstrasse 8-10, A-1040 Wien, Austria

E-Mail: hofi@aurora.anum.tuwien.ac.at
othmar@fsmat.at

This work described in this report was supported by the Special Research Program SFB F011 "AURORA" of the Austrian Science Fund FWF.

Introduction

In recent years, the importance of using special numerical integration schemes that reflect certain geometric properties or retain important conserved quantities of the flow of a differential equation has been widely recognized [13], [14]. Many of these methods are applicable to particular types of differential equations only. Examples of these are the Störmer/Verlet method and the exponential midpoint rule, which are discussed in detail in this report.

A cheap and efficient way to estimate the global error of a numerical method used to solve an ordinary differential equation (ODE) is the defect correction principle [22], [24]. The idea can also be used to successively improve the accuracy of the numerical solution ([2], [5], [8], [9], [10], [12], [20], and the references therein). In this acceleration technique, a number of *neighboring problems* have to be solved, which are not necessarily of the same type as the original problem. Therefore it may happen that the neighboring problems cannot be solved by the same geometric integrator as the original problem. In this paper, we present *splitting methods* [13] to avoid such difficulties.

Contents

1 Theoretical Considerations 3

1.1 Classical Defect Correction 3

1.2 Splitting Defect Correction 4

1.2.1 The Störmer/Verlet Method 5

1.3 Composition Methods 6

1.4 Convergence Orders for ISDeC Iterates 9

1.4.1 Order Results for Classical IDeC 9

1.4.2 Order Results for Schild's Method 9

1.4.3 Experimental Order Results for ISDeC Methods 12

1.4.4 Experimental Order Results for Simple ISDeC 15

1.4.5 Experimental Orders for Composition Methods 16

2 Numerical Results 19

2.1 Hamiltonian Systems – The Störmer-Verlet Method 19

2.1.1 Composition Methods 26

2.2 The Exponential Midpoint Rule 49

2.3 Exponential Integrators for Unsmooth Problems 62

2.3.1 The Test Equation 62

2.3.2 Exponential Splitting for the Schrödinger Equation . . . 63

A Auxiliary Results 67

Chapter 1

Theoretical Considerations

1.1 Classical Defect Correction

First, we describe the classical version of *iterated defect correction (IDeC)* [5], [8], [20]. Consider an initial value problem

$$\dot{z}(t) = f(t, z(t)), \quad z(t_0) = z_0, \tag{1.1}$$

to be solved on the interval $[t_0, t_{\text{end}}]$. Subsequently, we assume that a sufficiently smooth solution z of the analytical problem exists on the whole interval. The approximate solution $z_h^{[0]} := (z_0, \ldots, z_N)$ is obtained by some discretization method Φ on a uniform grid[1] $(t_0, \ldots, t_N)$, where $t_{i+1} - t_i = h,\ i = 0, \ldots, N-1$. Denote by $p^{[0]}(t)$ the polynomial of degree N interpolating the values of $z_h^{[0]}$. Using this interpolating function, we construct a neighboring problem associated with (1.1) whose exact solution is $p^{[0]}(t)$:

$$\dot{z}(t) = f(t, z(t)) + d^{[0]}(t), \quad z(t_0) = z_0, \tag{1.2}$$

where $d^{[0]}(t) := \dot{p}^{[0]}(t) - f(t, p^{[0]}(t))$. We now solve (1.2) using the same numerical method Φ and obtain an approximate solution $p_h^{[0]}$ for $p^{[0]}(t)$. This means that for the solution of the neighboring problem (1.2) we know the global error which is a good estimate for the unknown error of the original problem (1.1). This estimate can be used to improve the first solution,

$$z_h^{[1]} := z_h^{[0]} + \left(p^{[0]} - p_h^{[0]}\right).$$

Now, these values are used to define a new interpolating polynomial $p^{[1]}(t)$ by requiring $p^{[1]}(t_j) = z_j^{[1]}$. Again, $p^{[1]}(t)$ defines a neighboring problem in the same manner as in (1.2), where again the exact solution is known, and the numerical solution $p_h^{[1]}$ of this neighboring problem serves to obtain the second improved solution

$$z_h^{[2]} := z_h^{[0]} + \left(p^{[1]} - p_h^{[1]}\right).$$

[1]For the classical version of IDeC, piecewise equidistant grids are required for the classical order sequences to be observed, see for example [3], [4]. This restriction is not critical in our case, since many geometric integration methods rely on the assumption of equidistant grids to retain their advantageous properties [13].

This process can be continued iteratively. For obvious reasons one does not use one interpolating polynomial for the whole interval $[t_0, t_{\text{end}}]$ in practice. Instead, piecewise functions composed of polynomials of (moderate) degree m are defined to specify the neighboring problems.

In many situations, the defect correction principle yields an asymptotically correct error estimate and a successive improvement in the convergence orders of the respective iterates, up to a certain limit determined by the smoothness of the problem data and the value of m.

1.2 Splitting Defect Correction

If for the scheme described in Section 1.1, the basic numerical solution method Φ is a geometric integrator, the neighboring problem (1.2) may have a form to which the integrator cannot be applied straightforwardly. For example, if the Störmer/Verlet method is applied to a Hamiltonian system (see Sections 1.2.1 and 2.1), (1.2) is no longer an autonomous, separated system. Another example is the exponential midpoint rule designed for linear homogeneous systems, cf. Section 2.2.

In order to be able to use iterated defect correction even in these cases, we employ splitting methods, cf. [13]. To apply *Strang splitting* to (1.2), we split the time-dependent vector field into its components $f(t, y)$ and $d^{[0]}(t)$. We denote the numerical flow of $f(t, y)$ by $\Phi_{t,h}$, such that one step $(t, \eta_i) \mapsto (t+h, \eta_{i+1})$ with step size h of the basic scheme Φ applied to (1.1) can be written as $\eta_{i+1} = \Phi_{t,h}(\eta_i)$. The numerical flow $\Delta_{t,h}$ of the other component $d^{[0]}(t)$ is defined by the quadrature rule

$$\Delta_{t,h}(y) = y + \int_t^{t+h} D^{[0]}(\tau) d\tau, \tag{1.3}$$

where $D^{[0]}(t)$ is a piecewise polynomial interpolant of degree $\leq m-1$ of $d^{[0]}(t)$.

To explain this more precisely, we require some additional notation. Choose the grid $(t_0, \ldots, t_N)$ such that $N = N_1 m$ for some integer N_1. We split the integration interval into subintervals $J_i := [t_{im}, t_{(i+1)m}]$. On the interval J_i, we define interpolation nodes

$$\tau_{i,j} := t_{im} + hm\rho_j, \ j = 1, \ldots, m, \quad \text{where } 0 \leq \rho_1 < \rho_2 < \cdots < \rho_m \leq 1. \tag{1.4}$$

For the purpose of this paper, we use interpolation at either Gaussian or Radau points [1] in order to define $D^{[0]}(t)$. This implies that the maximal convergence order of IDeC iterates is $O(h^{2m})$ for Gaussian points and $O(h^{2m-1})$ for Radau points, respectively, see Section 1.4.

Using $\Phi_{t,h}$ and $\Delta_{t,h}$ from above, the numerical solution of (1.2) is computed using the numerical flow

$$\Psi_{t,h} = \Delta_{t+h/2,h/2} \circ \Phi_{t,h} \circ \Delta_{t,h/2}, \tag{1.5}$$

where $\circ$ denotes the *composition* of the numerical methods (which means that the result computed by one method is the starting value for the next method). We call the method where the solution of the neighboring problems is computed in this way *iterated splitting defect correction (ISDeC).*

1.2.1 The Störmer/Verlet Method

To illustrate the above considerations, we discuss the Störmer/Verlet method. This numerical solution method is a geometric integration scheme of order two which is particularly suited for the solution of *Hamiltonian systems* of ODEs, or more generally, *separated* ODEs.

Consider a system of two separated autonomous ODEs

$$\dot{p}(t) = f(p(t), q(t)), \quad \dot{q}(t) = g(p(t), q(t)). \tag{1.6}$$

One step of the Störmer/Verlet method for (1.6) is defined by

$$q_{i+1/2} = q_i + \frac{h}{2} g(p_i, q_{i+1/2}), \tag{1.7}$$

$$p_{i+1} = p_i + \frac{h}{2} \left(f(p_i, q_{i+1/2}) + f(p_{i+1}, q_{i+1/2}) \right), \tag{1.8}$$

$$q_{i+1} = q_{i+1/2} + \frac{h}{2} g(p_{i+1}, q_{i+1/2}). \tag{1.9}$$

For a Hamiltonian system, the method retains important conserved quantities of the exact flow like the angular momentum, see Section 2.1. In a Hamiltonian system, there exists a scalar function $H(p, q)$ such that

$$f(p, q) = -\nabla_q H(p, q), \quad g(p, q) = \nabla_p H(p, q). \tag{1.10}$$

Note that for the exact flow the Hamiltonian H is preserved, that is,

$$H(p(t), q(t)) = \text{const}$$

for every solution (p, q) of (1.6). The Störmer/Verlet method preserves the Hamiltonian H up to terms of order $O(h^2)$, even for very long time intervals. Other constants of motion, as for example the angular momentum, are discussed in [14], see also Section 2.1.

Obviously, the neighboring problem (1.2) is not a Hamiltonian system in general, the equations are not even posed as a separated system of autonomous differential equations. Consequently, the Störmer/Verlet method cannot be applied to (1.2) without the modifications of ISDeC.

1.3 Composition Methods

We now generalize the approach of ISDeC outlined in Section 1.2 for the case where the basic scheme Φ is a composition method.

As a first example, consider the Störmer/Verlet method from Section 1.2.1. This numerical scheme can be written as the composition of the *symplectic Euler rule* and its *adjoint method*. One step $(t_i, p_i, q_i) \mapsto (t_{i+1}, p_{i+1}, q_{i+1})$ of the symplectic Euler method ϕ applied to (1.6) is defined by

$$\begin{aligned} q_{i+1} &= q_i + hg(p_i, q_{i+1}), \\ p_{i+1} &= p_i + hf(p_i, q_{i+1}). \end{aligned} \tag{1.11}$$

The adjoint method ϕ^* is conversely defined by

$$\begin{aligned} p_{i+1} &= p_i + hf(p_{i+1}, q_i), \\ q_{i+1} &= q_i + hg(p_{i+1}, q_i). \end{aligned} \tag{1.12}$$

The numerical flow $\Phi_{t,h}$ defined by the Störmer/Verlet method (1.7), (1.8) and (1.9) can equivalently be expressed as

$$\Phi_{t,h} = \phi^*_{t+h/2,h/2} \circ \phi_{t,h/2}.$$

Remark: This numerical scheme is also denoted as *Version A* of the Störmer/Verlet method, while the method resulting from $\phi_{t+h/2,h/2} \circ \phi^*_{t,h/2}$ is the *dual scheme* denoted as *Version B*, see [13] and [14].

In this reformulation, we can apply the idea of splitting defect correction in several different ways. In addition to simply using (1.5), we could alternatively apply the splitting idea to ϕ or ϕ^* and use a composition of the resulting schemes to define the flow Ψ of the neighboring problem (1.2). This idea is discussed for general composition methods in the remainder of this section.

Consider a composition method

$$\Phi = \Phi^{[s]} \circ \cdots \circ \Phi^{[2]} \circ \Phi^{[1]}. \tag{1.13}$$

Then, the numerical method Ψ for the solution of the neighboring problem (1.2) can be defined by

$$\Psi_{t,h} = \Delta_{t+\hat{\delta}_{s+1}h,\delta_{s+1}h} \circ \Phi^{[s]} \circ \Delta_{t+\hat{\delta}_s h,\delta_s h} \circ \cdots \circ \Delta_{t+\hat{\delta}_2 h,\delta_2 h} \circ \Phi^{[1]} \circ \Delta_{t+\hat{\delta}_1 h,\delta_1 h}, \tag{1.14}$$

where $\delta_1, \ldots, \delta_{s+1}$ are given real numbers which satisfy

$$\delta_1 + \cdots + \delta_{s+1} = 1, \quad \hat{\delta}_j := \sum_{i=1}^{j-1} \delta_i,$$

and $\Delta_{t,h}$ is given by (1.3).

Examples. Let us discuss some examples of composition methods.

- *Symmetric composition of symmetric methods [13, Sec. V.3].*

$$\Phi^{[j]} = \phi_{t+\hat{\gamma}_j h, \gamma_j h}, \quad j = 1, \ldots, s, \tag{1.15}$$

where ϕ is a symmetric second order method, the coefficients $\gamma_s = \gamma_1, \gamma_{s-1} = \gamma_2, \ldots$ are symmetric, and $\hat{\gamma}_j := \sum_{i=1}^{j-1} \gamma_j$. Examples of possible choices for ϕ are the Störmer/Verlet scheme, the implicit midpoint rule, or the implicit trapezoidal rule. The coefficients γ_j may be chosen for example such as to yield Yoshida's method,

$$s = 3, \quad \gamma_1 = \gamma_3 = 1/(2 - 2^{1/3}), \quad \gamma_2 = -2^{1/3}/(2 - 2^{1/3}), \tag{1.16}$$

or Suzuki's method,

$$s = 5, \quad \gamma_1 = \gamma_2 = \gamma_4 = \gamma_5 = 1/(4 - 4^{1/3}), \quad \gamma_3 = -4^{1/3}/(4 - 4^{1/3}). \tag{1.17}$$

Both of these choices (in conjunction with a symmetric second-order basic scheme) yield methods of order 4, cf. [13, Sec. II.4]. A natural choice for the coefficients δ_j in the splitting (1.14) is

$$\delta_1 = \gamma_1/2, \qquad \delta_j = (\gamma_{j-1} + \gamma_j)/2, \quad j = 2, \ldots, s, \qquad \delta_{s+1} = \gamma_s/2, \tag{1.18}$$

since then Ψ can be written as

$$\Psi = \Psi^{[s]} \circ \cdots \circ \Psi^{[1]}, \tag{1.19}$$

where

$$\Psi^{[j]} = \Delta_{t+\hat{\gamma}_j h + \gamma_j h/2, \gamma_j h/2} \circ \phi_{t+\hat{\gamma}_j h, \gamma_j h} \circ \Delta_{t+\hat{\gamma}_j h, \gamma_j h/2}. \tag{1.20}$$

Consequently, $\Psi^{[j]}$ is a symmetric second-order method and Ψ has the same order as Φ, see [13, Sec. II.4].

- *Symmetric composition of first order methods.*
For s even we choose

$$\Phi^{[2j-1]} = \phi_{t+\hat{\gamma}_{2j-1} h, \gamma_{2j-1} h}, \quad \Phi^{[2j]} = \phi^*_{t+\hat{\gamma}_{2j} h, \gamma_{2j} h}, \quad j = 1, \ldots s/2, \tag{1.21}$$

where ϕ is an arbitrary first order method, ϕ^* the adjoint method of ϕ, and the coefficients γ_j satisfy

$$\gamma_s = \gamma_1, \gamma_{s-1} = \gamma_2, \ldots, \quad \hat{\gamma}_j := \sum_{i=1}^{j-1} \gamma_j.$$

As an example of such a composition the Störmer/Verlet method was discussed at the beginning of this section. A possible choice for the coefficients

γ_j is McLachlan's method (which yields a fourth-order method for suitable ϕ),

$$\begin{aligned} s = 10, \quad & \gamma_1 = \gamma_{10} = (14 - \sqrt{19})/108, && \gamma_2 = \gamma_9 = (146 + 5\sqrt{19})/540, \\ & \gamma_3 = \gamma_8 = (-23 - 20\sqrt{19})/270, && \gamma_4 = \gamma_7 = (-2 + 10\sqrt{19})/135, \\ & \gamma_5 = \gamma_6 = 1/5, \end{aligned} \tag{1.22}$$

cf. [13, Sec. V.3.1]. Again, the choice of the coefficients δ_j in (1.14) according to (1.18) ensures that Ψ has the same order as Φ.

A special case is given by the additional requirement $\gamma_{2j-1} = \gamma_{2j}$, $j = 1, \ldots, s/2$ in (1.21). Then, the definition of the resulting basic scheme Φ is included in the formulation (1.15), since for a first order method $\phi_{t,h}$, the composition $\phi^*_{t+h/2,h/2} \circ \phi_{t,h/2}$ is a symmetric second order method. In the representation (1.21) we have more freedom in choosing the coefficients δ_j: For each parameter $\lambda \in [0, 1]$ ($\lambda = 1$ corresponds to (1.18)), the choice

$$\begin{aligned} \delta_1 &= \lambda\gamma_1, \\ \delta_{2j} &= (1 - \lambda)(\gamma_{2j-1} + \gamma_{2j}), && j = 1, \ldots, s/2, \\ \delta_{2j+1} &= \lambda(\gamma_{2j} + \gamma_{2j+1}), && j = 1, \ldots, s/2 - 1, \\ \delta_{s+1} &= \lambda\gamma_s \end{aligned} \tag{1.23}$$

ensures that Ψ has the same order as Φ, cf. [13, Sec. II.4].

In this way, we may reformulate an IDeC method analyzed in [21] to fit into the context of the composition methods just discussed. The basic method is

$$\Phi_{t,h} = \phi^*_{t+h/2,h/2} \circ \phi_{t,h/2},$$

where ϕ and ϕ^* are the explicit and the implicit Euler methods, respectively. Consequently, Φ is the implicit trapezoidal rule. ISDeC is realized as

$$\Psi_{t,h} = \phi^*_{t+h/2,h/2} \circ \Delta_{t,h} \circ \phi_{t,h/2}. \tag{1.24}$$

In [21] it has been demonstrated for linear problems that the usage of Gaussian points in the quadrature rule (1.3) leads to an order sequence $O(h^2)$, $O(h^4), \ldots$ for the iteration error (the error of the respective IDeC iterate as compared with the fixed point of the iteration), which means that the order of the global error increases by two up to the convergence order of the fixed point, i. e. $O(h^{2m})$. This asymptotic behavior is the same as for the geometric integrators of this paper, see Chapter 2.

1.4 Convergence Orders for ISDeC Iterates

1.4.1 Order Results for Classical IDeC

It is well known that for sufficiently smooth non-stiff systems (1.1), the iterates $z_h^{[\nu]} = (z_0^{[\nu]}, \ldots, z_N^{[\nu]})$ computed by *classical* iterated defect correction (IDeC, see Section 1.1) satisfy

$$z_i^{[\nu]} - z(t_i) = O(h^{\min((\nu+1)p, m)}), \tag{1.25}$$

where $z(t)$ denotes the exact solution of (1.1) and p is the order of the basic discretization scheme Φ. Note that the maximal attainable order is $O(h^m)$. The proof (cf. e.g. [12]) of (1.25) is usually based on an asymptotic expansion of the global error of the basic solution method Φ.

1.4.2 Order Results for Schild's Method

The key idea in the convergence analysis of the ISDeC method which we want to outline here and which was given in [21] for the special case (1.24), is to estimate the iteration error of $z_h^{[\nu]}$ instead of the global error. First, we note that iterated defect correction converges to a fixed point p^* under fairly general assumptions [4], [5], [11]. The iteration error $z_h^{[\nu]} - p^*$ is the error of the respective iterates as compared with the fixed point. Order results analogous to (1.25) can then be derived by utilizing the approximation properties of the fixed point. This fixed point is easily identified as a certain collocation solution of (1.1): Let $p^*(t)$ denote the continuous piecewise polynomial function defined by $p^*(t) = p_i^*(t)$ for $t \in J_i$, where the $p_i^*(t)$ are polynomials of degree $\leq m$ satisfying the collocation relations

$$\dot{p}_i^*(\tau_{i,j}) = f\left(\tau_{i,j}, p_i^*(\tau_{i,j})\right), \quad i = 0, \ldots, N_1 - 1, \quad j = 1, \ldots, m. \tag{1.26}$$

The defect

$$d^*(t) := \dot{p}_i^*(t) - f\left(t, p^*(t)\right)$$

of $p^*(t)$ vanishes at all collocation nodes, so that the numerical flow $\Delta_{t,h}$ of $d^*(t)$ defined analogously to (1.3) for the defect correction step starting from $z_h^* := (p^*(t_0), \ldots, p^*(t_N))$ is the identity, and z_h^* is mapped onto itself.

If (1.1) is linear, one defect correction step $z_h^{[\nu]} \mapsto z_h^{[\nu+1]}$ can be interpreted as the application of an affine operator,

$$z_h^{[\nu+1]} = S_h z_h^{[\nu]} + v_h.$$

In this case, the iteration error $\varepsilon_h^{[\nu]} := z_h^{[\nu]} - p^*$ is propagated as

$$\varepsilon_h^{[\nu+1]} = S_h \varepsilon_h^{[\nu]}. \tag{1.27}$$

If we introduce Sobolev-like norms by

$$\|\varepsilon_h\|_k := \sum_{\kappa=0}^{k} \max_{0\le i\le N-1} \max_{t\in J_i} \left| \frac{d^\kappa}{dt^\kappa} q_i(t) \right|, \tag{1.28}$$

where $q_i(t)$ denotes the polynomial of degree $\le m$ which interpolates ε_h at t_l, $l = im, \ldots, (i+1)m$, the results of [21] for the special case (1.24) can be summarized in terms of the operator norms

$$\|S_h\|_{k,\ell} = \sup_{\varepsilon_h \neq 0} \frac{\|S_h \varepsilon_h\|_\ell}{\|\varepsilon_h\|_k},$$

which are given in Table 1.1.

$\ell \setminus k$	0	1	2	3	...	$m-1$	m
0	$O(h^0)$	$O(h)$	$O(h^2)$	$O(h^2)$	...	$O(h^2)$	$O(h^2)$
1		$O(h)$	$O(h^2)$	$O(h^2)$	...	$O(h^2)$	$O(h^2)$
2			$O(h)$	$O(h^2)$	...	$O(h^2)$	$O(h^2)$
$\vdots$				$\ddots$	$\ddots$	$\vdots$	$\vdots$
$m-1$						$O(h)$	$O(h^2)$
m							$O(h)$ or $O(h^2)$

Table 1.1: Orders of $\|S_h\|_{k,\ell}$ for Schild's method.

Here, $\|S_h\|_{m,m} = O(h^2)$ holds, if ρ_j from (1.4) satisfy

$$\sum_{j=1}^{m} \rho_j = \frac{m}{2}. \tag{1.29}$$

This relation holds in particular if ρ_j are symmetric in $[0,1]$ like Gaussian points[2]. Estimates of the iteration errors $\|\varepsilon_h^{[\nu]}\|_k$ are now easily derived from the following estimates for the iteration error of the basic solution, $\varepsilon_h^{[0]} = z_h^{[0]} - p^*$:

$$\begin{aligned} &\|\varepsilon_h^{[0]}\|_k = O(h^p), && k = 0, \ldots, m-p+1, \\ &\|\varepsilon_h^{[0]}\|_k = O(h^{m+1-k}), && k = m-p+2, \ldots, m-1, \\ &\|\varepsilon_h^{[0]}\|_m = \begin{cases} O(h^2) & \text{if } \rho_j \text{ satisfy (1.29)}, \\ O(h) & \text{otherwise.} \end{cases} \end{aligned} \tag{1.30}$$

p again denotes the order of the basic method Φ, for example $p = 2$ for the trapezoidal rule [21]. For the higher order composition methods considered in Section 1.2, we use a similar argument to analyze the iteration error, yet in that

[2] Actually, in [21] only the case of symmetric ρ_j is considered. The generalization (1.29) is given in Appendix A.

case $p = 4$ holds. Subsequently, we assume $m \geq p$, otherwise the ISDeC procedure does not make much sense. The estimates above follow from

$$\|z_h^{[0]} - z\|_k = O(h^p), \quad k = 0, \ldots, m.$$

This can be proven by means of an asymptotic expansion of the global error of Φ: If a sufficiently long error expansion exists, then there is a smooth function $e(t, h)$ such that

$$z_j^{[0]} - z(t_j) = e(t_j, h)h^p,$$

with $\frac{\partial^k}{\partial t^k} e(t, h) = O(1),\ k = 0, \ldots, m$. Consequently, for the polynomial q from (1.28) we conclude

$$\begin{aligned} \left| \frac{d^k}{dt^k} q_i(t) \right| &\leq \left| \frac{d^k}{dt^k} q_i(t) - \frac{\partial^k}{\partial t^k} e(t, h)h^p \right| + \left| \frac{\partial^k}{\partial t^k} e(t, h)h^p \right| \\ &\leq O(h^{m+p+1-k}) + O(h^p) = O(h^p), \quad k = 0, \ldots, m, \end{aligned}$$

which follows from standard results for polynomial collocation [16]). Moreover, we use the relations

$$\begin{aligned} \|p^* - z\|_0 &= \begin{cases} O(h^{m+1}) & \text{if } \rho_j \text{ define a collocation scheme of order} \geq m+1, \\ O(h^m) & \text{otherwise,} \end{cases} \\ \|p^* - z\|_k &= O(h^{m+1-k}), \quad k = 1, \ldots, m-1, \\ \|p^* - z\|_m &= \begin{cases} O(h^2) & \text{if } \rho_j \text{ satisfy (1.29),} \\ O(h) & \text{otherwise.} \end{cases} \end{aligned}$$

These are standard results for collocation methods [1], again taking into account [16]. The improved estimate $\|p^* - z\|_m = O(h^2)$ if (1.29) holds follows from Lemma 2 in Appendix A. The technical details are given in [17].

For a basic method Φ of order $p = 2$ and ρ_j satisfying (1.29), e.g. for the implicit trapezoidal rule and Gaussian points, the estimates of the initial iteration error $\varepsilon_h^{[0]} = z_h^{[0]} - p^*$ are simply

$$\|\varepsilon_h^{[0]}\|_k = O(h^2), \quad k = 0, \ldots, m.$$

Now assume that the estimate $\|S_h\|_{m,m} = O(h^2)$ holds. Then we may conclude

$$\|\varepsilon_h^{[\nu+1]}\|_k \leq \|\varepsilon_h^{[\nu+1]}\|_m \leq \|S_h\|_{m,m} \|\varepsilon_h^{[\nu]}\|_m \leq Ch^2 \|\varepsilon_h^{[\nu]}\|_m = O(h^{2\nu+2}), \tag{1.31}$$

which implies the order sequence

$$O(h^2), O(h^4), O(h^6), \ldots \tag{1.32}$$

of the iteration errors $\|\varepsilon_h^{[\nu]}\|_k,\ k = 0, \ldots, m,\ \nu = 0, 1, 2, \ldots$.

If (1.29) does not hold, $\|S_h\|_{m,m} = O(h)$ in general. Using

$$\begin{aligned} &\|\varepsilon_h^{[0]}\|_k = O(h^2), \quad k = 0, \ldots, m-1, \\ &\|\varepsilon_h^{[0]}\|_m = O(h) \end{aligned}$$

and the estimates

$$\begin{aligned} \|\varepsilon_h^{[\nu+1]}\|_0 &\le \|S_h\|_{0,2}\|\varepsilon_h^{[\nu]}\|_2 &&\le Ch^2\|\varepsilon_h^{[\nu]}\|_2, \\ \|\varepsilon_h^{[\nu+1]}\|_k &\le \|S_h\|_{k,k+1}\|\varepsilon_h^{[\nu]}\|_{k+1} &&\le Ch^2\|\varepsilon_h^{[\nu]}\|_{k+1}, \quad k = 1, \ldots, m-1, \\ \|\varepsilon_h^{[\nu+1]}\|_m &\le \|S_h\|_{m,m}\|\varepsilon_h^{[\nu]}\|_m &&\le Ch\|\varepsilon_h^{[\nu]}\|_m \end{aligned}$$

(cf. Table 1.1), we obtain an order sequence for $\|\varepsilon_h^{[\nu]}\|_0$, $\nu = 0, 1, 2, \ldots$:

$$O(h^2), O(h^4), \ldots, O(h^{2m-2}), O(h^{2m-1}), \ldots, \tag{1.33}$$

i. e. the order of $\|\varepsilon_h^{[\nu]}\|_0$ increases by two in every defect correction step up to $\nu = m-2$. For $\nu > m-2$ the order increases only by one in every defect correction step.

1.4.3 Experimental Order Results for ISDeC Methods

The investigations from above for Schild's method motivate to compute $\|S_h\|_{k,\ell}$ and the corresponding orders numerically for other ISDeC algorithms applied to simple test problems in order to gain insight into the convergence behavior of the algorithm. To this end we consider the *test equation*

$$y' = \lambda y, \quad y(0) = 0, \quad t \in [0, 1]. \tag{1.34}$$

The basic scheme Φ is composed according to (1.21), where the components $\Phi^{[j]}$ are chosen as

$$\Phi^{[j]}(y) = \mathrm{e}^{\gamma_j h\lambda} y, \tag{1.35}$$

which represents the exact flow of (1.34), or alternatively as a numerical flow

$$\Phi^{[j]}(y) = R(\gamma_j h\lambda) y, \tag{1.36}$$

where $R(z)$ denotes the A-stability function of $\Phi^{[j]}(y)$ [15]. A matrix representation of the operator S_h can be computed explicitly using techniques developed in [2]. Instead of (1.28), for the purpose of obtaining empirical order results we define Sobolev-like norms by[3]

$$\|\varepsilon_h\|_k = h^{-1/2}\sqrt{\|\varepsilon_h\|_{\ell_2}^2 + \|D_h^{(1)}\varepsilon_h\|_{\ell_2}^2 + \|D_h^{(2)}\varepsilon_h\|_{\ell_2}^2 + \cdots + \|D_h^{(k)}\varepsilon_h\|_{\ell_2}^2}, \tag{1.37}$$

[3]Note that we do not include the component ε_0 in ε_h, which is implicitly assumed to be 0.

with $\varepsilon_h = (\varepsilon_0, \ldots, \varepsilon_N)^T \in \mathbb{R}^N$ and matrices $D_h^{(\kappa)}$ to be specified below, such that (1.28) and (1.37) are equivalent uniformly in h (see also [21]). In (1.37), we use discrete Euclidean norms

$$\|\varepsilon_h\|_{\ell_2}^2 := \sum_{k=0}^{N} |\varepsilon_k|^2.$$

For $D_h^{(\kappa)}$ we choose divided difference operators of order κ, where differences are only formed from components ε_j belonging to the same interpolation interval J_i, and the implicitly given component $\varepsilon_0 = 0$ has to be taken into account. E. g., for $N = 6$, $m = 3$, we have

$$D_h^{(1)} = \frac{1}{h} \begin{pmatrix} 1 & & & & & \\ -1 & 1 & & & & \\ & -1 & 1 & & & \\ & & -1 & 1 & & \\ & & & -1 & 1 & \\ & & & & -1 & 1 \end{pmatrix},$$

$$D_h^{(2)} = \frac{1}{h^2} \begin{pmatrix} -2 & 1 & & & & \\ 1 & -2 & 1 & & & \\ & & 1 & -2 & 1 & \\ & & & 1 & -2 & 1 \end{pmatrix},$$

$$D_h^{(3)} = \frac{1}{h^3} \begin{pmatrix} 3 & -3 & 1 & & & \\ & & -1 & 3 & -3 & 1 \end{pmatrix}.$$

Note that the matrix norms $\|S_h\|_{k,\ell} = \sup_{\varepsilon_h \neq 0} \frac{\|S_h \varepsilon_h\|_\ell}{\|\varepsilon_h\|_k}$ can be explicitly computed as $\|S_h\|_{k,\ell} = \sqrt{\mu_1}$, where $\mu_1 \geq \mu_2 \geq \cdots \geq \mu_N \geq 0$ are the (real!) eigenvalues of the generalized eigenvalue problem

$$S_h^T V_{h,\ell} S_h x = \mu V_{h,k} x \tag{1.38}$$

with positive definite matrices

$$V_{h,k} = I_N + (D_h^{(1)})^T D_h^{(1)} + (D_h^{(2)})^T D_h^{(2)} + \cdots + (D_h^{(k)})^T D_h^{(k)} \in \mathbb{R}^{N \times N}. \tag{1.39}$$

To see this, we use the following lemma:

Lemma 1 *Let $V, \tilde{V} \in \mathbb{R}^{N \times N}$ be symmetric, positive definite matrices, and define a norm by*

$$\|x\|_V := \sqrt{\langle x, Vx \rangle} = \sqrt{x^T V x}. \tag{1.40}$$

Now, an associated matrix norm defined as

$$\|A\|_{V,\tilde{V}} := \max_{\|x\|_{\tilde{V}} = 1} \|Ax\|_V, \quad A \in \mathbb{R}^{N \times N}, \tag{1.41}$$

can be computed from

$$\|A\|_{V,\tilde{V}} = \sqrt{\lambda_1}, \tag{1.42}$$

where $\lambda_1 \geq \lambda_2 \geq \cdots \geq \lambda_N \geq 0$ *denote the eigenvalues of the generalized eigenvalue problem*

$$A^T V A x = \lambda \tilde{V} x. \tag{1.43}$$

Proof. We wish to compute the maximum of $\|Ax\|_V$ under the constraint $\|x\|_{\tilde{V}} = 1$, which is the same as the square root of the maximum of $x^T A^T V A x$ under the constraint $1 - x^T \tilde{V} x = 0$.

We define a Lagrangian function with Lagrange multiplier λ by

$$h(x, \lambda) = x^T A^T V A x + \lambda \cdot (1 - x^T \tilde{V} x).$$

We note that

$$\nabla_x h(x, \lambda) = 2(A^T V A x - \lambda \tilde{V} x)^T,$$

whence a solution x of our maximization problem must necessarily be a generalized eigenvector x of (1.43) satisfying $\|x\|_{\tilde{V}} = 1$. The maximal value is equal to

$$\sqrt{x^T A^T V A x} = \sqrt{\lambda x^T \tilde{V} x} = \sqrt{\lambda},$$

where λ denotes the eigenvalue associated with x. Thus, we need to show that all eigenvalues of (1.43) are real and nonnegative.

From (1.43) we obtain the eigenvalue problem

$$\tilde{V}^{-1} A^T V A x = \lambda x,$$

since $\tilde{V}$ is nonsingular from our assumptions. Here, the matrix $\tilde{V}^{-1} A^T V A$ is not symmetric in general. However, there exist nonsingular, lower triangular matrices $L, \tilde{L}$ such that

$$\begin{aligned} V &= L L^T, \\ \tilde{V} &= \tilde{L} \tilde{L}^T, \end{aligned}$$

which can be computed by Cholesky factorization. Now,

$$\begin{aligned} \tilde{L}^T (\tilde{V}^{-1} A^T V A)(\tilde{L}^T)^{-1} &= \tilde{L}^T (\tilde{L}^T)^{-1} \tilde{L}^{-1} A^T V A (\tilde{L}^{-1})^T \\ &= \tilde{L}^{-1} (A^T V A)(\tilde{L}^{-1})^T \\ &= \underbrace{(\tilde{L}^{-1} A^T L)}_{=:H} \cdot \underbrace{(\tilde{L}^{-1} A^T L)^T}_{=H^T} \\ &=: G, \end{aligned}$$

and thus G is symmetric. Consequently, $\tilde{V}^{-1} A^T V A$ is similar to a symmetric matrix, whence all eigenvalues of $\tilde{V}^{-1} A^T V A$ are real. By observing that G is also positive semidefinite, we conclude that the eigenvalues are nonnegative. □

We now give a detailed description of two particular experiments, and give a summary of observations from similar experiments. The test runs were implemented in C++ using "quad-double" precision, see `http://crd.lbl.gov/~dhbailey/mpdist/`. This extended precision (approximately 64 decimal digits) was necessary, because the terms $(D_h^{(\kappa)})^T D_h^{(\kappa)}$ constituting (1.39) differ significantly in their order of magnitude, which made it impossible to get reasonable results by using ordinary floating point arithmetic. For the linear algebra the Template Numerical Toolkit (TNT) together with the JAMA/C++ library was used, see `http://math.nist.gov/tnt/`. Some minor modifications were necessary in order to make JAMA/C++ work with quad-double.

1.4.4 Experimental Order Results for Simple ISDeC

For the first experiment we choose $\lambda = -1$ in (1.34) and $m = 6$, ρ_j from (1.4) are Gaussian points, as basic scheme we use the implicit midpoint rule, and ISDeC is realized according to Section 1.2. The results are given in Table 1.2. We see that

$N = 96$							
$\ell \setminus k$	0	1	2	3	4	5	6
0	$1.38 \cdot 10^{-01}$	$7.28 \cdot 10^{-04}$	$6.67 \cdot 10^{-06}$	$5.53 \cdot 10^{-06}$	$5.53 \cdot 10^{-06}$	$5.53 \cdot 10^{-06}$	$5.53 \cdot 10^{-06}$
1		$8.45 \cdot 10^{-03}$	$4.60 \cdot 10^{-05}$	$1.44 \cdot 10^{-05}$	$1.44 \cdot 10^{-05}$	$1.44 \cdot 10^{-05}$	$1.44 \cdot 10^{-05}$
2			$7.32 \cdot 10^{-03}$	$4.04 \cdot 10^{-05}$	$1.90 \cdot 10^{-05}$	$1.90 \cdot 10^{-05}$	$1.90 \cdot 10^{-05}$
3				$5.89 \cdot 10^{-03}$	$3.42 \cdot 10^{-05}$	$2.30 \cdot 10^{-05}$	$2.30 \cdot 10^{-05}$
4					$4.24 \cdot 10^{-03}$	$2.64 \cdot 10^{-05}$	$2.64 \cdot 10^{-05}$
5						$2.45 \cdot 10^{-03}$	$3.04 \cdot 10^{-05}$
6							$3.38 \cdot 10^{-05}$

$N = 192$							
$\ell \setminus k$	0	1	2	3	4	5	6
0	$1.38 \cdot 10^{-01}$	$3.63 \cdot 10^{-04}$	$1.67 \cdot 10^{-06}$	$1.38 \cdot 10^{-06}$	$1.38 \cdot 10^{-06}$	$1.38 \cdot 10^{-06}$	$1.38 \cdot 10^{-06}$
1		$4.22 \cdot 10^{-03}$	$1.15 \cdot 10^{-05}$	$3.61 \cdot 10^{-06}$	$3.61 \cdot 10^{-06}$	$3.61 \cdot 10^{-06}$	$3.61 \cdot 10^{-06}$
2			$3.66 \cdot 10^{-03}$	$1.01 \cdot 10^{-05}$	$4.75 \cdot 10^{-06}$	$4.75 \cdot 10^{-06}$	$4.75 \cdot 10^{-06}$
3				$2.95 \cdot 10^{-03}$	$8.55 \cdot 10^{-06}$	$5.75 \cdot 10^{-06}$	$5.75 \cdot 10^{-06}$
4					$2.12 \cdot 10^{-03}$	$6.59 \cdot 10^{-06}$	$6.59 \cdot 10^{-06}$
5						$1.22 \cdot 10^{-03}$	$7.60 \cdot 10^{-06}$
6							$8.46 \cdot 10^{-06}$

Observed order $N = 96 \to N = 192$							
$\ell \setminus k$	0	1	2	3	4	5	6
0	0.00	1.00	2.00	2.00	2.00	2.00	2.00
1		1.00	2.00	2.00	2.00	2.00	2.00
2			1.00	2.00	2.00	2.00	2.00
3				1.00	2.00	2.00	2.00
4					1.00	2.00	2.00
5						1.00	2.00
6							2.00

Table 1.2: Empirical orders of $\|S_h\|_{\ell,k}$. ISDeC based on IMR, $m = 6$ Gaussian points.

in this case the values of $\|S_h\|_{k,\ell}$ agree with Table 1.1.

This experiment was repeated with other polynomial degrees m, with the exact flow as basic method, with RadauIIA-points ρ_j (which do not satisfy (1.29)), and with collocation points

$$\rho_j = \frac{3}{2}\frac{j(j+1)}{(m+1)(m+2)}, \tag{1.44}$$

which satisfy (1.29) but for $m \geq 3$ are not symmetric in $[0,1]$. In each case the obtained values for the orders of $\|S_h\|_{k,\ell}$ agreed with Table 1.1. Particularly, $\|S_h\|_{m,m} = O(h^2)$ for ρ_j from (1.44).

Repeating the reasoning of Section 1.4.2 we conclude that the following order sequences of the iteration errors $\|\varepsilon_h^{[\nu]}\|_0$, $\nu = 0, 1, \ldots$ (computed according to (1.37)) are to be expected for simple ISDeC:

- If (1.29) is satisfied, cf. (1.32):

$$O(h^2),\ O(h^4),\ O(h^6), \ldots$$

- If (1.29) is not satisfied, cf. (1.33):

$$\begin{aligned}
m = 4: &\quad O(h^2),\ O(h^4),\ O(h^6),\ O(h^7),\ O(h^8),\ O(h^9), \ldots \\
m = 5: &\quad O(h^2),\ O(h^4),\ O(h^6),\ O(h^8),\ O(h^9),\ O(h^{10}), \ldots \\
m = 6: &\quad O(h^2),\ O(h^4),\ O(h^6),\ O(h^8),\ O(h^{10}),\ O(h^{11}), \ldots \\
m = 7: &\quad O(h^2),\ O(h^4),\ O(h^6),\ O(h^8),\ O(h^{10}),\ O(h^{12}), \ldots \\
&\ \vdots
\end{aligned}$$

These values are confirmed by the numerical results of Chapter 2.

1.4.5 Experimental Orders for Composition Methods

For the second experiment we again choose $\lambda = -1$ and $m = 6$ Gaussian points ρ_j. As basic scheme Φ we use Suzuki's composition method (1.17) based on the implicit midpoint rule. The results are given in Table 1.3, the observed orders agree well with the scheme given in Table 1.4.

The experiment was repeated with Yoshida's and McLachlan's composition schemes (based on the implict midpoint rule and the explicit and implicit Euler methods, respectively), with other polynomial degrees m, with RadauIIA points ρ_j, and with ρ_j chosen according to (1.44). In each case the obtained values for the orders of $\|S_h\|_{k,\ell}$ agreed with Table 1.4.

$N = 96$							
$\ell \setminus k$	0	1	2	3	4	5	6
0	$1.03 \cdot 10^{-02}$	$5.58 \cdot 10^{-05}$	$3.05 \cdot 10^{-07}$	$1.68 \cdot 10^{-09}$	$1.54 \cdot 10^{-11}$	$1.30 \cdot 10^{-11}$	$1.30 \cdot 10^{-11}$
1		$4.88 \cdot 10^{-03}$	$2.68 \cdot 10^{-05}$	$1.49 \cdot 10^{-07}$	$8.51 \cdot 10^{-10}$	$2.93 \cdot 10^{-11}$	$2.93 \cdot 10^{-11}$
2			$4.45 \cdot 10^{-03}$	$2.48 \cdot 10^{-05}$	$1.41 \cdot 10^{-07}$	$8.50 \cdot 10^{-10}$	$3.48 \cdot 10^{-11}$
3				$3.74 \cdot 10^{-03}$	$2.13 \cdot 10^{-05}$	$1.28 \cdot 10^{-07}$	$9.44 \cdot 10^{-10}$
4					$2.73 \cdot 10^{-03}$	$1.64 \cdot 10^{-05}$	$1.21 \cdot 10^{-07}$
5						$1.58 \cdot 10^{-03}$	$1.16 \cdot 10^{-05}$
6							$2.08 \cdot 10^{-05}$

$N = 192$							
$\ell \setminus k$	0	1	2	3	4	5	6
0	$9.21 \cdot 10^{-03}$	$2.49 \cdot 10^{-05}$	$6.80 \cdot 10^{-08}$	$1.87 \cdot 10^{-10}$	$9.51 \cdot 10^{-13}$	$8.10 \cdot 10^{-13}$	$8.10 \cdot 10^{-13}$
1		$2.44 \cdot 10^{-03}$	$6.70 \cdot 10^{-06}$	$1.86 \cdot 10^{-08}$	$5.32 \cdot 10^{-11}$	$1.83 \cdot 10^{-12}$	$1.83 \cdot 10^{-12}$
2			$2.22 \cdot 10^{-03}$	$6.19 \cdot 10^{-06}$	$1.77 \cdot 10^{-08}$	$5.31 \cdot 10^{-11}$	$2.18 \cdot 10^{-12}$
3				$1.87 \cdot 10^{-03}$	$5.33 \cdot 10^{-06}$	$1.60 \cdot 10^{-08}$	$5.90 \cdot 10^{-11}$
4					$1.37 \cdot 10^{-03}$	$4.11 \cdot 10^{-06}$	$1.51 \cdot 10^{-08}$
5						$7.89 \cdot 10^{-04}$	$2.91 \cdot 10^{-06}$
6							$5.20 \cdot 10^{-06}$

Observed order $N = 96 \to N = 192$							
$\ell \setminus k$	0	1	2	3	4	5	6
0	0.16	1.16	2.17	3.17	4.02	4.00	4.00
1		1.00	2.00	3.00	4.00	4.00	4.00
2			1.00	2.00	3.00	4.00	4.00
3				1.00	2.00	3.00	4.00
4					1.00	2.00	3.00
5						1.00	2.00
6							2.00

Table 1.3: Empirical orders of $\|S_h\|_{\ell,k}$. ISDeC based on Suzuki (IMR), $m = 6$ Gaussian points.

$\ell \setminus k$	0	1	2	3	4	...	$m-3$	$m-2$	$m-1$	m
0	$O(h^0)$	$O(h)$	$O(h^2)$	$O(h^3)$	$O(h^4)$	...	$O(h^4)$	$O(h^4)$	$O(h^4)$	$O(h^4)$
1		$O(h)$	$O(h^2)$	$O(h^3)$	$O(h^4)$	...	$O(h^4)$	$O(h^4)$	$O(h^4)$	$O(h^4)$
2			$O(h)$	$O(h^2)$	$O(h^3)$	...	$O(h^4)$	$O(h^4)$	$O(h^4)$	$O(h^4)$
$\vdots$				$\ddots$	$\ddots$	$\ddots$	$\vdots$	$\vdots$	$\vdots$	$\vdots$
$m-3$							$O(h)$	$O(h^2)$	$O(h^3)$	$O(h^4)$
$m-2$								$O(h)$	$O(h^2)$	$O(h^3)$
$m-1$									$O(h)$	$O(h^2)$
m										$O(h)$ or $O(h^2)$

Table 1.4: General pattern of observed orders of $\|S_h\|_{k,\ell}$ for Yoshida, Suzuki, McLachlan. Order $O(h^2)$ for $\|S_h\|_{m,m}$ holds for ρ_j which satisfy (1.29).

Using (1.30) with $p = 4$ and the estimates

$$
\begin{aligned}
\|\varepsilon_h^{[\nu+1]}\|_0 &\le \|S_h\|_{0,4}\|\varepsilon_h^{[\nu]}\|_4 \quad\quad\; \le\; Ch^4\|\varepsilon_h^{[\nu]}\|_4, \\
\|\varepsilon_h^{[\nu+1]}\|_k &\le \|S_h\|_{k,k+3}\|\varepsilon_h^{[\nu]}\|_{k+3} \le\; Ch^4\|\varepsilon_h^{[\nu]}\|_{k+3}, \quad k = 1, \ldots, m-3, \\
\|\varepsilon_h^{[\nu+1]}\|_{m-2} &\le \|S_h\|_{m-2,m}\|\varepsilon_h^{[\nu]}\|_m \le\; Ch^3\|\varepsilon_h^{[\nu]}\|_m, \\
\|\varepsilon_h^{[\nu+1]}\|_{m-1} &\le \|S_h\|_{m-1,m}\|\varepsilon_h^{[\nu]}\|_m \le\; Ch^2\|\varepsilon_h^{[\nu]}\|_m, \\
\|\varepsilon_h^{[\nu+1]}\|_m &\le \|S_h\|_{m,m}\|\varepsilon_h^{[\nu]}\|_m \le \begin{cases} Ch^2\|\varepsilon_h^{[\nu]}\|_m, & \text{if (1.29) is satisfied,} \\ Ch\|\varepsilon_h^{[\nu]}\|_m, & \text{otherwise,} \end{cases}
\end{aligned}
$$

(see Table 1.4), we can again derive order sequences for the iteration errors $\varepsilon_h^{[\nu]}$. We demonstrate this for the special case $m = 6$:

- If (1.29) is not satisfied:

	$k=0$	$k=1$	$k=2$	$k=3$	$k=4$	$k=5$	$k=6$
$\|\varepsilon_h^{[0]}\|_k$	$O(h^4)$	$O(h^4)$	$O(h^4)$	$O(h^4)$	$O(h^3)$	$O(h^2)$	$O(h^1)$
$\|\varepsilon_h^{[1]}\|_k$	$O(h^7)$	$O(h^7)$	$O(h^6)$	$O(h^5)$	$O(h^4)$	$O(h^3)$	$O(h^2)$
$\|\varepsilon_h^{[2]}\|_k$	$O(h^8)$	$O(h^8)$	$O(h^7)$	$O(h^6)$	$O(h^5)$	$O(h^4)$	$O(h^3)$

  This leads to the order sequences for $\|\varepsilon_h^{[\nu]}\|_0$

$$\begin{aligned}
m = 6: &\quad O(h^4),\ O(h^7),\ O(h^8),\ O(h^9),\ O(h^{10}),\ O(h^{11}),\dots\\
m = 7: &\quad O(h^4),\ O(h^8),\ O(h^9),\ O(h^{10}),\ O(h^{11}),\ O(h^{12}),\dots\\
m = 8: &\quad O(h^4),\ O(h^8),\ O(h^{10}),\ O(h^{11}),\ O(h^{12}),\ O(h^{13}),\dots\\
m = 9: &\quad O(h^4),\ O(h^8),\ O(h^{11}),\ O(h^{12}),\ O(h^{13}),\ O(h^{14}),\dots\\
&\ \ \vdots
\end{aligned}$$

  which are also observed in the numerical experiments reported in Chapter2.

- If (1.29) is satisfied:

	$k=0$	$k=1$	$k=2$	$k=3$	$k=4$	$k=5$	$k=6$
$\|\varepsilon_h^{[0]}\|_k$	$O(h^4)$	$O(h^4)$	$O(h^4)$	$O(h^4)$	$O(h^3)$	$O(h^2)$	$O(h^2)$
$\|\varepsilon_h^{[1]}\|_k$	$O(h^7)$	$O(h^7)$	$O(h^6)$	$O(h^6)$	$O(h^5)$	$O(h^4)$	$O(h^4)$
$\|\varepsilon_h^{[2]}\|_k$	$O(h^9)$	$O(h^9)$	$O(h^8)$	$O(h^8)$	$O(h^7)$	$O(h^6)$	$O(h^6)$

  This leads to the order sequences for $\|\varepsilon_h^{[\nu]}\|_0$

$$\begin{aligned}
m = 6: &\quad O(h^4),\ O(h^7),\ O(h^9),\ O(h^{11}),\ O(h^{13}),\ O(h^{15}),\dots\\
m = 7: &\quad O(h^4),\ O(h^8),\ O(h^{10}),\ O(h^{12}),\ O(h^{14}),\ O(h^{16}),\dots\\
m = 8: &\quad O(h^4),\ O(h^8),\ O(h^{10}),\ O(h^{12}),\ O(h^{14}),\ O(h^{16}),\dots\\
m = 9: &\quad O(h^4),\ O(h^8),\ O(h^{11}),\ O(h^{13}),\ O(h^{15}),\ O(h^{17}),\dots\\
&\ \ \vdots
\end{aligned}$$

  Note that the actually observed orders for $m = 6$ and $m = 9$ were in fact higher in the numerical experiments reported in Chapter 2 than the orders concluded from Table 1.4. We actually observed the following order sequences:

$$\begin{aligned}
m = 6: &\quad O(h^4),\ O(h^8),\ O(h^{10}),\ O(h^{12}),\ O(h^{14}),\ O(h^{16}),\dots\\
m = 9: &\quad O(h^4),\ O(h^8),\ O(h^{12}),\ O(h^{14}),\ O(h^{16}),\ O(h^{18}),\dots
\end{aligned}$$

Chapter 2

Numerical Results

2.1 Hamiltonian Systems – The Störmer-Verlet Method

First (and most comprehensively), we discuss the Störmer/Verlet method introduced in Section 1.2.1. This method demonstrates its advantages particularly when applied to Hamiltonian systems (1.6) and (1.10). The example we consider here is the *Kepler problem*, defined by the Hamiltonian

$$H(p_1, p_2, q_1, q_2) = \frac{1}{2}(p_1^2 + p_2^2) - \frac{1}{\sqrt{q_1^2 + q_2^2}}, \tag{2.1}$$

cf. [13, Sec. I.2]. The initial values are given as

$$q_1(0) = 1 - e, \quad q_2(0) = 0, \quad \dot{q}_1(0) = 0, \quad \dot{q}_2(0) = \sqrt{\frac{1+e}{1-e}}, \tag{2.2}$$

where $0 \leq e < 1$. In our experiments we use $e = 0.6$.

The exact solution of the Kepler problem is periodic with period 2π. Consequently, we choose the integration interval $[t_0, t_{\text{end}}] = [0, 2\pi]$. Note that the Hamiltonian H is constant along the exact flow of the problem. Moreover, the angular momentum

$$L(p_1, p_2, q_1, q_2) = q_1 p_2 - q_2 p_1 \tag{2.3}$$

is preserved.

Now, we discuss the asymptotic order of the iterates computed by ISDeC based on the Störmer/Verlet method. First, we remark that under certain circumstances, the ISDeC iteration converges to a fixed point p^* (in the sense that $\lim_{\nu\to\infty} z_j^{[\nu]} = p^*(t_j),\ j = 0\ldots, N$). This fixed point is a piecewise polynomial function of degree $\leq m$, and from the definition of $\Delta_{t,h}$ it is clear that this fixed point is characterized by $\dot{p}^*(\tau_{i,j}) - f(\tau_{i,j}, p^*(\tau_{i,j})) = 0$, where $\tau_{i,j}$ are the points where $D^{[0]}$ interpolates $d^{[0]}$, see Section 1.2. This means that in this situation the ISDeC iterates converge to a *collocation polynomial* [5].

Figures 2.1 to 2.5 give the absolute errors of the respective ISDeC iterates with respect to the fixed point at $t_{\text{end}} = 2\pi$, using interpolation of the defect at m Gaussian points $\tau_{i,j}$, where $m = 4, \ldots, 8$. In the diagrams, the left column refers

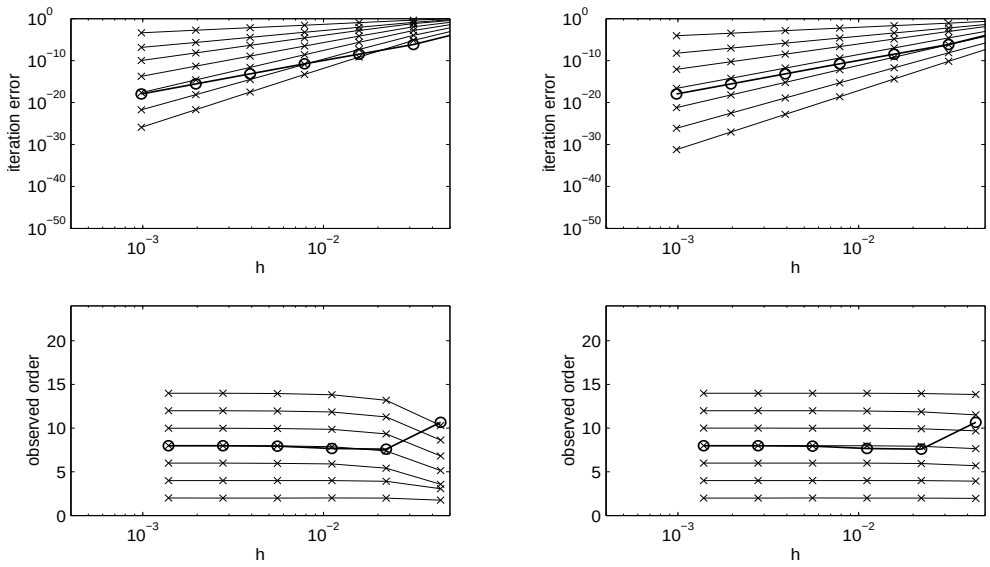

Figure 2.1: ISDeC, $m = 4$ Gaussian points, based on Störmer/Verlet for Kepler problem.

to Version A of the Störmer/Verlet method, while the right column gives the results for Version B (cf. Section 1.2.1). Obviously, the results are virtually the same, so we do not distinguish between the two versions in our discussion. In the top diagrams we give the iteration errors on a logarithmic scale plotted against the (equidistant) step size h, while the diagrams below show the empirical orders of the iteration errors. The circles $\circ$ illustrate the errors and the convergence orders for the fixed points, i. e., collocation solutions of order 8, 10, 12, 14 and 16, respectively. The convergence orders as compared to the fixed points are $O(h^2)$, $O(h^4)$, $O(h^6), \ldots$. This corresponds to classical theory which predicts the order to increase by two in every step if the data is sufficiently smooth, see Section 1.4 and [5]. From the triangle inequality it is clear that the global errors of the iterates as compared to the exact solution have orders $O(h^2)$, $O(h^4), \ldots$, $O(h^{2m})$, which do not increase further than the order of the fixed point.

Next, we consider the same procedure, where instead of Gaussian points we choose $\tau_{i,j}$ as the Radau points in (1.3), see for example [1]. This means that the maximal attainable convergence orders are 7, 9, 11, 13 and 15, respectively. The order sequences of the iteration errors are similar as for Gaussian points. In the first few steps, an increase of two is observed. However, from some point on the increase is reduced to only one order we gain in every step. The first iterate that is affected by this reduction is determined by the polynomial degree m used for the interpolation in ISDeC. This phenomenon is explained in Section 1.4. Consequently, for $m = 4$ we observe an order sequence for the iteration error of $O(h^2)$, $O(h^4)$, $O(h^6)$, $O(h^7), \ldots$. For higher polynomial degrees m, the order reduction occurs in later steps, for $m = 5$ the fourth iterate has an iteration

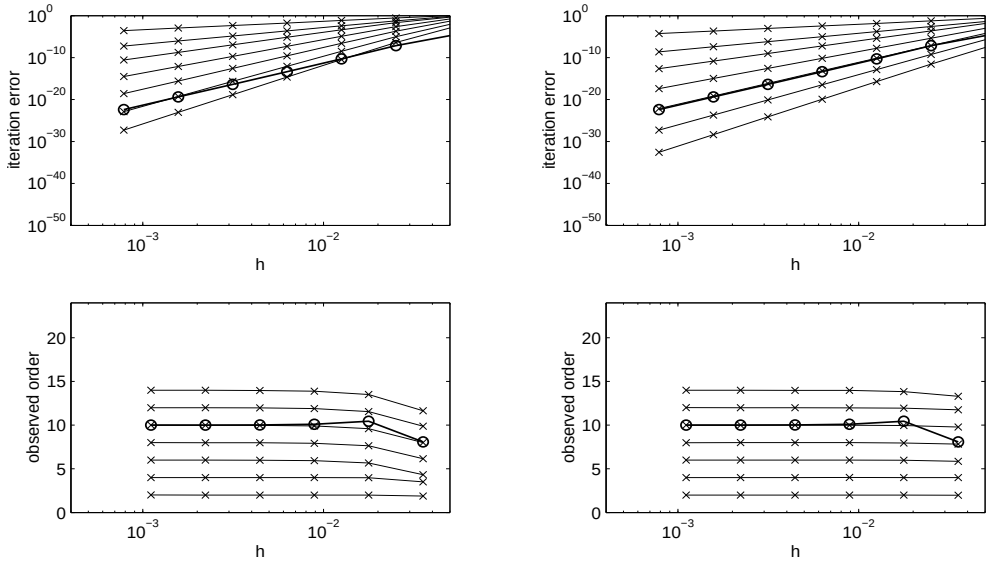

Figure 2.2: ISDeC, $m = 5$ Gaussian points, based on Störmer/Verlet for Kepler problem.

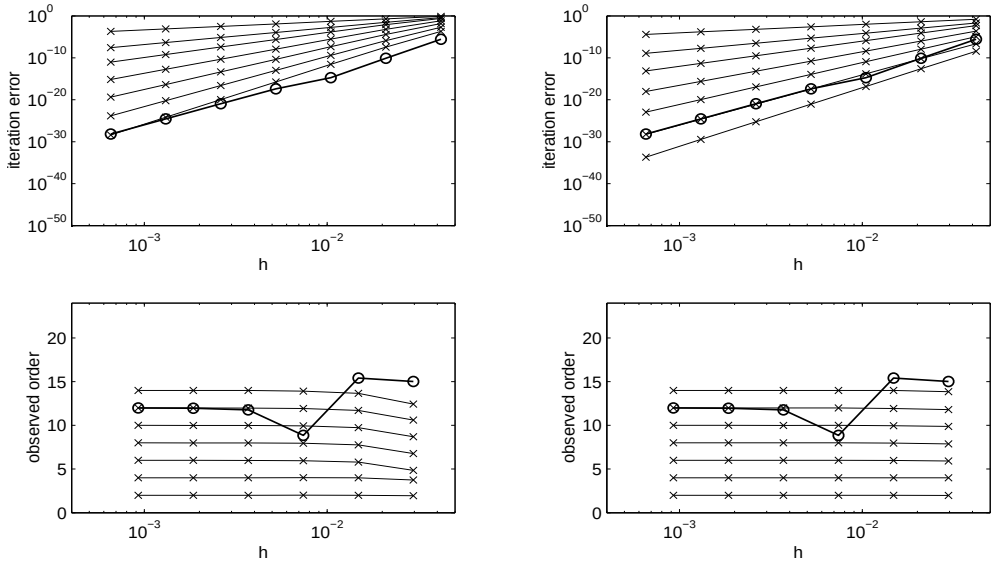

Figure 2.3: ISDeC, $m = 6$ Gaussian points, based on Störmer/Verlet for Kepler problem.

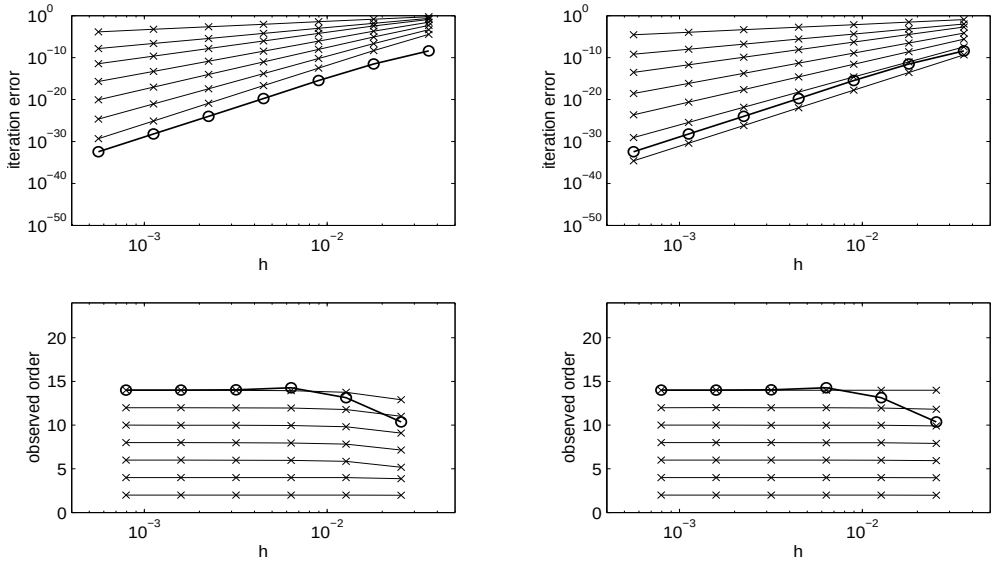

Figure 2.4: ISDeC, $m = 7$ Gaussian points, based on Störmer/Verlet for Kepler problem.

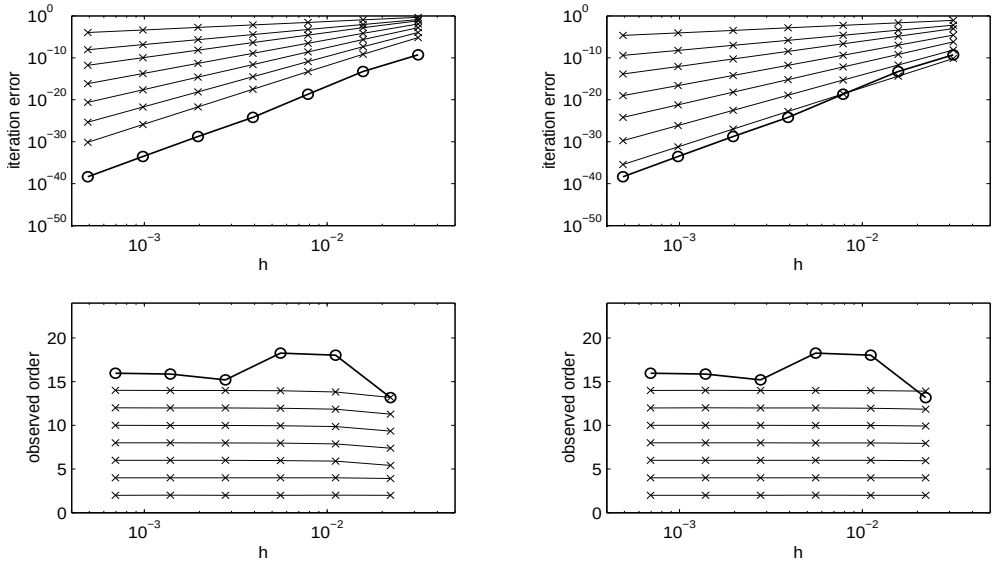

Figure 2.5: ISDeC, $m = 8$ Gaussian points, based on Störmer/Verlet for Kepler problem.

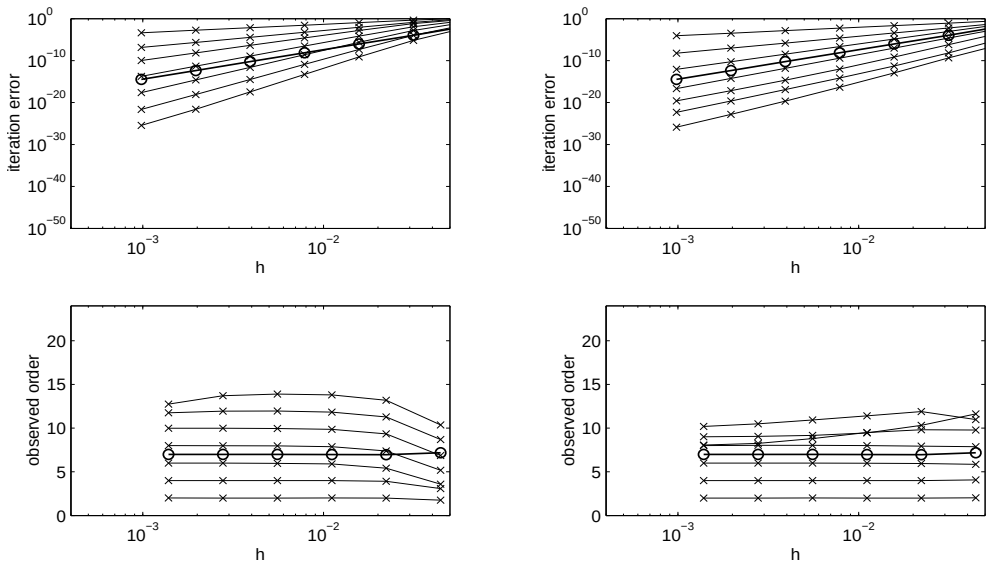

Figure 2.6: ISDeC, $m = 4$ Radau points, based on Störmer/Verlet for Kepler problem.

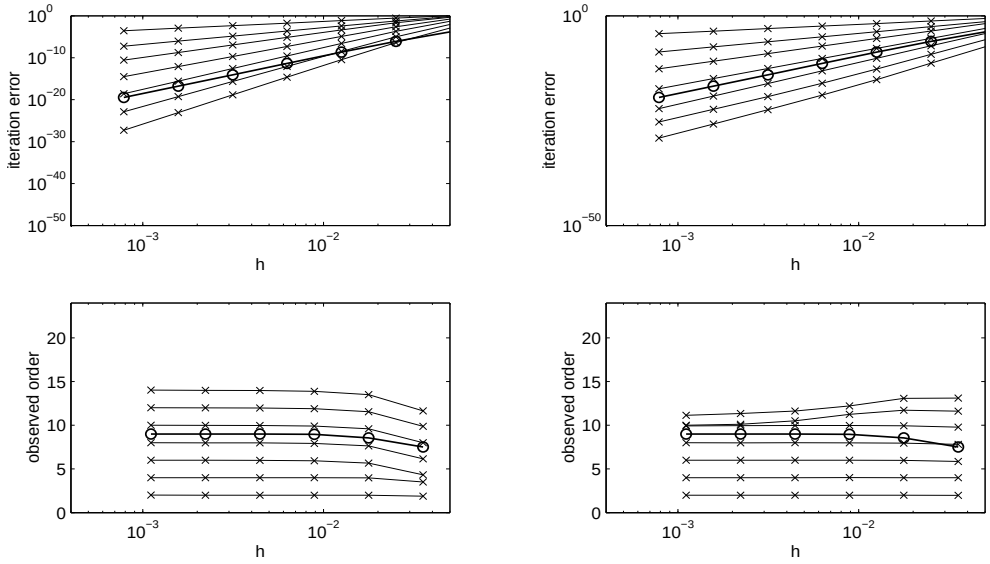

Figure 2.7: ISDeC, $m = 5$ Radau points, based on Störmer/Verlet for Kepler problem.

error of $O(h^9)$, for $m = 6$ the fifth iterate is reduced to order $O(h^{11})$, and so on, cf. Section 1.4. The results are given in Figures 2.6 to 2.10.

Finally, we take a look at the invariants which are preserved by the exact flow. We only consider ISDeC based on Gaussian points here. It is well known that both the Störmer/Verlet method and the fixed point of ISDeC, defined by collocation at Gaussian points, retain the angular momentum (2.3) exactly [13] (this is not

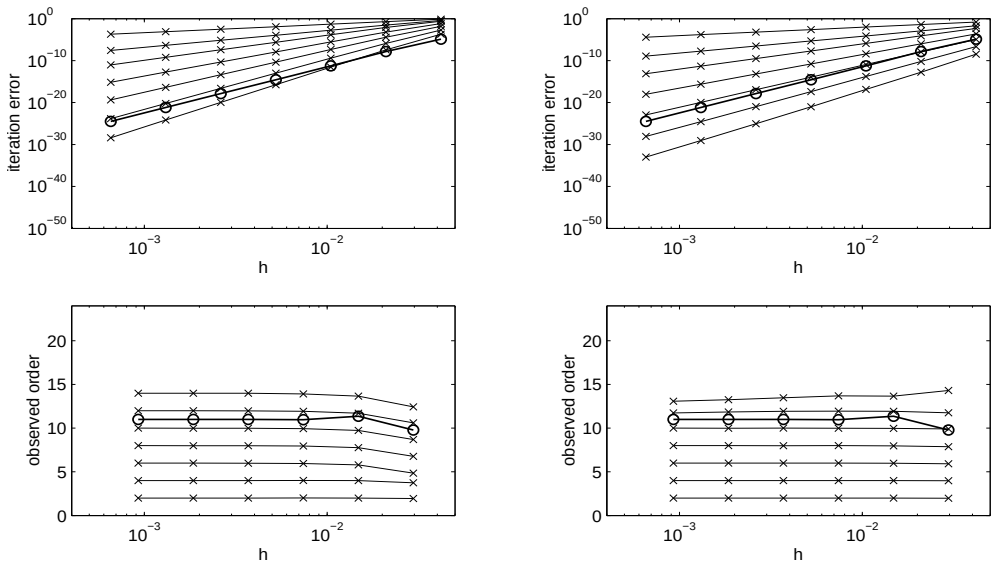

Figure 2.8: ISDeC, $m = 6$ Radau points, based on Störmer/Verlet for Kepler problem.

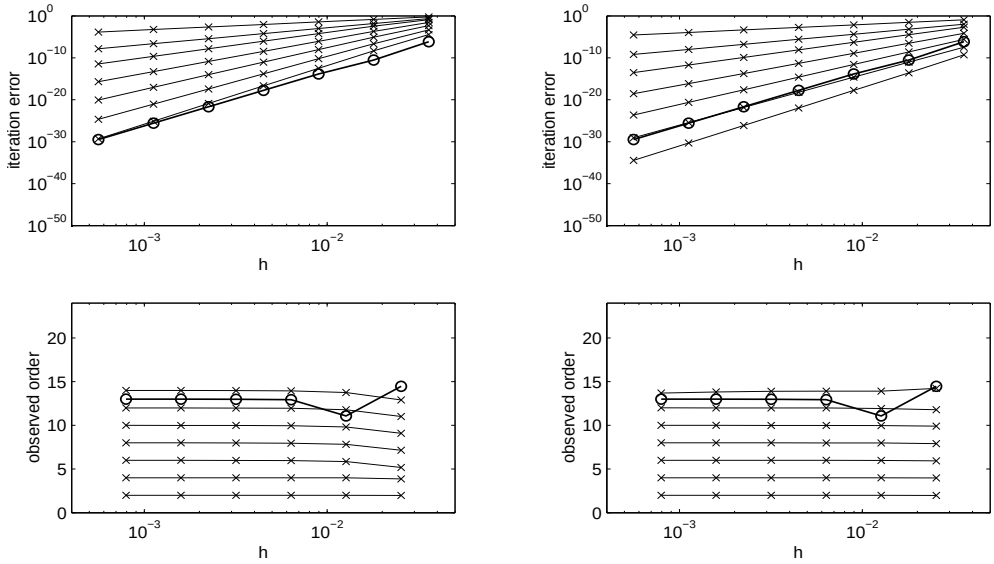

Figure 2.9: ISDeC, $m = 7$ Radau points, based on Störmer/Verlet for Kepler problem.

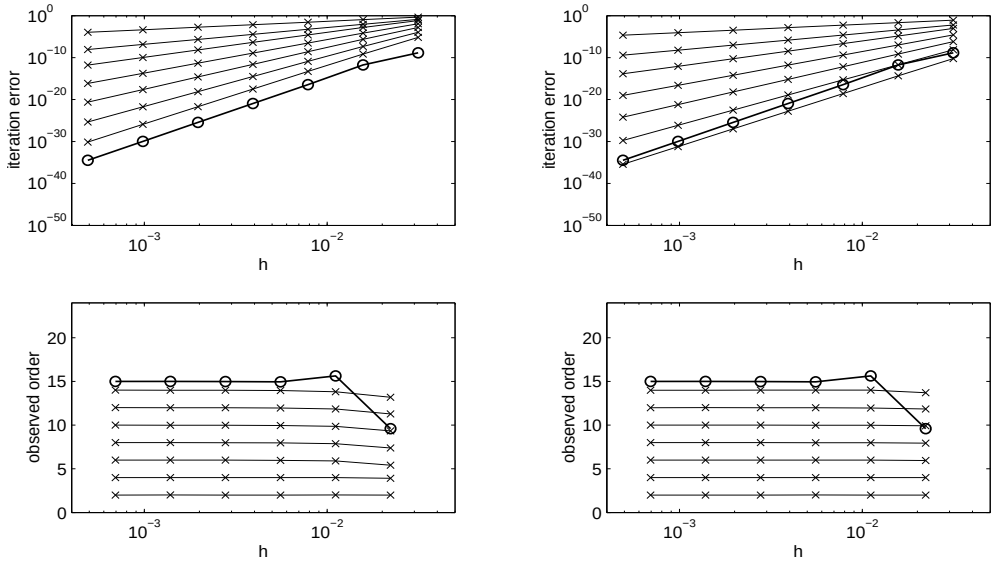

Figure 2.10: ISDeC, $m = 8$ Radau points, based on Störmer/Verlet for Kepler problem.

true for the fixed points defined by Radau points). This is not precisely the case for the ISDeC iterates, however. Table 2.1 shows that the angular momentum is preserved up to terms of the order of the iteration error (as compared with the fixed point p^*). The example in Table 2.1 was computed for $m = 6$, and it is clear from Figures 2.1 to 2.5 that for other degrees of the interpolation polynomial the same conservation properties of the ISDeC iterates must hold.

hm	Störmer	ISDeC 1	ISDeC 2	ISDeC 3	ISDeC 4	ISDeC 5	ISDeC 6
$2\pi/25$	0	$2.73 \cdot 10^{-01}$	$6.03 \cdot 10^{-02}$	$2.89 \cdot 10^{-02}$	$3.95 \cdot 10^{-03}$	$6.10 \cdot 10^{-04}$	$5.18 \cdot 10^{-05}$
$2\pi/50$	0	$2.27 \cdot 10^{-02}$	$2.36 \cdot 10^{-03}$	$3.11 \cdot 10^{-04}$	$1.24 \cdot 10^{-05}$	$4.96 \cdot 10^{-07}$	$1.22 \cdot 10^{-08}$
$2\pi/100$	0	$1.43 \cdot 10^{-03}$	$4.52 \cdot 10^{-05}$	$1.47 \cdot 10^{-06}$	$1.54 \cdot 10^{-08}$	$1.56 \cdot 10^{-10}$	$9.93 \cdot 10^{-13}$
$2\pi/200$	0	$8.90 \cdot 10^{-05}$	$7.39 \cdot 10^{-07}$	$6.00 \cdot 10^{-09}$	$1.59 \cdot 10^{-11}$	$4.03 \cdot 10^{-14}$	$6.48 \cdot 10^{-17}$
$2\pi/400$	0	$5.55 \cdot 10^{-06}$	$1.17 \cdot 10^{-08}$	$2.37 \cdot 10^{-11}$	$1.58 \cdot 10^{-14}$	$9.99 \cdot 10^{-18}$	$4.02 \cdot 10^{-21}$
$2\pi/800$	0	$3.47 \cdot 10^{-07}$	$1.83 \cdot 10^{-10}$	$9.27 \cdot 10^{-14}$	$1.55 \cdot 10^{-17}$	$2.45 \cdot 10^{-21}$	$2.46 \cdot 10^{-25}$
$2\pi/1600$	0	$2.17 \cdot 10^{-08}$	$2.86 \cdot 10^{-12}$	$3.62 \cdot 10^{-16}$	$1.51 \cdot 10^{-20}$	$5.98 \cdot 10^{-25}$	$1.51 \cdot 10^{-29}$
$2\pi/25$		3.59	4.68	6.54	8.32	10.26	12.05
$2\pi/50$		3.99	5.71	7.72	9.65	11.63	13.58
$2\pi/100$		4.01	5.93	7.94	9.92	11.92	13.90
$2\pi/200$		4.00	5.98	7.98	9.97	11.98	13.98
$2\pi/400$		4.00	6.00	8.00	9.99	11.99	14.00
$2\pi/800$		4.00	6.00	8.00	10.00	12.00	13.99
$2\pi/1600$							

Table 2.1: Error in the angular momentum for ISDeC based on Störmer/Verlet, $m = 6$.

If we consider the preservation of the Hamiltonian (2.1), the situation is different. Here, theory predicts that the Hamiltonian is preserved by the Störmer/Verlet method only up to terms of order h^2. However, this order estimate is not affected by the length of the time interval considered, see [14]. The fixed point p^* of

ISDeC preserves the Hamiltonian exactly if Gaussian points τ_{ij} are used for the interpolation [13]. As for the angular momentum, this is not the case for Radau points. Consequently, in Table 2.2, we give the errors in the Hamiltonian of the numerical solution computed by the Störmer/Verlet method, and of the ISDeC iterates when $m = 6$ Gaussian points are used. Note that in the particular case of the Kepler problem (2.1), the asymptotic quality of the Störmer/Verlet method is even better than the worst case theoretical estimate. The important point, however, is that the ISDeC iterates preserve the Hamiltonian only up to terms of the order of the iteration error.

hm	Störmer	ISDeC 1	ISDeC 2	ISDeC 3	ISDeC 4	ISDeC 5	ISDeC 6
$2\pi/25$	$2.53 \cdot 10^{-03}$	$9.44 \cdot 10^{-01}$	$1.87 \cdot 10^{-01}$	$1.16 \cdot 10^{-01}$	$1.51 \cdot 10^{-02}$	$2.52 \cdot 10^{-03}$	$2.12 \cdot 10^{-04}$
$2\pi/50$	$4.86 \cdot 10^{-05}$	$9.10 \cdot 10^{-02}$	$8.09 \cdot 10^{-03}$	$1.33 \cdot 10^{-03}$	$5.12 \cdot 10^{-05}$	$2.16 \cdot 10^{-06}$	$5.32 \cdot 10^{-08}$
$2\pi/100$	$7.61 \cdot 10^{-07}$	$5.79 \cdot 10^{-03}$	$1.58 \cdot 10^{-04}$	$6.34 \cdot 10^{-06}$	$6.46 \cdot 10^{-08}$	$6.86 \cdot 10^{-10}$	$4.37 \cdot 10^{-12}$
$2\pi/200$	$1.19 \cdot 10^{-08}$	$3.61 \cdot 10^{-04}$	$2.59 \cdot 10^{-06}$	$2.59 \cdot 10^{-08}$	$6.70 \cdot 10^{-11}$	$1.78 \cdot 10^{-13}$	$2.86 \cdot 10^{-16}$
$2\pi/400$	$1.85 \cdot 10^{-10}$	$2.25 \cdot 10^{-05}$	$4.10 \cdot 10^{-08}$	$1.02 \cdot 10^{-10}$	$6.63 \cdot 10^{-14}$	$4.41 \cdot 10^{-17}$	$1.78 \cdot 10^{-20}$
$2\pi/800$	$2.89 \cdot 10^{-12}$	$1.41 \cdot 10^{-06}$	$6.42 \cdot 10^{-10}$	$4.01 \cdot 10^{-13}$	$6.50 \cdot 10^{-17}$	$1.08 \cdot 10^{-20}$	$1.09 \cdot 10^{-24}$
$2\pi/1600$	$4.52 \cdot 10^{-14}$	$8.79 \cdot 10^{-08}$	$1.00 \cdot 10^{-11}$	$1.57 \cdot 10^{-15}$	$6.36 \cdot 10^{-20}$	$2.64 \cdot 10^{-24}$	$6.65 \cdot 10^{-29}$
$2\pi/25$	5.70	3.37	4.53	6.45	8.20	10.19	11.96
$2\pi/50$	6.00	3.97	5.68	7.71	9.63	11.62	13.57
$2\pi/100$	6.00	4.00	5.93	7.94	9.91	11.91	13.90
$2\pi/200$	6.01	4.00	5.98	7.99	9.98	11.98	13.97
$2\pi/400$	6.00	4.00	6.00	7.99	9.99	12.00	14.00
$2\pi/800$	6.00	4.00	6.00	8.00	10.00	12.00	14.00
$2\pi/1600$							

Table 2.2: Error in the Hamiltonian for ISDeC based on Störmer/Verlet, $m = 6$.

2.1.1 Composition Methods

In this section, we consider the higher-order composition methods described in Section 1.3, where we use the Störmer/Verlet method as the basic scheme. Again, we solve the Kepler problem (2.1). In Figures 2.11 to 2.17 we give the results for Suzuki's method and ISDeC based on interpolation at Gaussian points, see Section 1.3. Again, the top row of each figure gives the iteration errors and error of the fixed point on a logarithmic scale, while the bottom row gives the resulting empirical orders. For the left columns, Version A of the Störmer/Verlet method is used as the basic scheme, and the right columns give the analogous results for the dual Version B (which shows the same behavior as Version A).

We observe that the basic scheme has order 4 as predicted, and the increase in the order of the iteration error is at least 2 in every step. This of course implies that the order of the global error increases in the same way up to the theoretical maximum given by the order of the fixed point, Gaussian collocation. For $m = 6$, $m = 7$ and $m = 8$, the first ISDeC iterate yields a numerical approximation of order 8, even. Thus, the increase in the attainable order is 4 in the first step, but drops back to 2 in the further course of the iteration. For $m = 9$ and $m = 10$, we

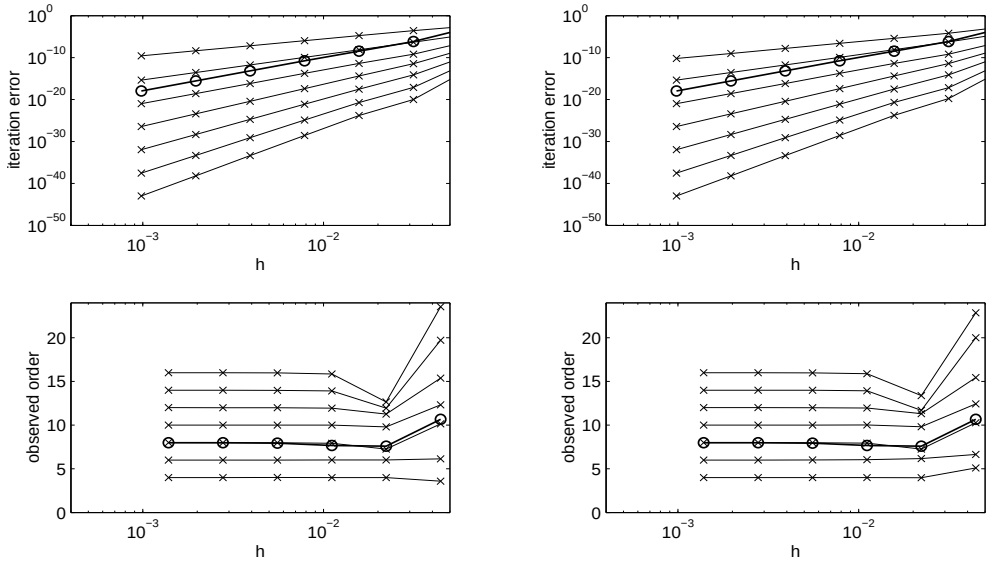

Figure 2.11: ISDeC, $m = 4$ Gaussian points, based on Suzuki for Kepler problem.

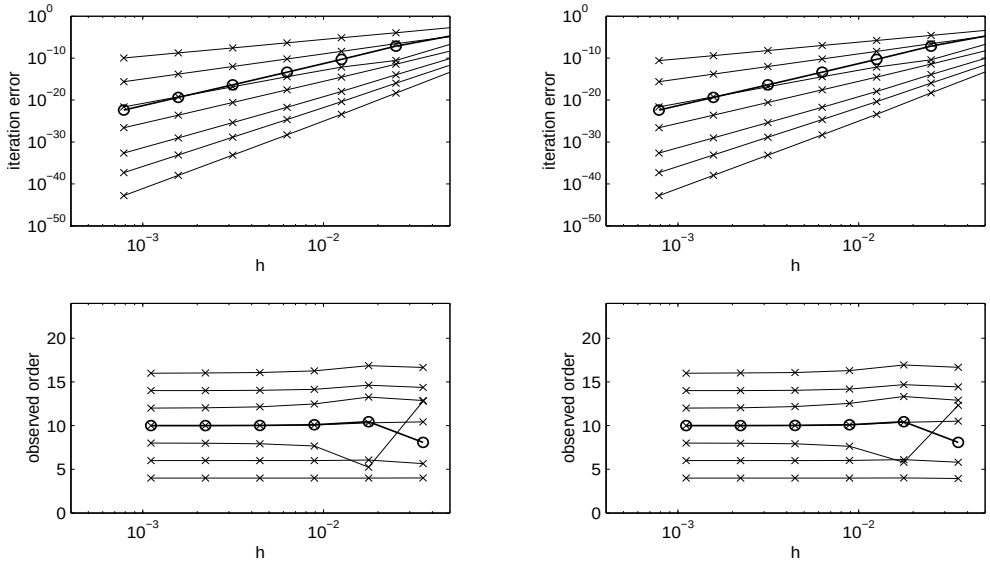

Figure 2.12: ISDeC, $m = 5$ Gaussian points, based on Suzuki for Kepler problem.

observe order sequences $O(h^4)$, $O(h^8)$, $O(h^{12})$, $O(h^{14})$, $O(h^{16}), \ldots$. These order sequences become plausible in the light of the discussion in Section 1.4. For some of the iterates, we observe even higher orders than predicted by our theoretical considerations, however.

Figures 2.18 to 2.24 give the same results, where the interpolation is based on Radau points. The iteration error shows a different asymptotic behavior as that

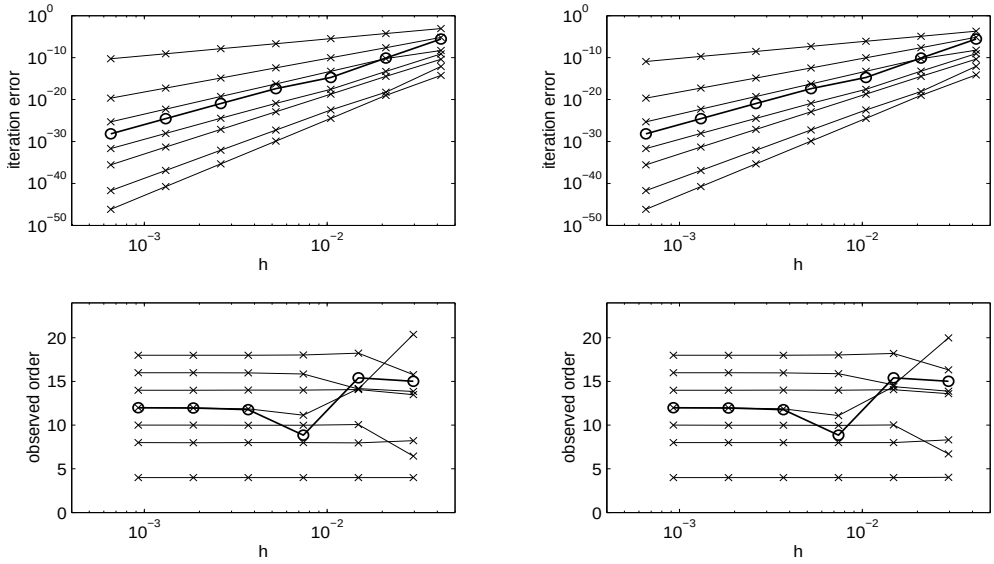

Figure 2.13: ISDeC, $m = 6$ Gaussian points, based on Suzuki for Kepler problem.

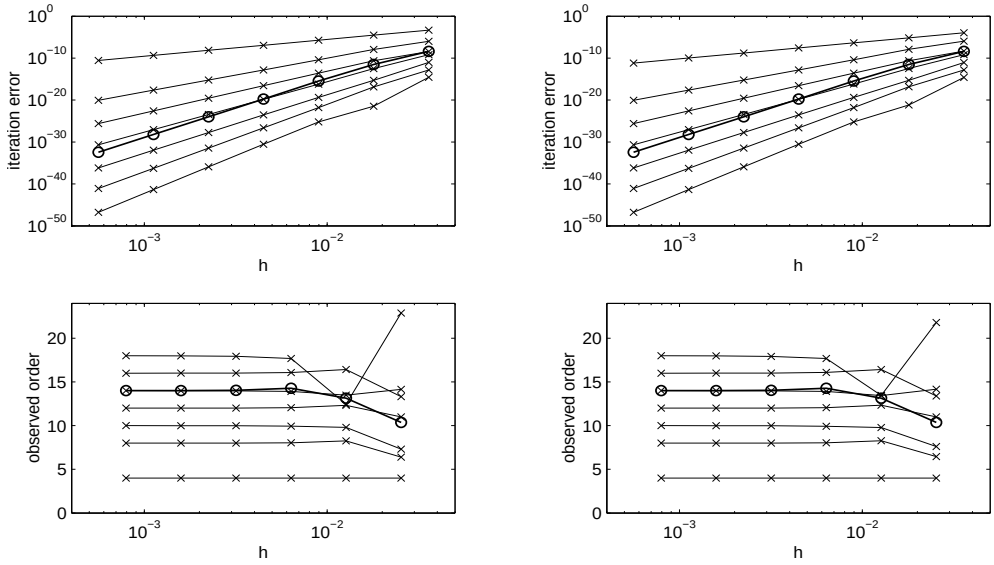

Figure 2.14: ISDeC, $m = 7$ Gaussian points, based on Suzuki for Kepler problem.

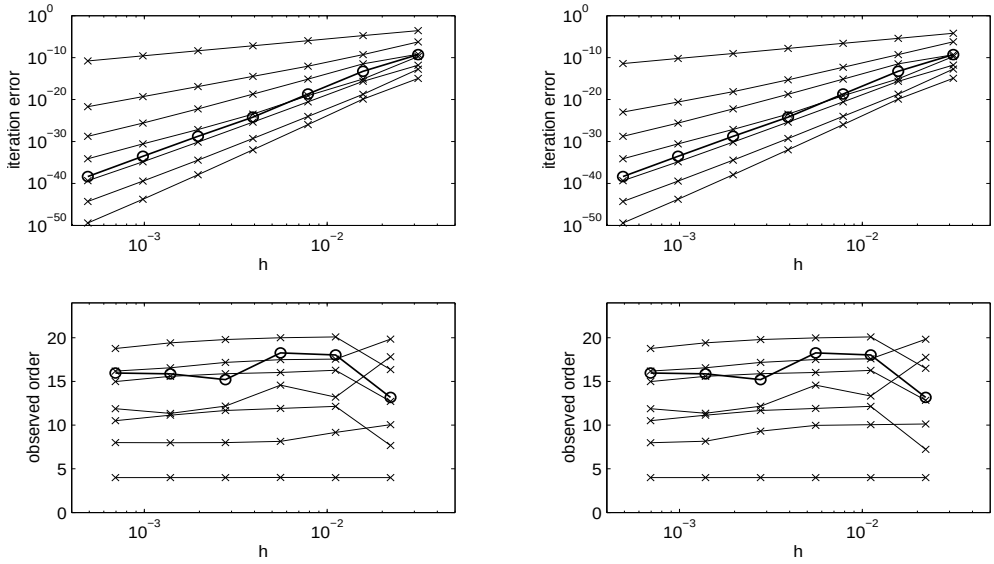

Figure 2.15: ISDeC, $m = 8$ Gaussian points, based on Suzuki for Kepler problem.

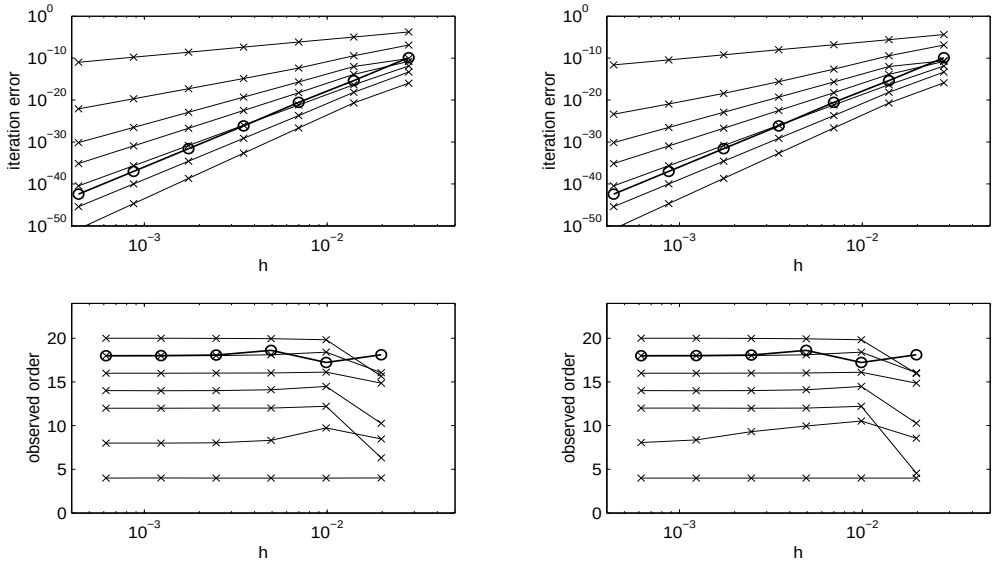

Figure 2.16: ISDeC, $m = 9$ Gaussian points, based on Suzuki for Kepler problem.

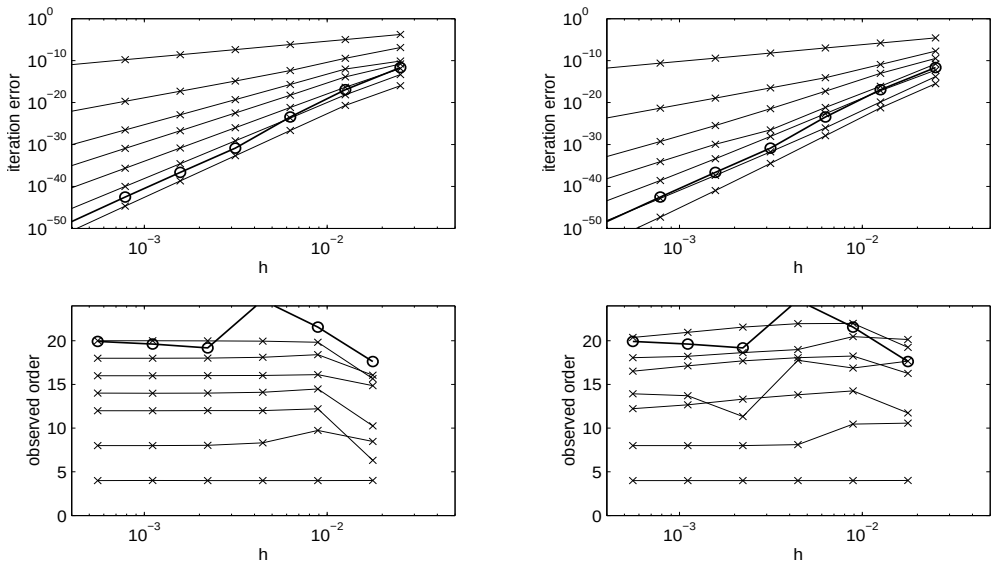

Figure 2.17: ISDeC, $m = 10$ Gaussian points, based on Suzuki for Kepler problem.

observed in the case of Gaussian points. This can be attributed to the fact that Radau points do not satisfy (1.29). While the results for Radau points can fully be explained by the considerations in Section 1.4, the more favorable behavior for Gaussian points is not entirely clear.

For Radau points, the increase in the orders of the iteration errors of the respective ISDeC iterates is generally one in every step, while for symmetric points like Gaussian points, the increase is two in general, see Section 1.4. If the degree of the interpolation polynomial is sufficiently large, a faster acceleration in the convergence order is observed. Namely, for degree $m = 5$, the first iteration step yields an increase from order 4 to 6, while for $m = 4$ only order 5 is obtained. For $m = 6$ and $m = 7$, the increase in the first step amounts to 3 and 4, even (but the increase drops back to 1 in each of the succeeding steps). For $m = 8$ we observe an order sequence $O(h^4)$, $O(h^8)$, $O(h^{10})$, $O(h^{11}), \ldots$. For $m = 9$ this is improved to $O(h^4)$, $O(h^8)$, $O(h^{11})$, $O(h^{12}), \ldots$. Finally, for $m = 10$ we observe $O(h^4)$, $O(h^8)$, $O(h^{12})$, $O(h^{13}), \ldots$. Refer to Section 1.4 for an explanation of this behavior.

The fixed points have lower orders in the case of Radau points as compared to Gaussian points, however. This of course limits the maximal attainable order of the global error as discussed before.

Finally, we discuss the geometric properties of Suzuki's method based on the Störmer/Verlet method. The composition method which serves as a basis for ISDeC preserves the angular momentum, see Table 2.3 and [13]. Unfortunately, the same does not hold for the ISDeC iterates. As in the case of ISDeC based

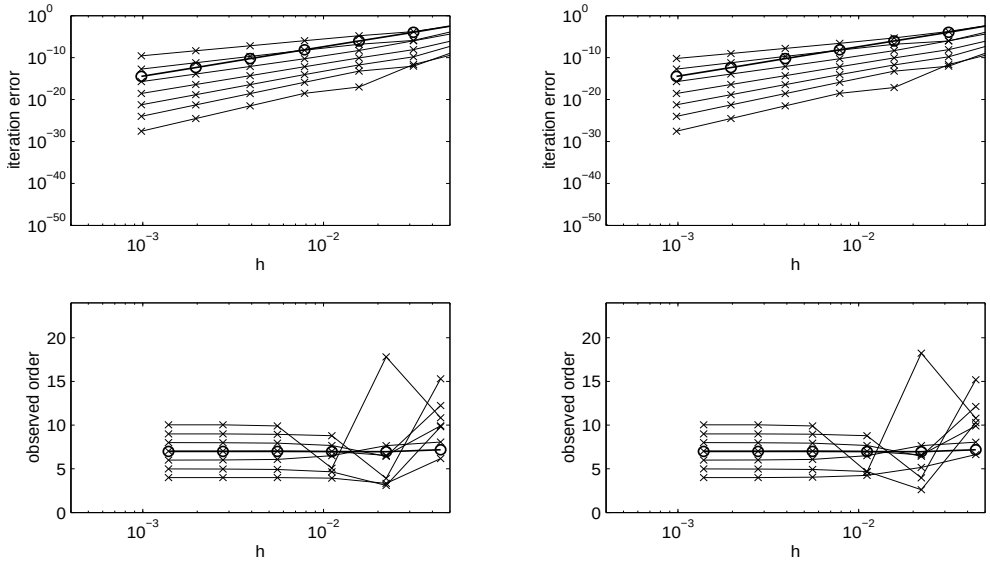

Figure 2.18: ISDeC, $m = 4$ Radau points, based on Suzuki for Kepler problem.

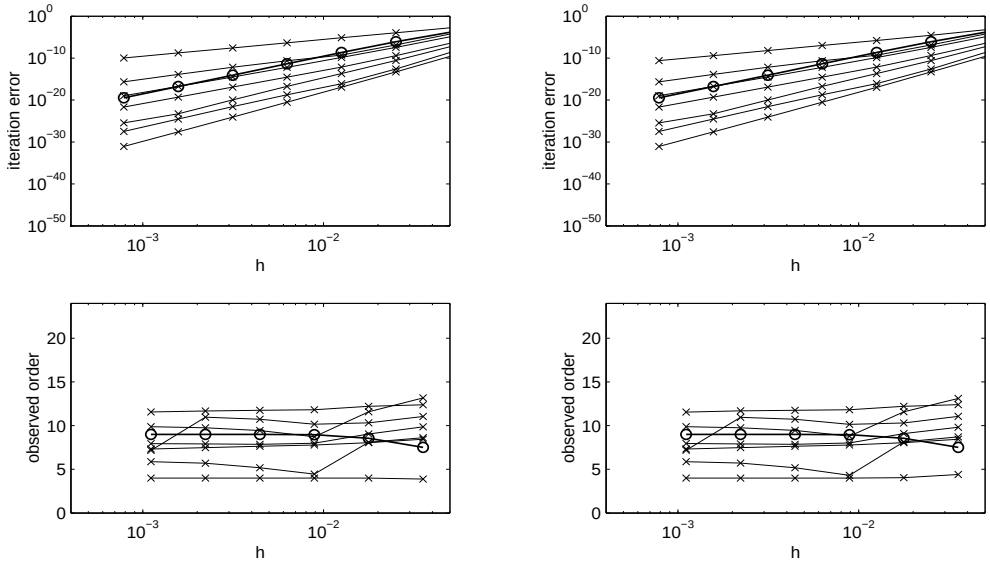

Figure 2.19: ISDeC, $m = 5$ Radau points, based on Suzuki for Kepler problem.

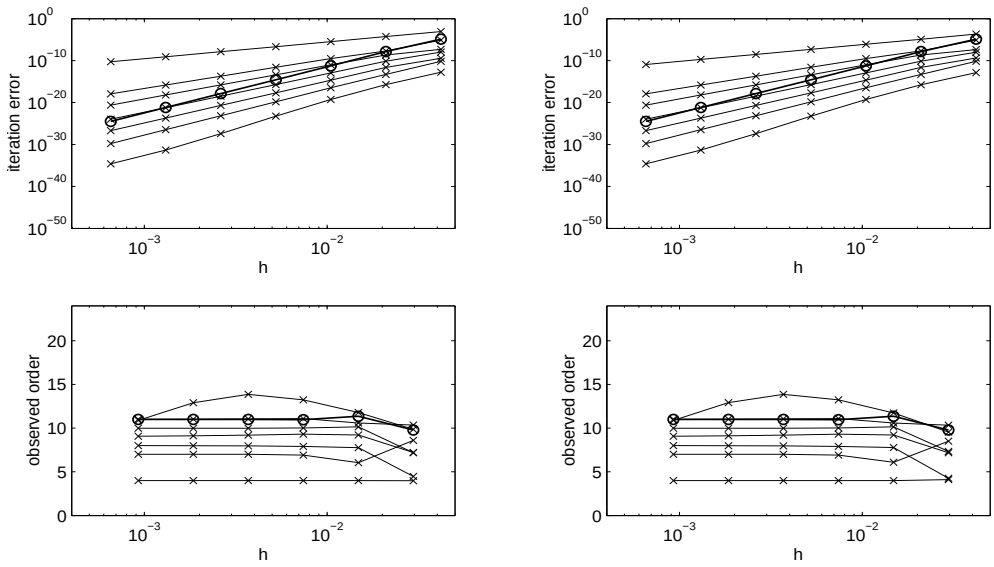

Figure 2.20: ISDeC, $m = 6$ Radau points, based on Suzuki for Kepler problem.

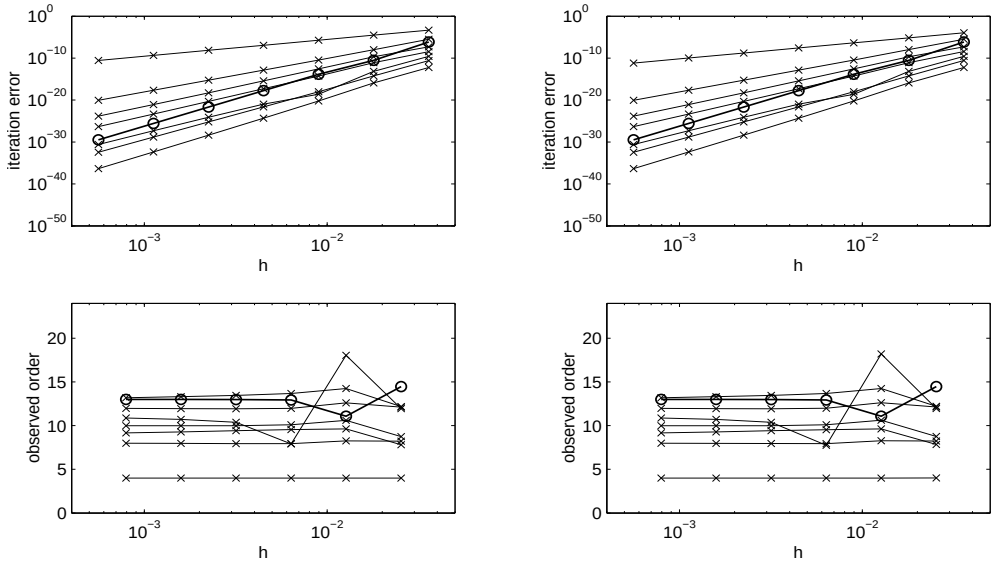

Figure 2.21: ISDeC, $m = 7$ Radau points, based on Suzuki for Kepler problem.

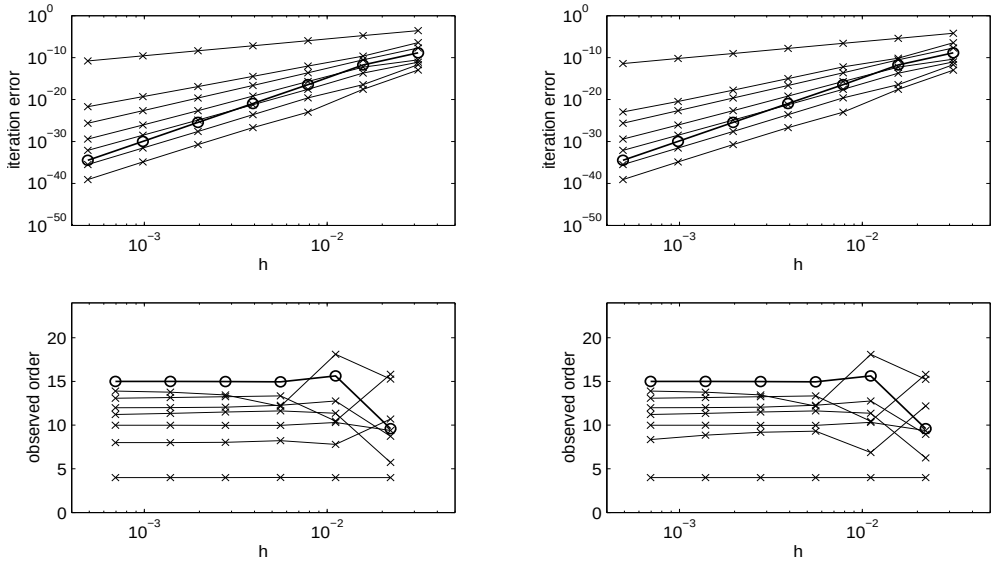

Figure 2.22: ISDeC, $m = 8$ Radau points, based on Suzuki for Kepler problem.

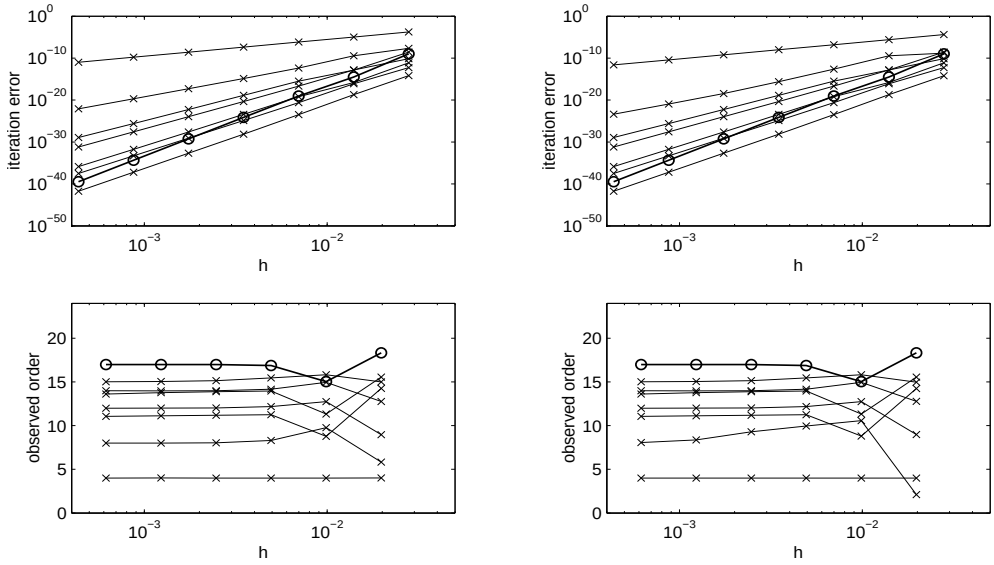

Figure 2.23: ISDeC, $m = 9$ Radau points, based on Suzuki for Kepler problem.

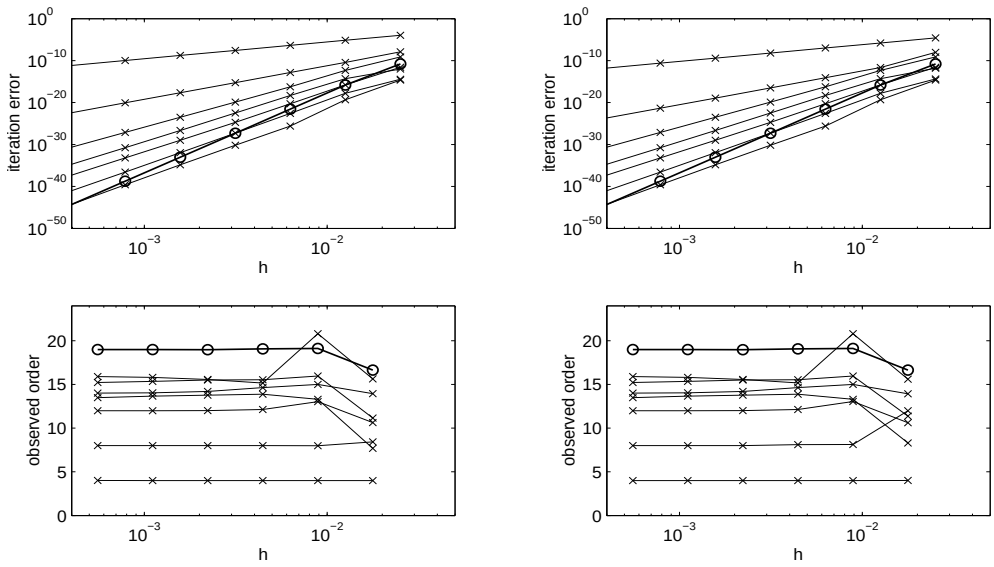

Figure 2.24: ISDeC, $m = 10$ Radau points, based on Suzuki for Kepler problem.

on the Störmer/Verlet method, this invariant is conserved only up to terms of the order of the iteration error in general if Gaussian points are used. Recall that the fixed point p^* retains the angular momentum exactly. Table 2.3 shows the corresponding results, which are even a little more favorable for some of the iterates than we would expect in general.

hm	Suzuki	ISDeC 1	ISDeC 2	ISDeC 3	ISDeC 4	ISDeC 5	ISDeC 6
$2\pi/25$	0	$4.35 \cdot 10^{-07}$	$3.20 \cdot 10^{-09}$	$3.91 \cdot 10^{-12}$	$3.81 \cdot 10^{-13}$	$1.99 \cdot 10^{-14}$	$3.80 \cdot 10^{-16}$
$2\pi/50$	0	$1.73 \cdot 10^{-09}$	$6.62 \cdot 10^{-13}$	$1.90 \cdot 10^{-15}$	$1.59 \cdot 10^{-18}$	$1.11 \cdot 10^{-19}$	$2.17 \cdot 10^{-23}$
$2\pi/100$	0	$6.73 \cdot 10^{-12}$	$1.65 \cdot 10^{-16}$	$1.10 \cdot 10^{-19}$	$7.52 \cdot 10^{-24}$	$4.01 \cdot 10^{-25}$	$6.56 \cdot 10^{-29}$
$2\pi/200$	0	$2.63 \cdot 10^{-14}$	$4.05 \cdot 10^{-20}$	$6.78 \cdot 10^{-24}$	$1.87 \cdot 10^{-28}$	$1.52 \cdot 10^{-30}$	$6.95 \cdot 10^{-35}$
$2\pi/400$	0	$1.03 \cdot 10^{-16}$	$9.90 \cdot 10^{-24}$	$4.15 \cdot 10^{-28}$	$3.08 \cdot 10^{-33}$	$5.80 \cdot 10^{-36}$	$6.73 \cdot 10^{-41}$
$2\pi/800$	0	$4.01 \cdot 10^{-19}$	$2.42 \cdot 10^{-27}$	$2.54 \cdot 10^{-32}$	$4.79 \cdot 10^{-38}$	$2.21 \cdot 10^{-41}$	$6.44 \cdot 10^{-47}$
$2\pi/1600$	0	$1.57 \cdot 10^{-21}$	$5.90 \cdot 10^{-31}$	$1.55 \cdot 10^{-36}$	$7.33 \cdot 10^{-43}$	$8.44 \cdot 10^{-47}$	$6.15 \cdot 10^{-53}$
$2\pi/25$		7.97	12.24	11.01	17.87	17.45	24.06
$2\pi/50$		8.01	11.97	14.08	17.69	18.08	18.34
$2\pi/100$		8.00	11.99	13.99	15.30	18.01	19.85
$2\pi/200$		8.00	12.00	14.00	15.89	18.00	19.98
$2\pi/400$		8.00	12.00	14.00	15.97	18.00	20.00
$2\pi/800$		8.00	12.00	14.00	16.00	18.00	20.00
$2\pi/1600$							

Table 2.3: Error in the angular momentum for ISDeC based on Suzuki, $m = 6$.

The Hamiltonian is not preserved in general by Suzuki's method based on Störmer/Verlet. This can also be observed in Table 2.4. Again, the iterates preserve the invariant up to terms of an order correlated with the iteration error as compared with the fixed point.

If instead of Suzuki's method, we use Yoshida's method to obtain a fourth order

hm	Suzuki	ISDeC 1	ISDeC 2	ISDeC 3	ISDeC 4	ISDeC 5	ISDeC 6
$2\pi/25$	$1.01 \cdot 10^{-11}$	$1.77 \cdot 10^{-06}$	$1.31 \cdot 10^{-08}$	$1.41 \cdot 10^{-11}$	$1.74 \cdot 10^{-12}$	$2.38 \cdot 10^{-13}$	$1.58 \cdot 10^{-13}$
$2\pi/50$	$2.40 \cdot 10^{-15}$	$6.99 \cdot 10^{-09}$	$2.73 \cdot 10^{-12}$	$7.70 \cdot 10^{-15}$	$6.52 \cdot 10^{-18}$	$4.55 \cdot 10^{-19}$	$5.60 \cdot 10^{-21}$
$2\pi/100$	$5.82 \cdot 10^{-19}$	$2.73 \cdot 10^{-11}$	$6.82 \cdot 10^{-16}$	$4.48 \cdot 10^{-19}$	$2.75 \cdot 10^{-23}$	$1.63 \cdot 10^{-24}$	$2.78 \cdot 10^{-28}$
$2\pi/200$	$1.42 \cdot 10^{-22}$	$1.07 \cdot 10^{-13}$	$1.67 \cdot 10^{-19}$	$2.76 \cdot 10^{-23}$	$7.17 \cdot 10^{-28}$	$6.18 \cdot 10^{-30}$	$2.93 \cdot 10^{-34}$
$2\pi/400$	$3.46 \cdot 10^{-26}$	$4.16 \cdot 10^{-16}$	$4.09 \cdot 10^{-23}$	$1.69 \cdot 10^{-27}$	$1.19 \cdot 10^{-32}$	$2.36 \cdot 10^{-35}$	$2.84 \cdot 10^{-40}$
$2\pi/800$	$8.46 \cdot 10^{-30}$	$1.63 \cdot 10^{-18}$	$9.98 \cdot 10^{-27}$	$1.03 \cdot 10^{-31}$	$1.84 \cdot 10^{-37}$	$8.99 \cdot 10^{-41}$	$2.72 \cdot 10^{-46}$
$2\pi/1600$	$2.06 \cdot 10^{-33}$	$6.35 \cdot 10^{-21}$	$2.44 \cdot 10^{-30}$	$6.31 \cdot 10^{-36}$	$2.82 \cdot 10^{-42}$	$3.43 \cdot 10^{-46}$	$2.59 \cdot 10^{-52}$
$2\pi/25$	12.04	7.98	12.23	10.84	18.03	19.00	24.75
$2\pi/50$	12.01	8.00	11.97	14.07	17.86	18.09	24.26
$2\pi/100$	12.00	8.00	12.00	13.99	15.23	18.01	19.86
$2\pi/200$	12.00	8.01	12.00	14.00	15.88	18.00	19.98
$2\pi/400$	12.00	8.00	12.00	14.00	15.98	18.00	19.99
$2\pi/800$	12.00	8.00	12.00	13.99	15.99	18.00	20.00
$2\pi/1600$							

Table 2.4: Error in the Hamiltonian for ISDeC based on Suzuki, $m = 6$.

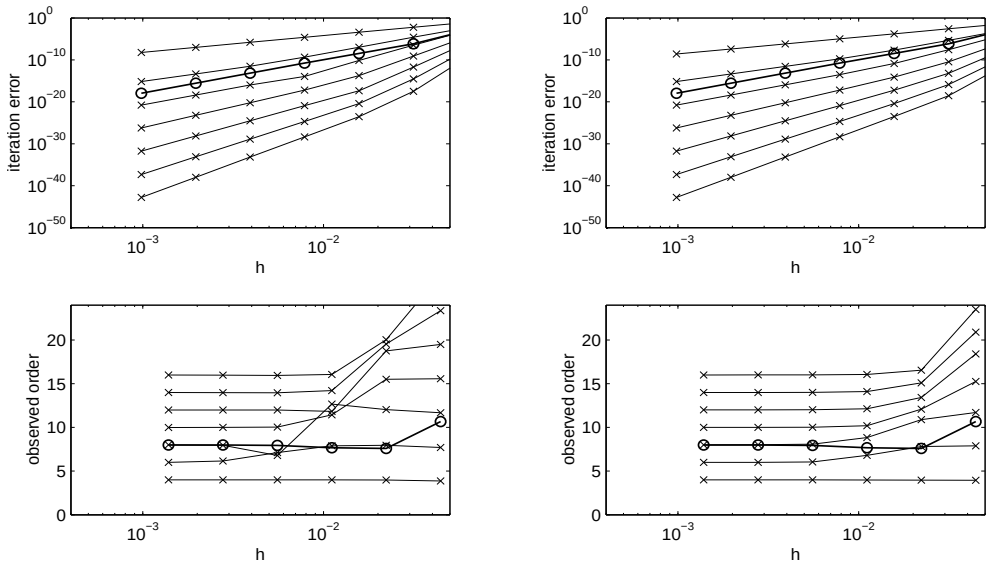

Figure 2.25: ISDeC, $m = 4$ Gaussian points, based on Yoshida for Kepler problem.

method from the Störmer/Verlet method, and leave all other algorithmic details of ISDeC unaltered, we obtain precisely the same results, see Tables 2.25– 2.39.

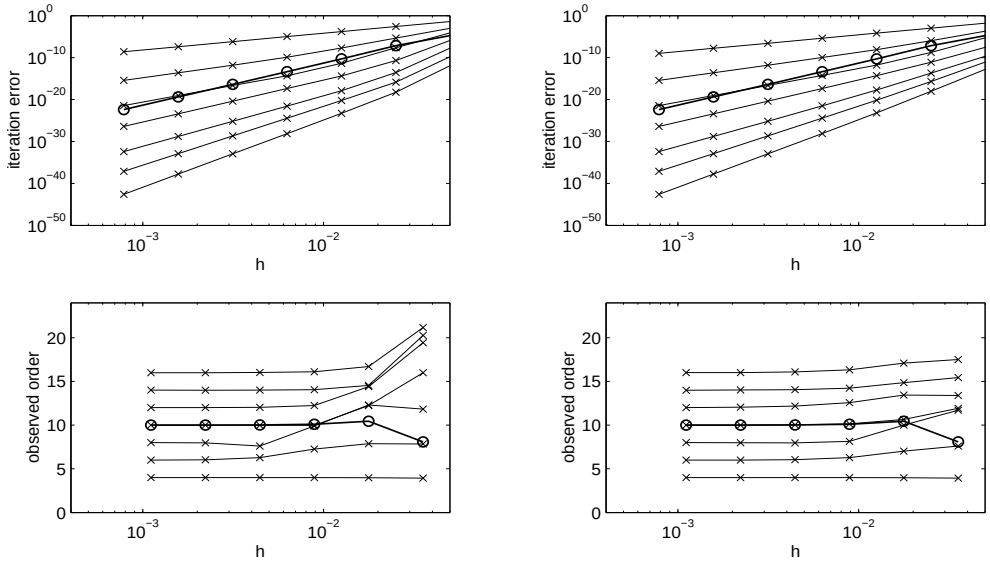

Figure 2.26: ISDeC, $m = 5$ Gaussian points, based on Yoshida for Kepler problem.

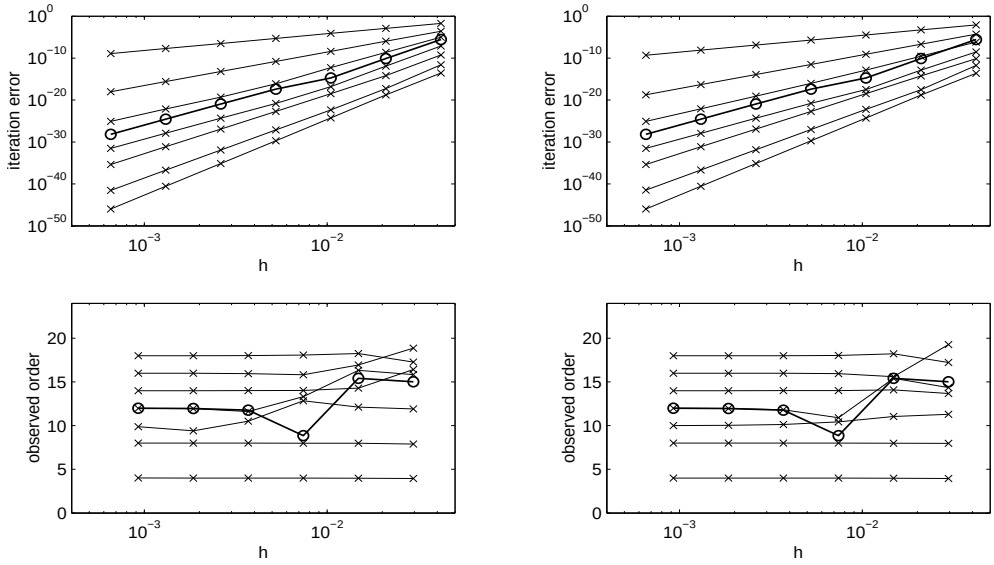

Figure 2.27: ISDeC, $m = 6$ Gaussian points, based on Yoshida for Kepler problem.

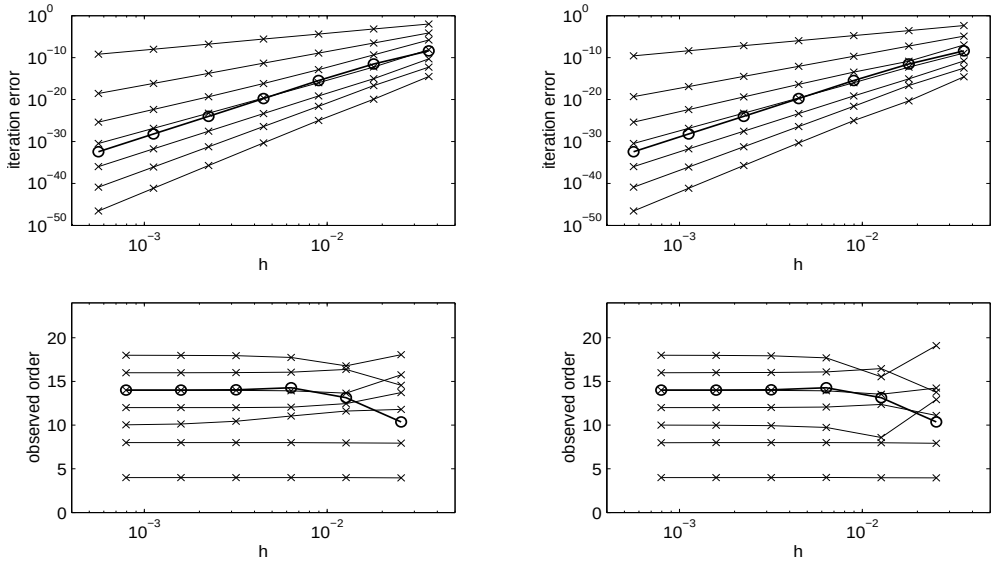

Figure 2.28: ISDeC, $m = 7$ Gaussian points, based on Yoshida for Kepler problem.

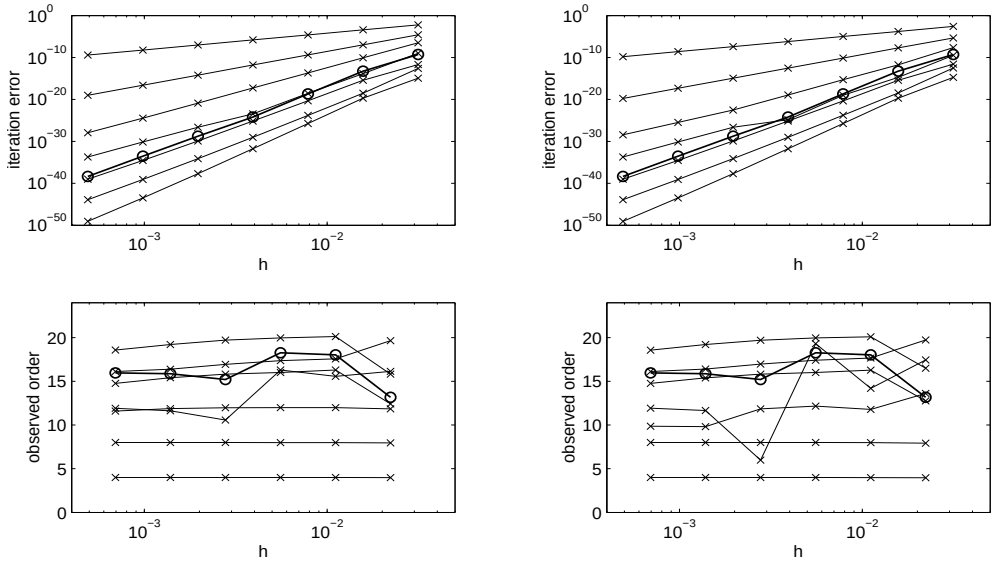

Figure 2.29: Yoshida, Gauss, $m = 8$

Figure 2.30: ISDeC, $m = 8$ Gaussian points, based on Yoshida for Kepler problem.

As a last example for ISDeC with a high-order composition method as basic method applied to the Hamiltonian system (2.1), we consider McLachlan's method (cf. Section 1.3) based on the symplectic Euler methods (1.11) and (1.12). We construct a symmetric fourth-order method Ψ for the solution of the neighboring problems (1.2) as described in Section 1.3. In the following figures, the left

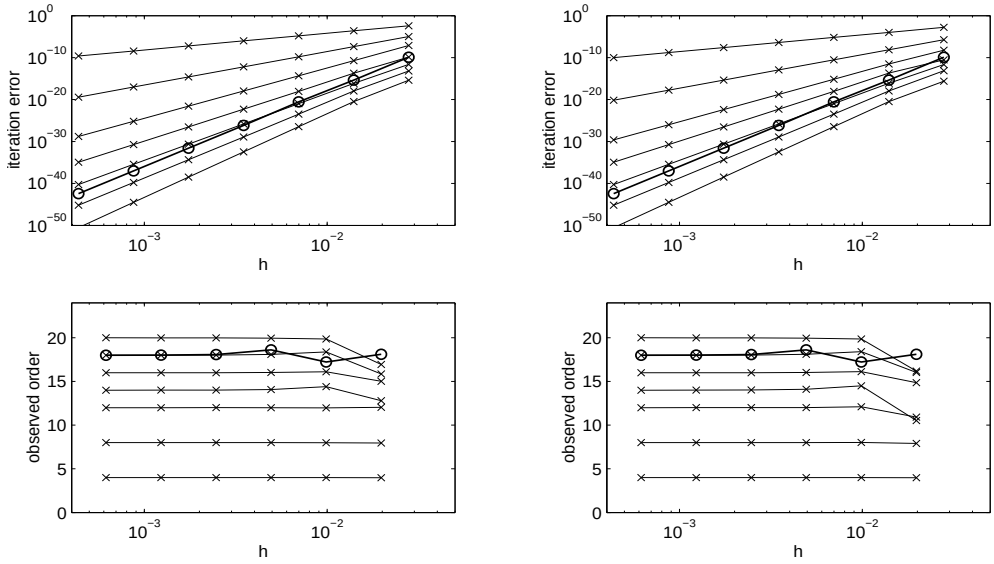

Figure 2.31: ISDeC, $m = 9$ Gaussian points, based on Yoshida for Kepler problem.

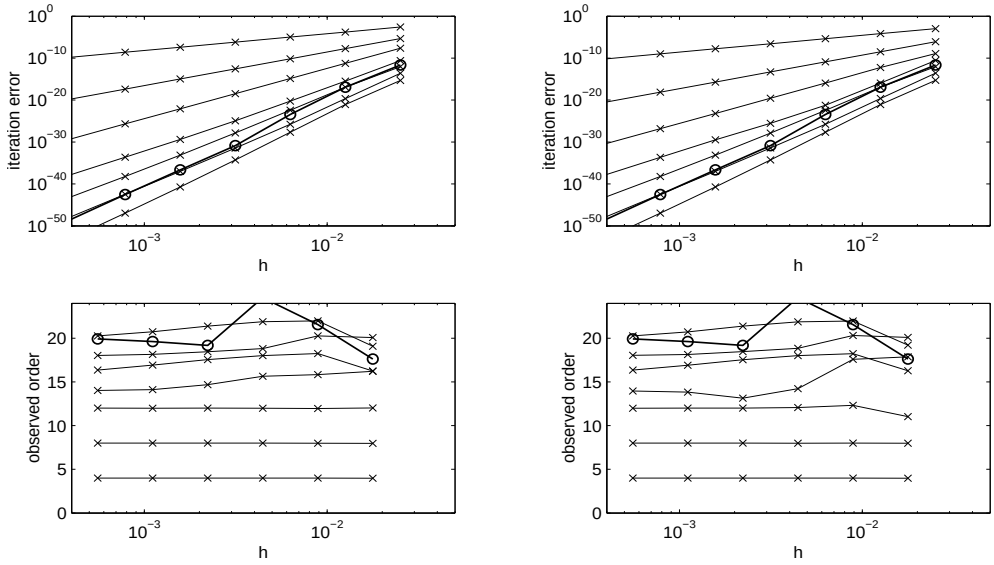

Figure 2.32: ISDeC, $m = 10$ Gaussian points, based on Yoshida for Kepler problem.

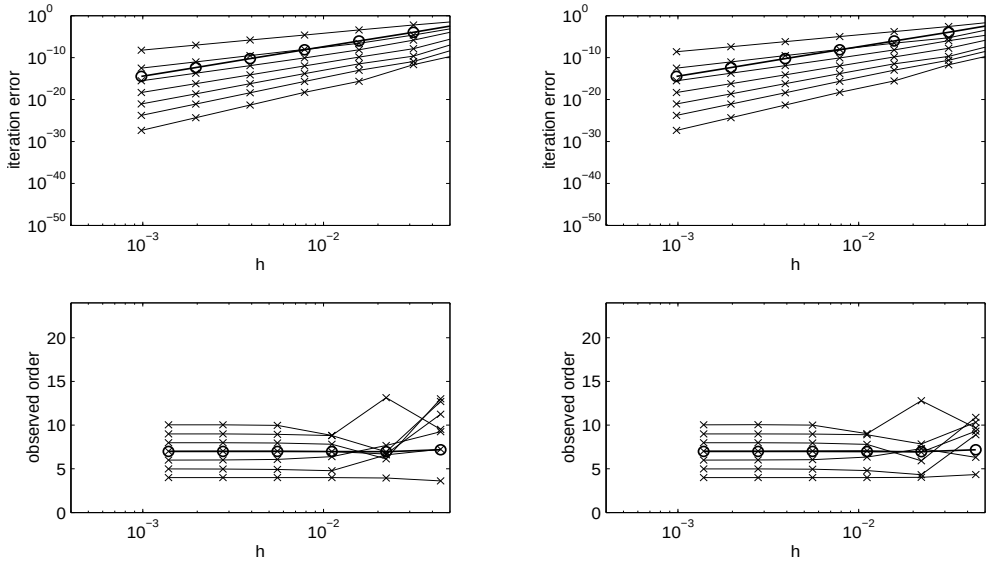

Figure 2.33: ISDeC, $m = 4$ Radau points, based on Yoshida for Kepler problem.

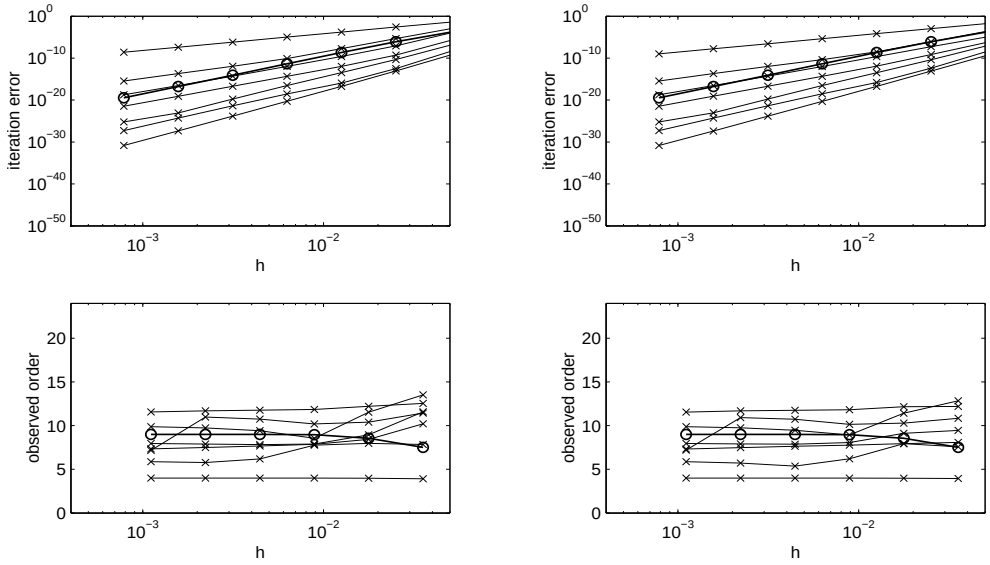

Figure 2.34: ISDeC, $m = 5$ Radau points, based on Yoshida for Kepler problem.

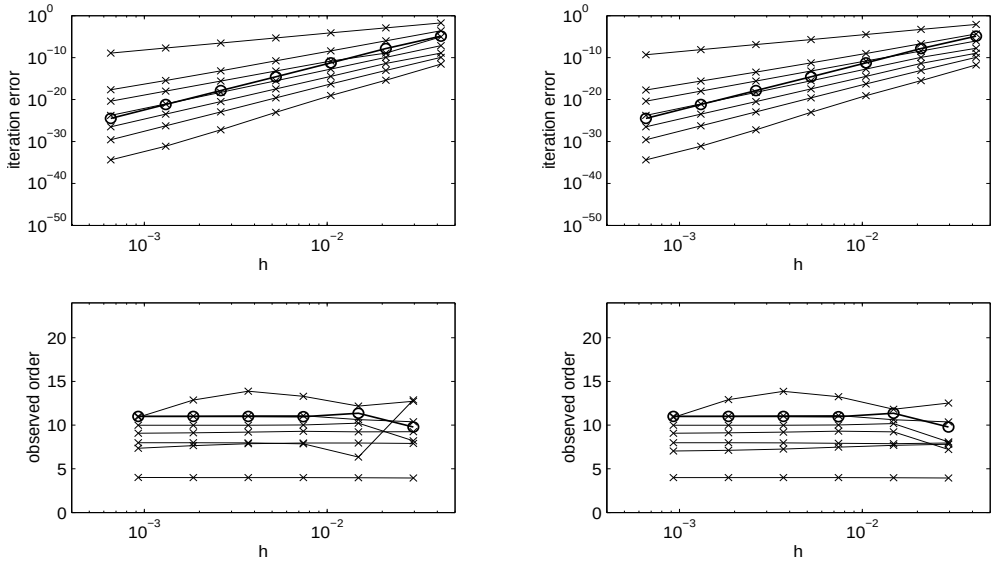

Figure 2.35: ISDeC, $m = 6$ Radau points, based on Yoshida for Kepler problem.

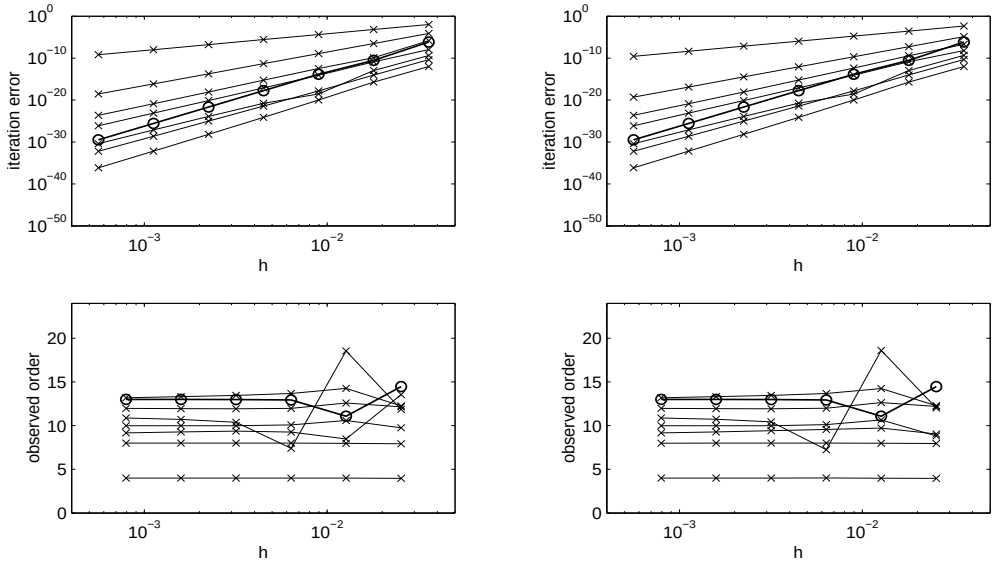

Figure 2.36: ISDeC, $m = 7$ Radau points, based on Yoshida for Kepler problem.

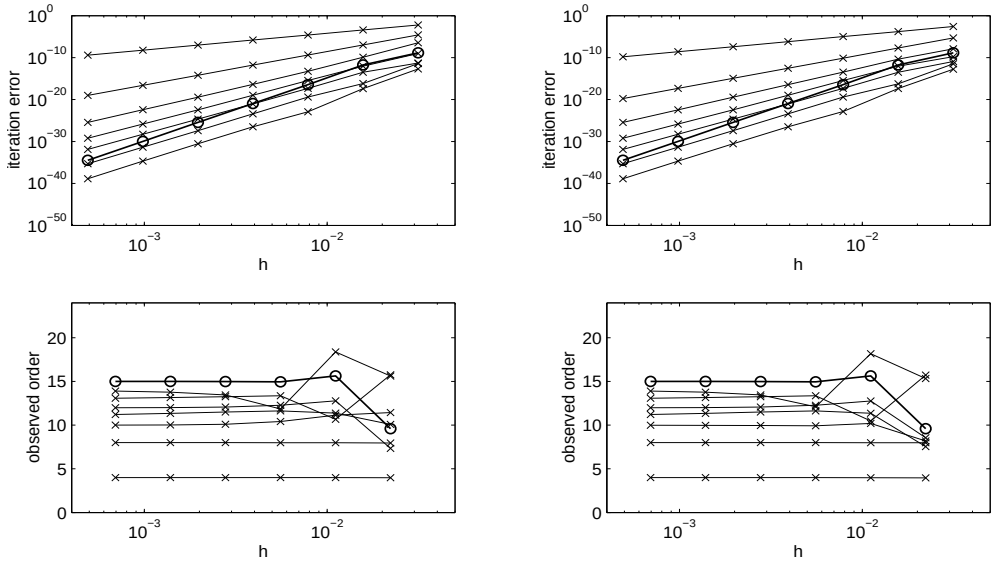

Figure 2.37: ISDeC, $m = 8$ Radau points, based on Yoshida for Kepler problem.

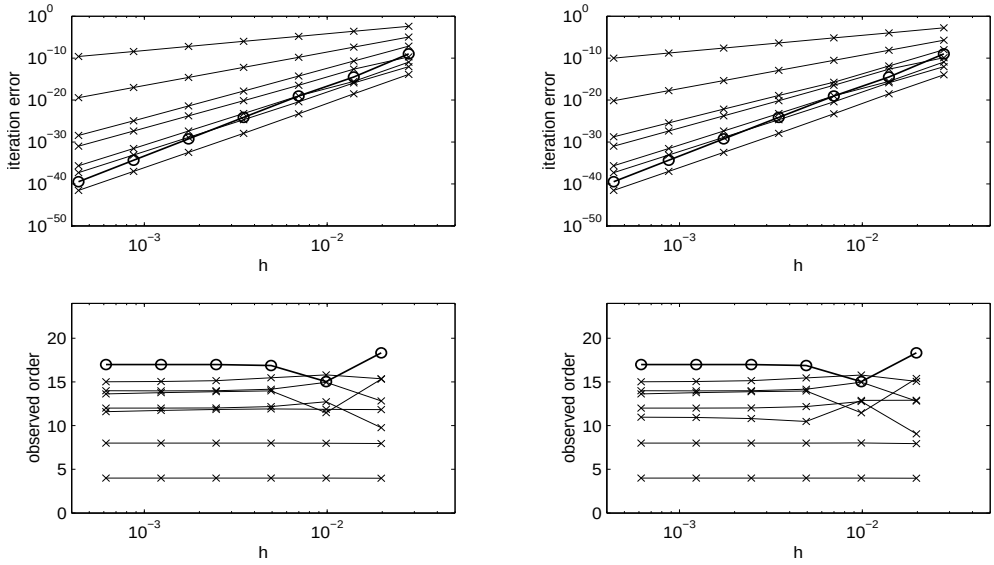

Figure 2.38: ISDeC, $m = 9$ Radau points, based on Yoshida for Kepler problem.

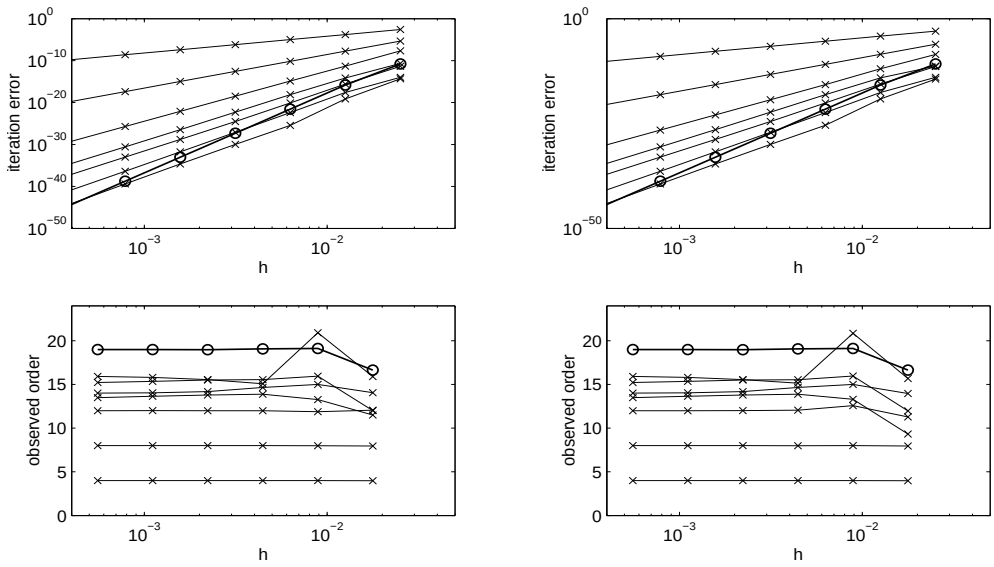

Figure 2.39: ISDeC, $m = 10$ Radau points, based on Yoshida for Kepler problem.

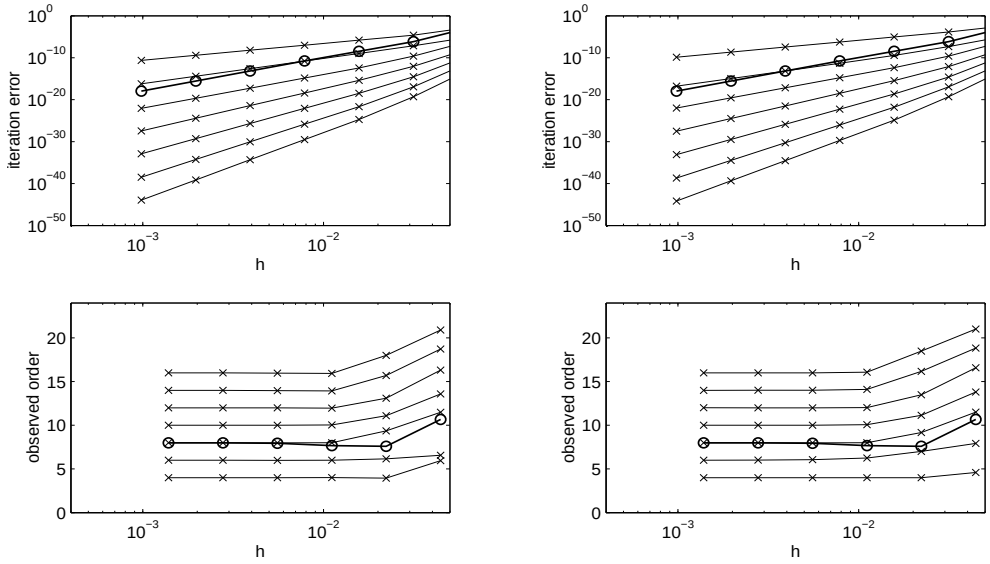

Figure 2.40: ISDeC, $m = 4$ Gaussian points, based on McLachlan for Kepler problem.

columns refer to the scheme as defined by (1.21), while for the right columns, the results for the dual methods are given, where the roles of ϕ and ϕ^* are exchanged. The order sequences given in Tables 2.40– 2.53 for McLachlan's method are the same as those observed for Suzuki's and Yoshida's methods.

Remark: Acceleration techniques for geometric integrators are also considered in [6]. Particularly, the conservation properties of the iterates obtained by *extrap-*

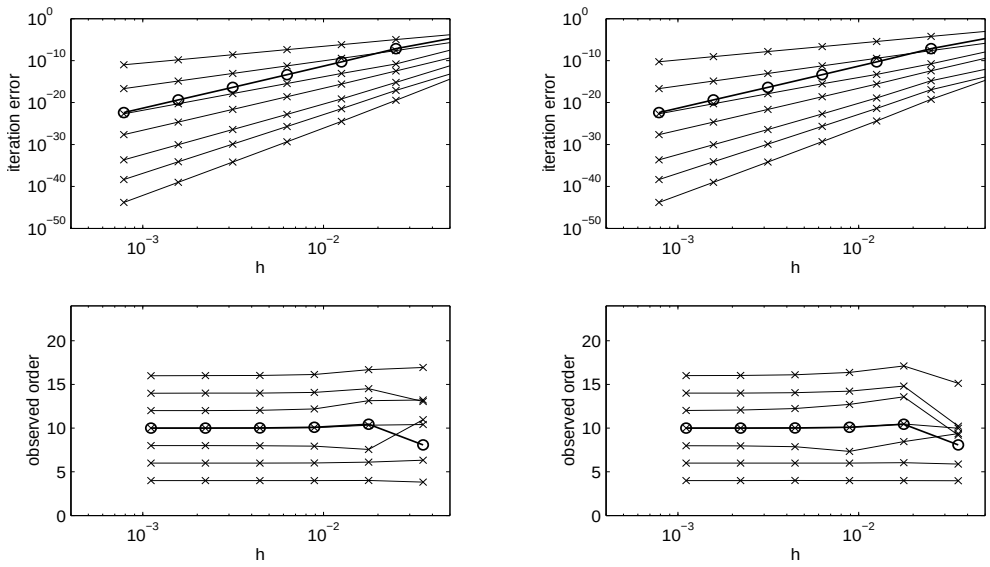

Figure 2.41: ISDeC, $m = 5$ Gaussian points, based on McLachlan for Kepler problem.

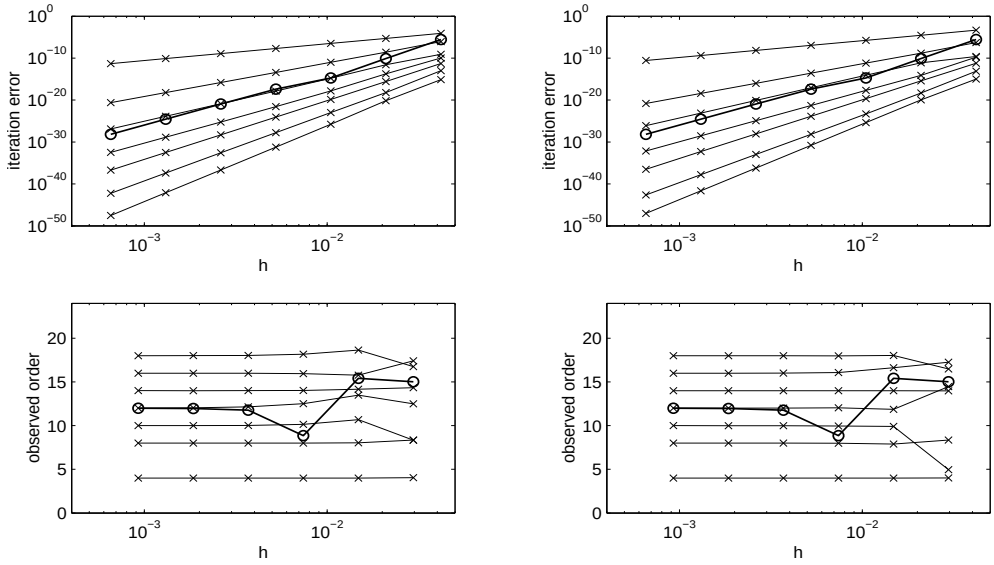

Figure 2.42: ISDeC, $m = 6$ Gaussian points, based on McLachlan for Kepler problem.

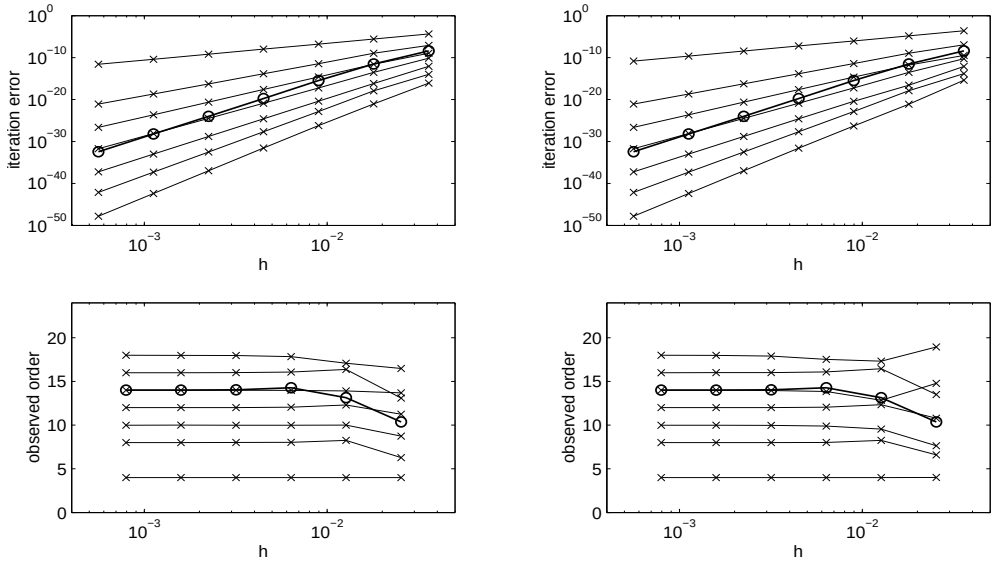

Figure 2.43: ISDeC, $m = 7$ Gaussian points, based on McLachlan for Kepler problem.

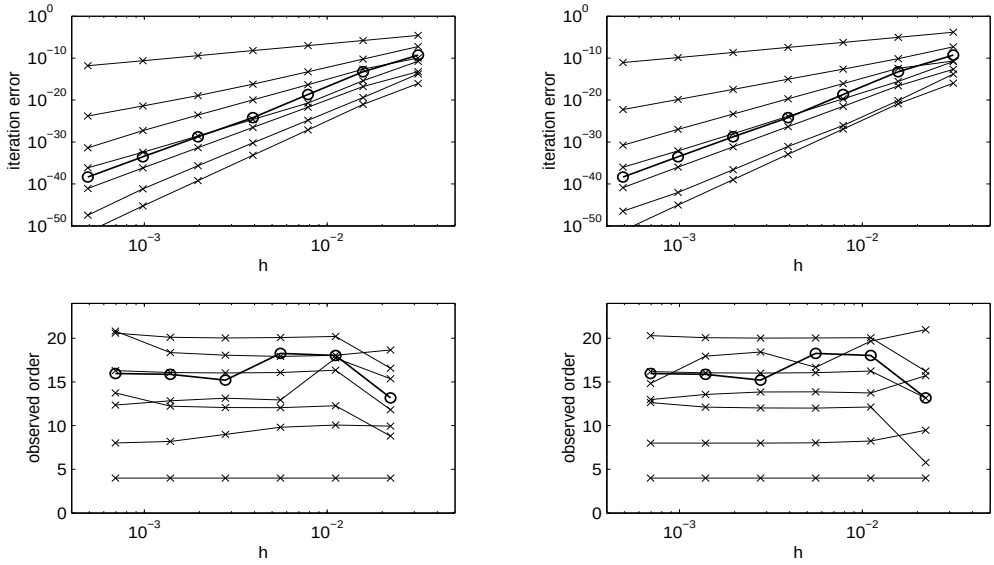

Figure 2.44: ISDeC, $m = 8$ Gaussian points, based on McLachlan for Kepler problem.

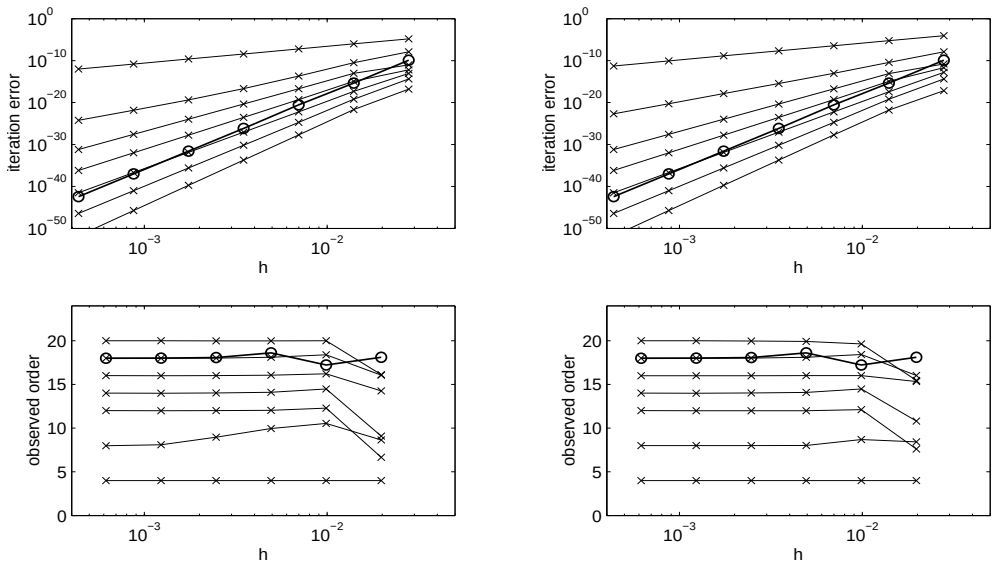

Figure 2.45: ISDeC, $m = 9$ Gaussian points, based on McLachlan for Kepler problem.

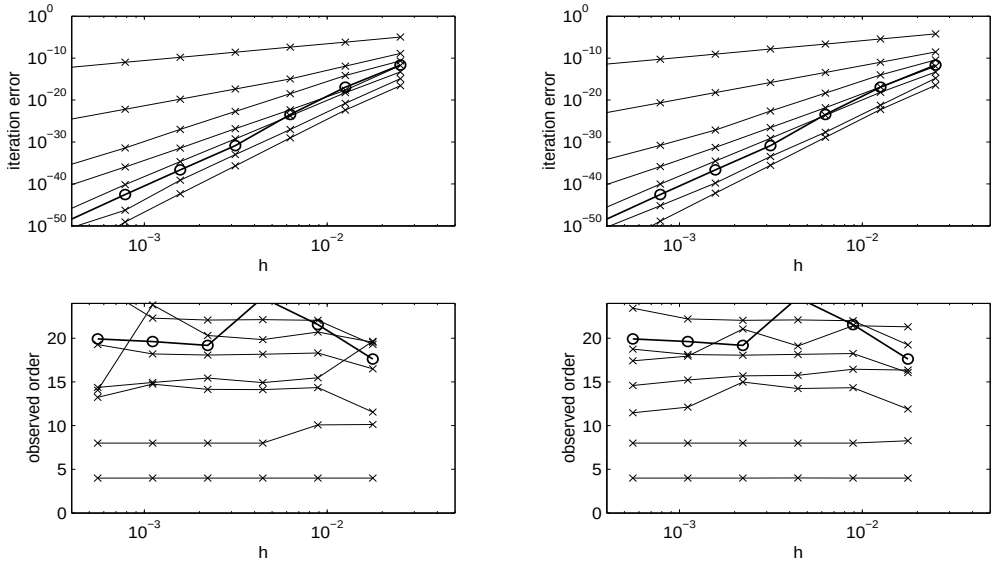

Figure 2.46: ISDeC, $m = 10$ Gaussian points, based on McLachlan for Kepler problem.

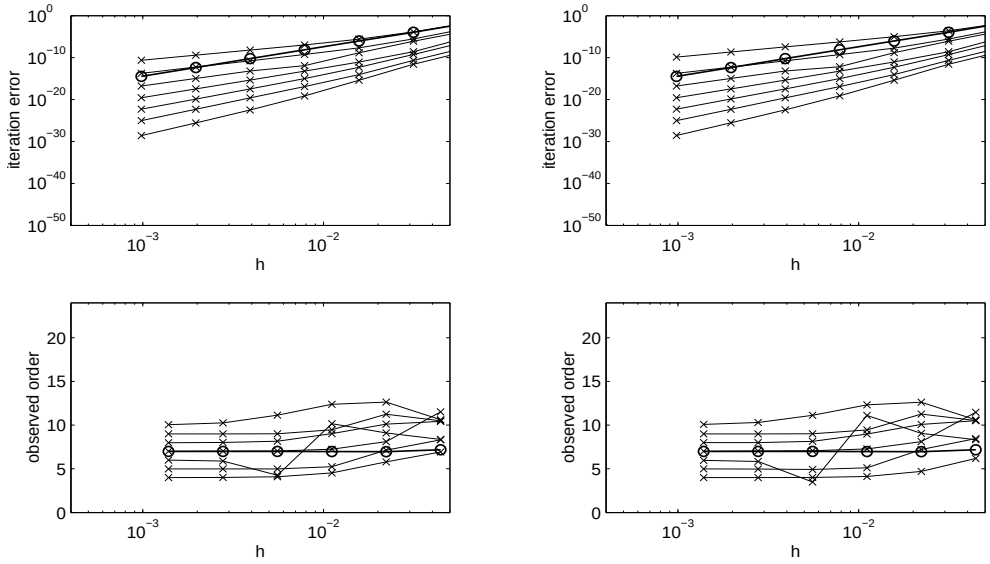

Figure 2.47: ISDeC, $m = 4$ Radau points, based on McLachlan for Kepler problem.

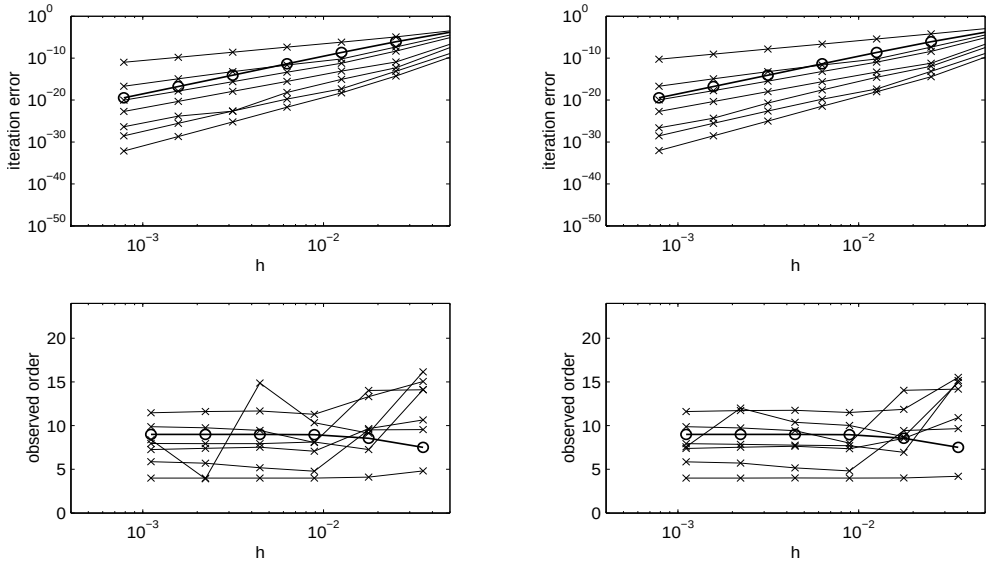

Figure 2.48: ISDeC, $m = 5$ Radau points, based on McLachlan for Kepler problem.

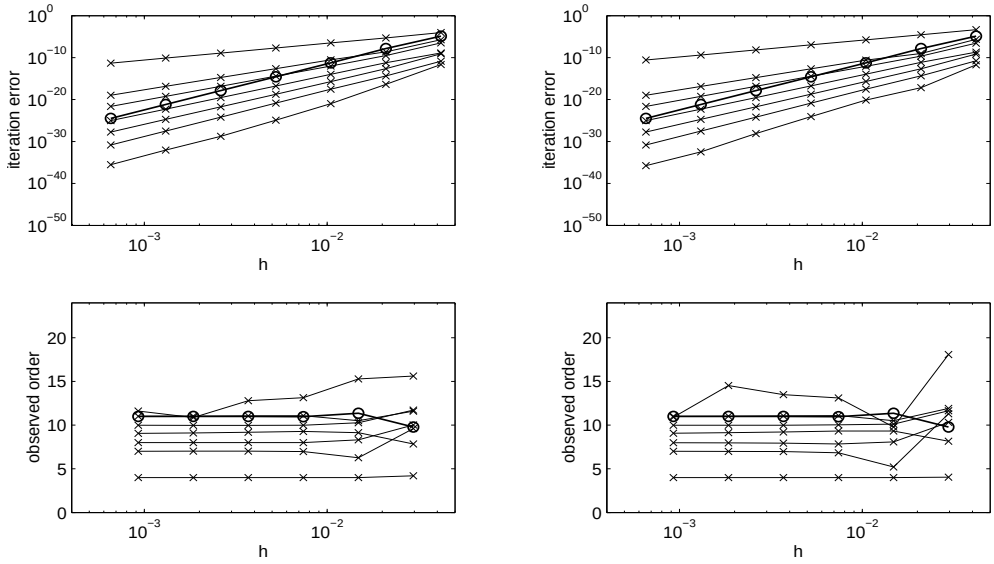

Figure 2.49: ISDeC, $m = 6$ Radau points, based on McLachlan for Kepler problem.

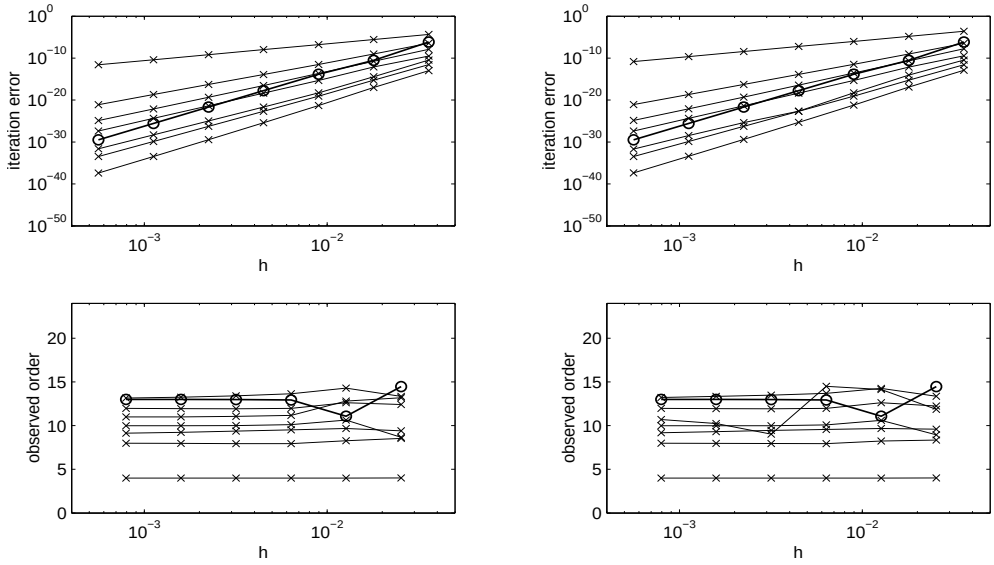

Figure 2.50: ISDeC, $m = 7$ Radau points, based on McLachlan for Kepler problem.

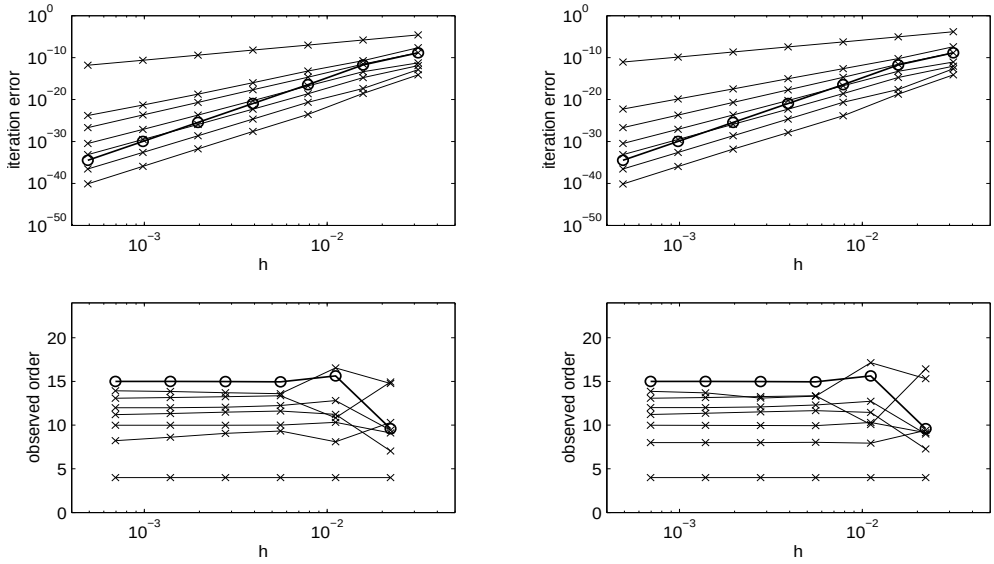

Figure 2.51: ISDeC, $m = 8$ Radau points, based on McLachlan for Kepler problem.

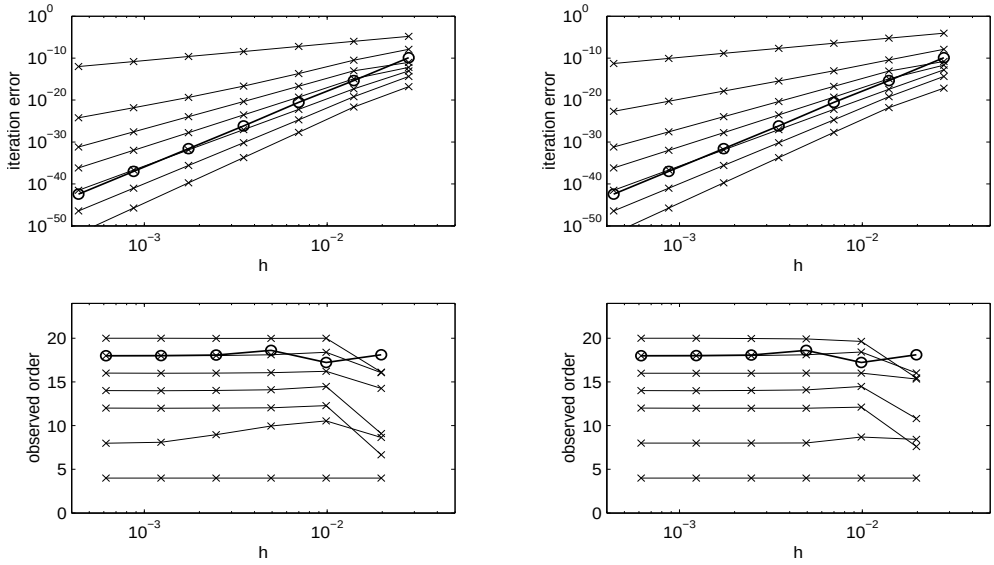

Figure 2.52: ISDeC, $m = 9$ Radau points, based on McLachlan for Kepler problem.

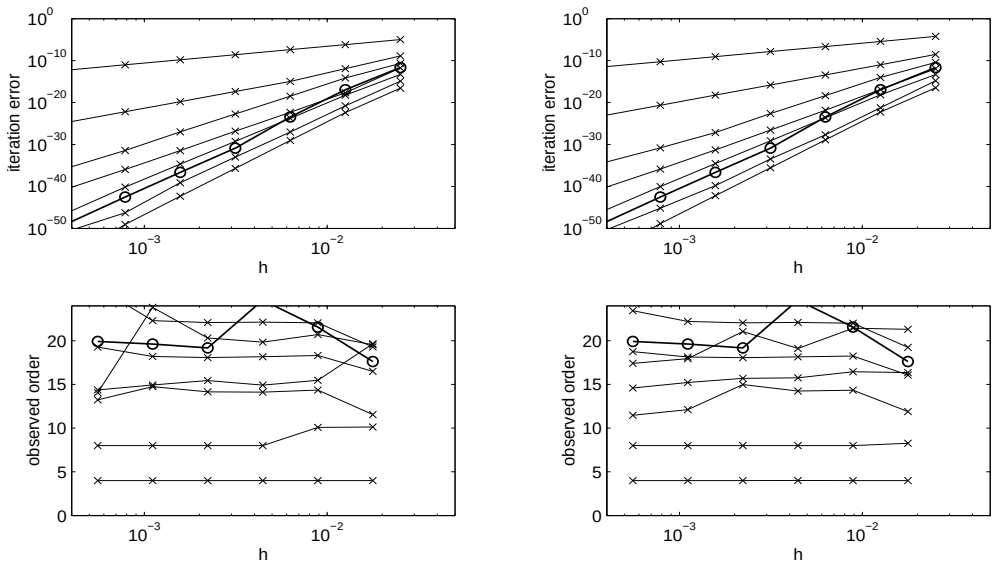

Figure 2.53: ISDeC, $m = 10$ Radau points, based on McLachlan for Kepler problem.

olation from Yoshida's method are considered. It turns out that the favorable geometric properties of the basic method are not retained, the invariants are only conserved up to terms of a certain asymptotic order. The approximation quality is quite high, however. Consequently, the situation is quite similar to the one discussed here.

2.2 The Exponential Midpoint Rule

In this section, we consider ISDeC based on the exponential midpoint rule, which is a second order method defined for linear homogeneous ODEs

$$\dot{y}(t) = A(t)y(t) \tag{2.4}$$

by

$$\Phi_{t,h}(y) = \exp\left(hA(t + h/2)\right) y. \tag{2.5}$$

If ISDeC based on the exponential midpoint rule is applied to smooth problems, the same behavior as for the Störmer/Verlet method can be observed. We demonstrate this for an example taken from [7], where

$$A(t) = \begin{pmatrix} 0 & t & -0.4\cos(t) \\ -t & 0 & 0.1t \\ 0.4\cos(t) & -0.1t & 0 \end{pmatrix}. \tag{2.6}$$

The system matrix is skew-symmetric, and the flow of the differential equation preserves the Euclidean norm. Consequently, for our initial values

$$y(0) = (0, 0, 1)^T,$$

the exact solution stays on the unit sphere.

For our numerical experiments, we consider the solution on the interval $[t_0, t_{\text{end}}] = [0, 5]$ and record the error at $t_{\text{end}} = 5$. Since we do not have two different versions of the basic method as in the case of Störmer/Verlet, in the figures below we give the results for different degrees m of the interpolation polynomial for ISDeC in one figure, the left column referring to the lower degree. Again, the top row of each figure gives the iteration error of the respective ISDeC iterates, while the bottom row shows the corresponding empirical orders of the iteration errors.

To summarize, the behavior for ISDeC based on the exponential midpoint rule is the same as for Störmer/Verlet. The order of the iteration error increases in steps of two for Gaussian points, while the speed of this convergence acceleration is slower for Radau points. The highest attainable convergence order as compared with the true solution is limited by the accuracy of the fixed point p^*, which is a collocation solution at Gaussian points and Radau points, respectively. The results are given in Figures 2.54 to 2.59.

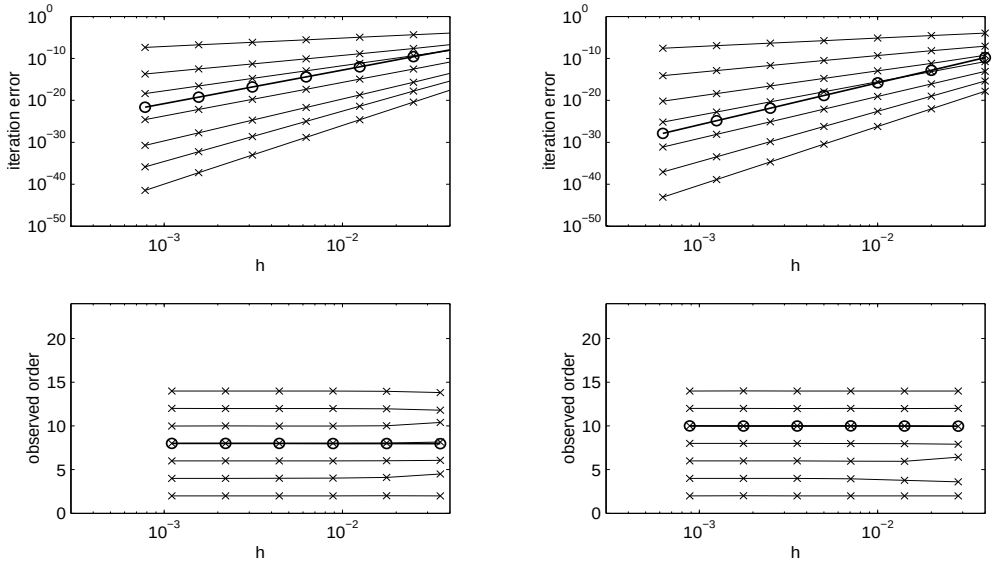

Figure 2.54: ISDeC, $m = 4$ and $m = 5$ Gaussian points, based on EMR for (2.6).

The geometric properties of the ISDeC iterates based on the exponential midpoint rule when applied to (2.6) are comparable to the results for the Störmer/Verlet method applied to Hamiltonian systems. The basic approximation shares the property of the exact flow that the Euclidean norm of the solution is preserved.

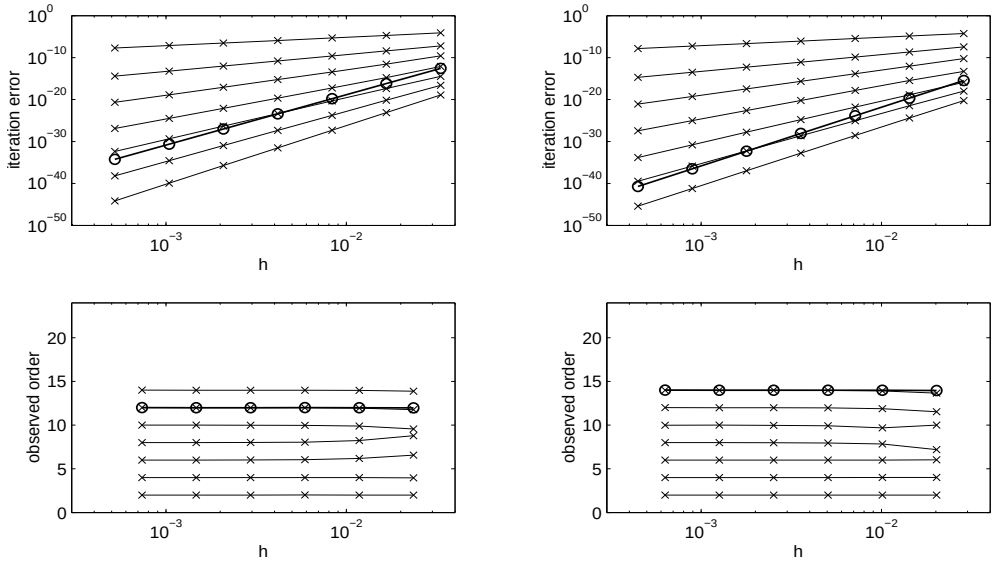

Figure 2.55: ISDeC, $m = 6$ and $m = 7$ Gaussian points, based on EMR for (2.6).

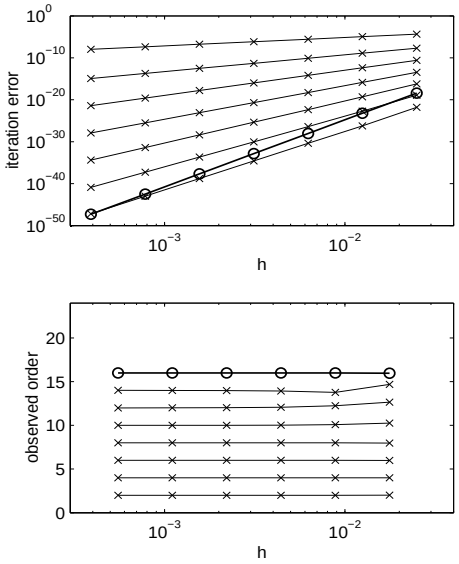

Figure 2.56: ISDeC, $m = 8$ Gaussian points, based on EMR for (2.6).

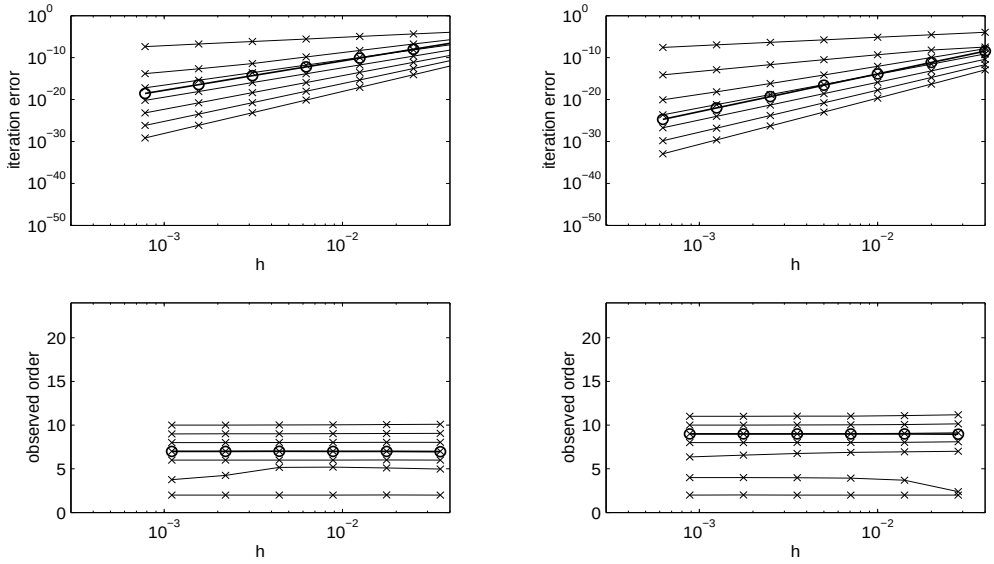

Figure 2.57: ISDeC, $m = 4$ and $m = 5$ Radau points, based on EMR for (2.6).

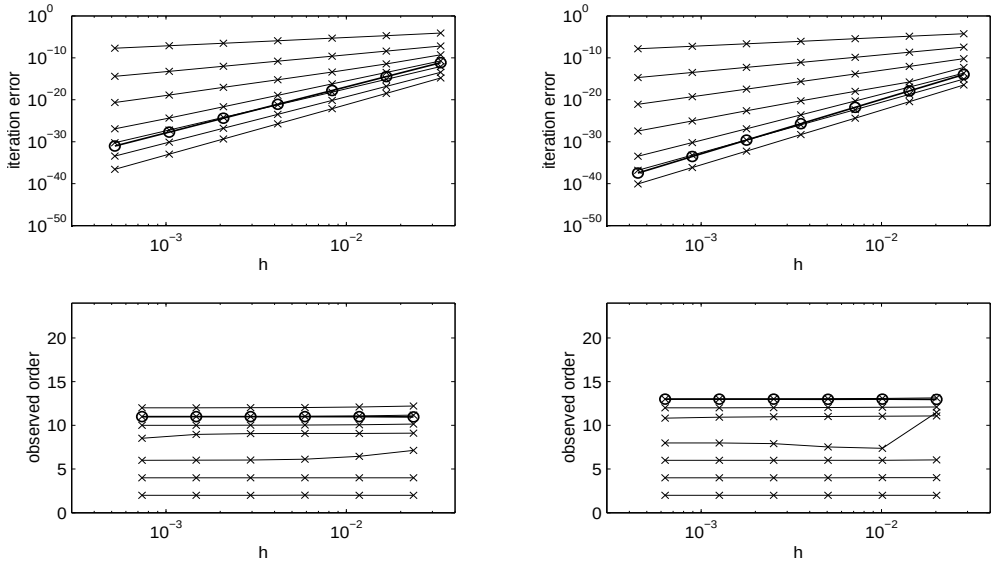

Figure 2.58: ISDeC, $m = 6$ and $m = 7$ Radau points, based on EMR for (2.6).

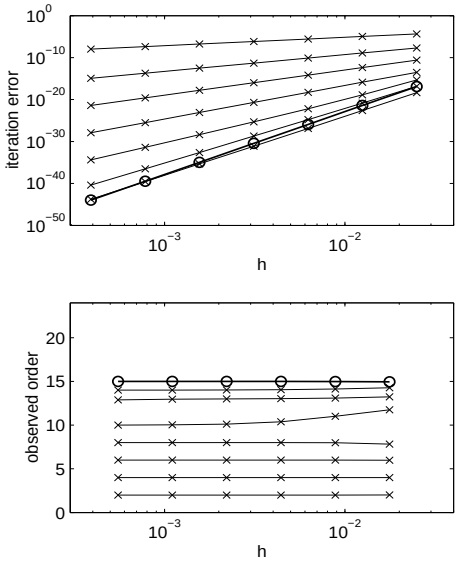

Figure 2.59: ISDeC, $m = 8$ Radau points, based on EMR for (2.6).

This does not hold for the ISDeC iterates in general: The norm is preserved up to terms of the order of the iteration error as compared with the fixed point if Gaussian points are used. This behavior is clearly visible from Table 2.5, where the results for $m = 6$ are given. Note that the fixed point, Gaussian collocation, preserves the Euclidean norm precisely, see [13].

hm	EMR	ISDeC 1	ISDeC 2	ISDeC 3	ISDeC 4	ISDeC 5	ISDeC 6
1/5	0	$3.23 \cdot 10^{-08}$	$1.40 \cdot 10^{-10}$	$3.18 \cdot 10^{-13}$	$1.76 \cdot 10^{-15}$	$8.52 \cdot 10^{-18}$	$3.29 \cdot 10^{-20}$
1/10	0	$2.06 \cdot 10^{-09}$	$1.52 \cdot 10^{-12}$	$8.87 \cdot 10^{-16}$	$2.00 \cdot 10^{-18}$	$1.94 \cdot 10^{-21}$	$1.68 \cdot 10^{-24}$
1/20	0	$1.29 \cdot 10^{-10}$	$2.11 \cdot 10^{-14}$	$3.11 \cdot 10^{-18}$	$2.02 \cdot 10^{-21}$	$4.63 \cdot 10^{-25}$	$9.73 \cdot 10^{-29}$
1/40	0	$8.07 \cdot 10^{-12}$	$3.19 \cdot 10^{-16}$	$1.18 \cdot 10^{-20}$	$1.99 \cdot 10^{-24}$	$1.12 \cdot 10^{-28}$	$5.85 \cdot 10^{-33}$
1/80	0	$5.04 \cdot 10^{-13}$	$4.94 \cdot 10^{-18}$	$4.58 \cdot 10^{-23}$	$1.94 \cdot 10^{-27}$	$2.74 \cdot 10^{-32}$	$3.56 \cdot 10^{-37}$
1/160	0	$3.15 \cdot 10^{-14}$	$7.71 \cdot 10^{-20}$	$1.78 \cdot 10^{-25}$	$1.90 \cdot 10^{-30}$	$6.69 \cdot 10^{-36}$	$2.17 \cdot 10^{-41}$
1/320	0	$1.97 \cdot 10^{-15}$	$1.20 \cdot 10^{-21}$	$6.97 \cdot 10^{-28}$	$1.85 \cdot 10^{-33}$	$1.63 \cdot 10^{-39}$	$1.32 \cdot 10^{-45}$
1/5							
1/10		3.97	6.53	8.49	9.78	12.10	14.26
1/20		4.00	6.17	8.16	9.95	12.03	14.08
1/40		4.00	6.05	8.04	9.99	12.01	14.02
1/80		4.00	6.01	8.01	10.00	12.00	14.00
1/160		4.00	6.00	8.01	10.00	12.00	14.00
1/320		4.00	6.01	8.00	10.00	12.00	14.00

Table 2.5: Error in the norm for ISDeC based on EMR, $m = 6$.

To conclude the discussion of the exponential midpoint rule, we give numerical results for the fourth order composition methods discussed in Section 1.3, where the exponential midpoint rule serves as the basic method Φ. In this case, we consider the Suzuki and the Yoshida method[1]. The order results are again the

[1]Since the exponential midpoint rule itself cannot be written as a composition of first order

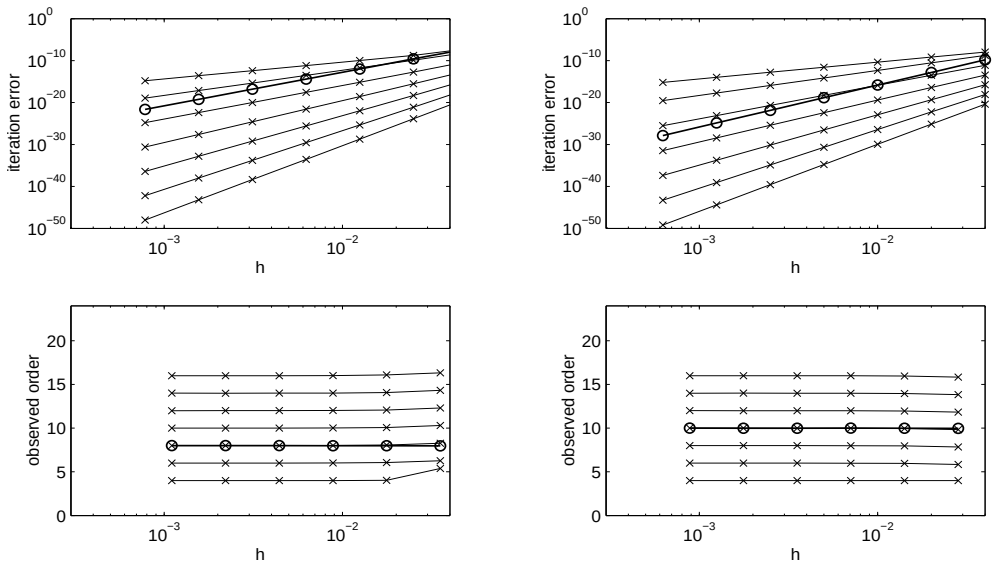

Figure 2.60: ISDeC, $m = 4$ and $m = 5$ Gaussian points, based on Suzuki for (2.6).

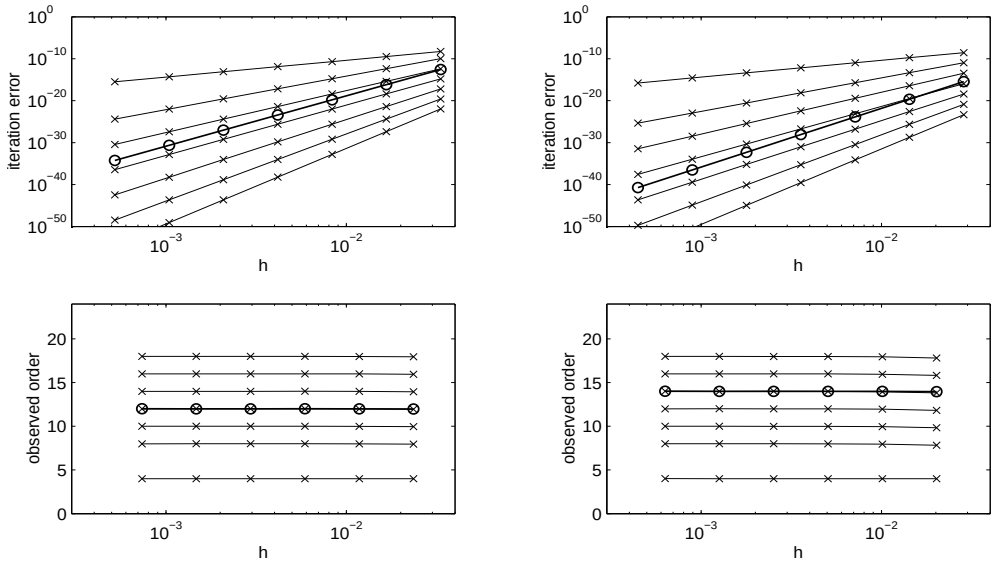

Figure 2.61: ISDeC, $m = 6$ and $m = 7$ Gaussian points, based on Suzuki for (2.6).

same as in Section 2.1, where the Störmer/Verlet method served as the basic method. From the discussion in Section 1.4 we indeed expected the results to be independent from the choice of the basic scheme. The iteration errors and associated orders are given in Figures 2.60 to 2.75.

methods, we have no analogue to McLachlan's method in this section.

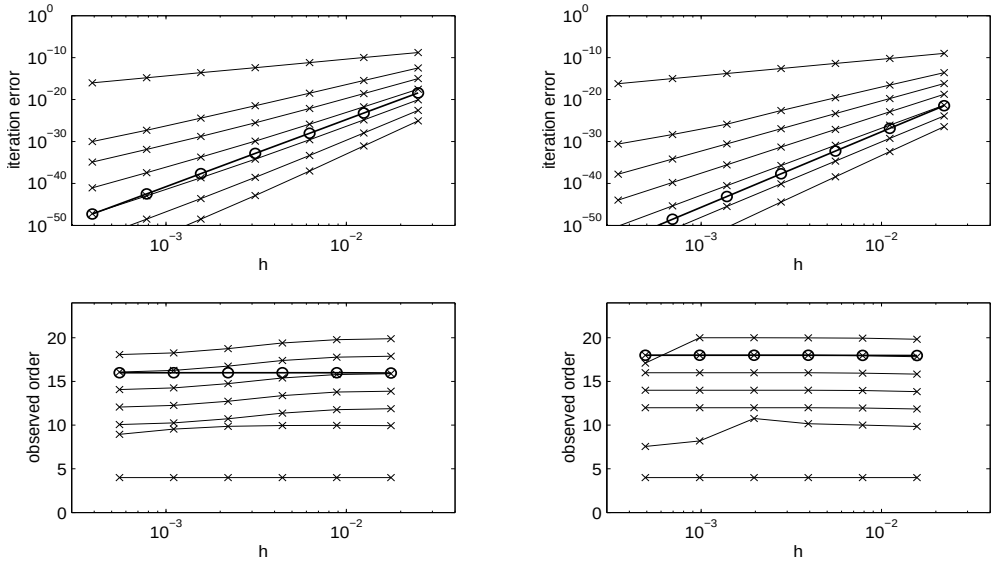

Figure 2.62: ISDeC, $m = 8$ and $m = 9$ Gaussian points, based on Suzuki for (2.6).

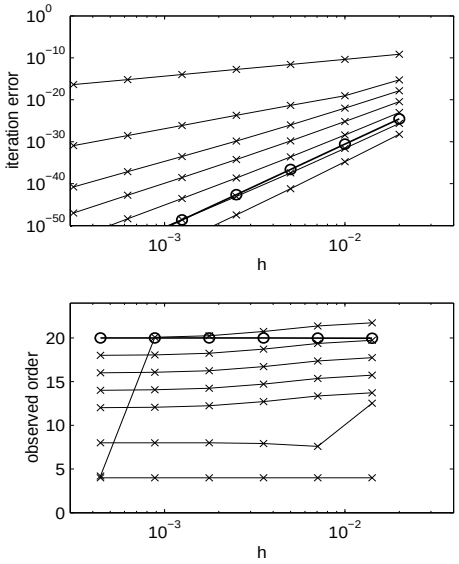

Figure 2.63: ISDeC, $m = 10$ Gaussian points, based on Suzuki for (2.6).

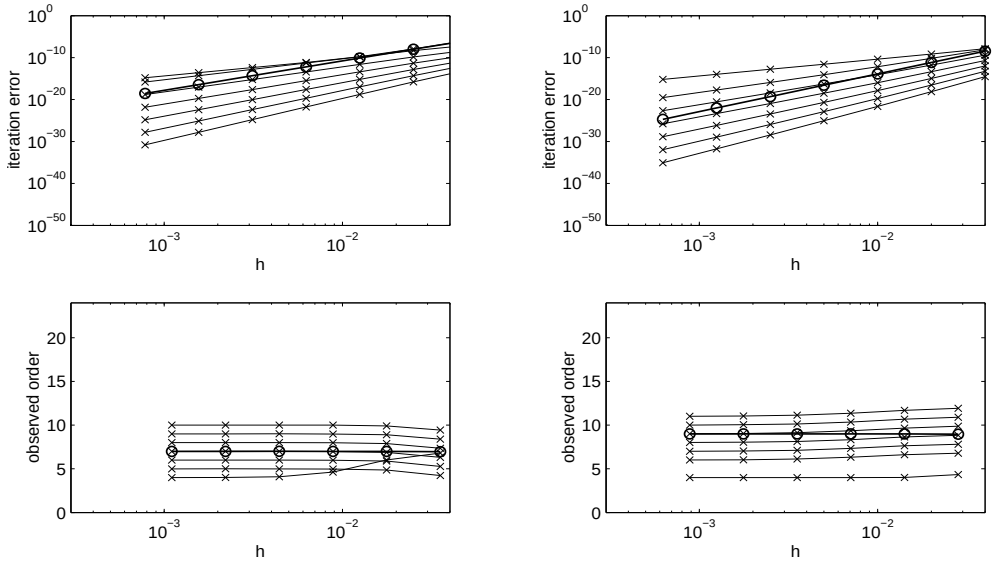

Figure 2.64: ISDeC, $m = 4$ and $m = 5$ Radau points, based on Suzuki for (2.6).

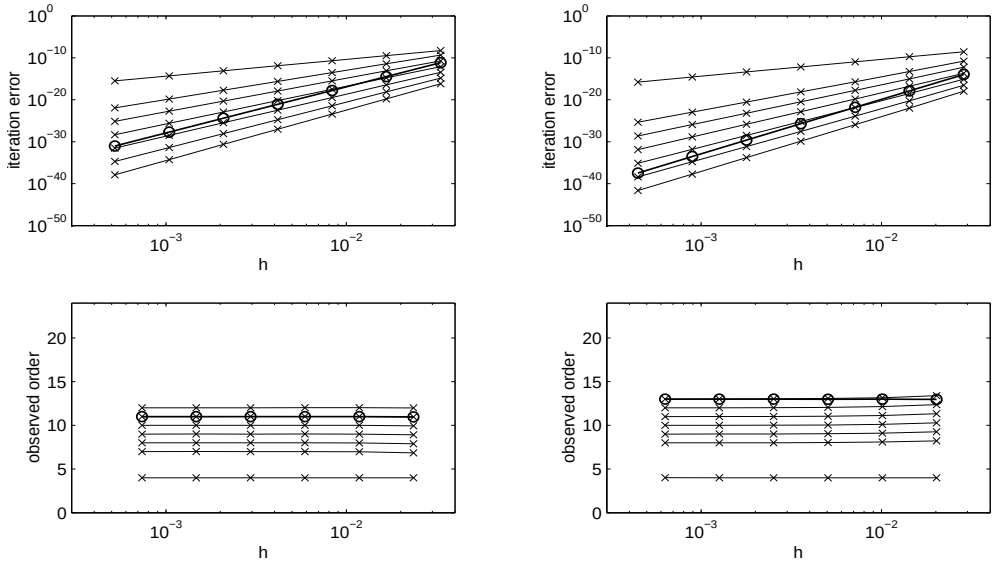

Figure 2.65: ISDeC, $m = 6$ and $m = 7$ Radau points, based on Suzuki for (2.6).

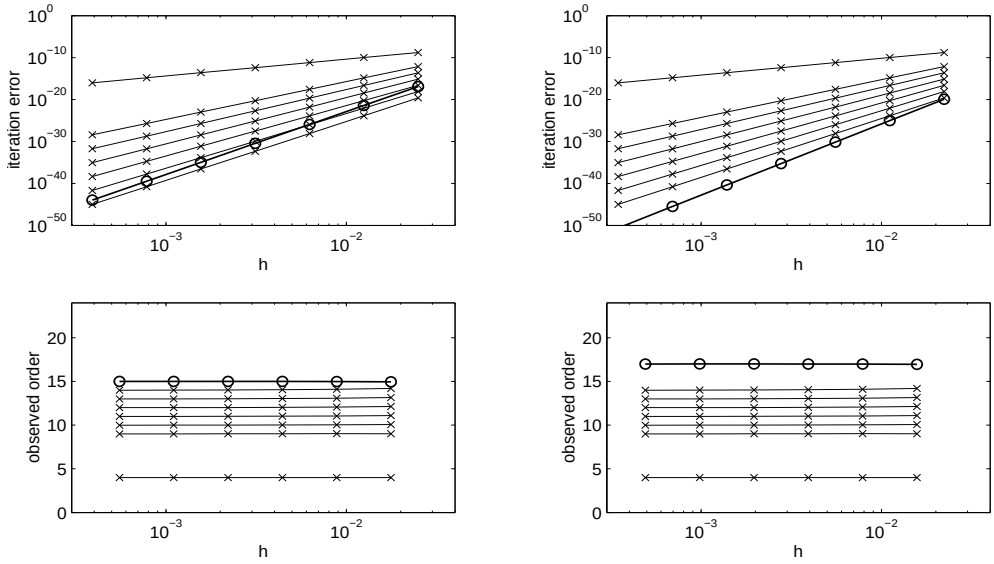

Figure 2.66: ISDeC, $m = 8$ and $m = 9$ Radau points, based on Suzuki for (2.6).

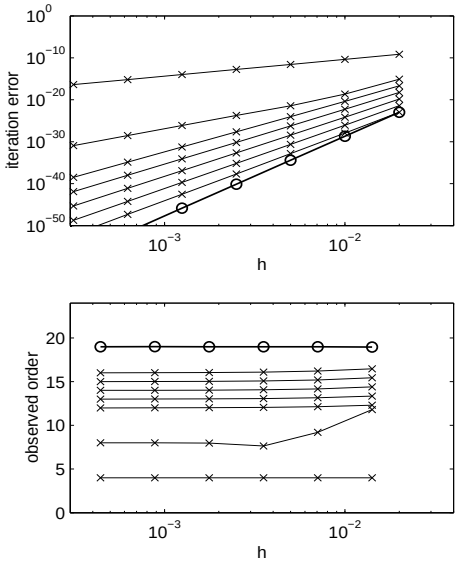

Figure 2.67: ISDeC, $m = 10$ Radau points, based on Suzuki for (2.6).

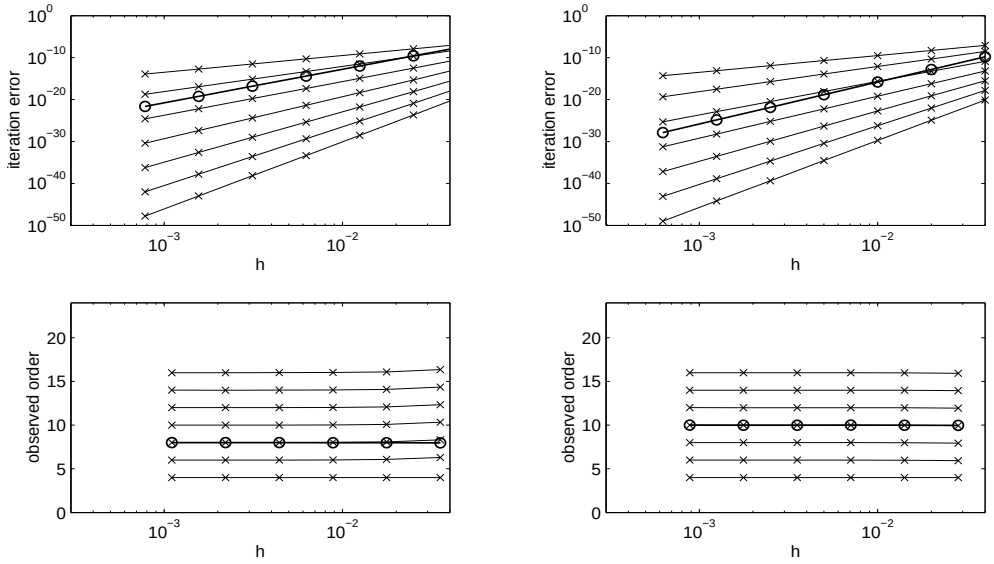

Figure 2.68: ISDeC, $m = 4$ and $m = 5$ Gaussian points, based on Yoshida for (2.6).

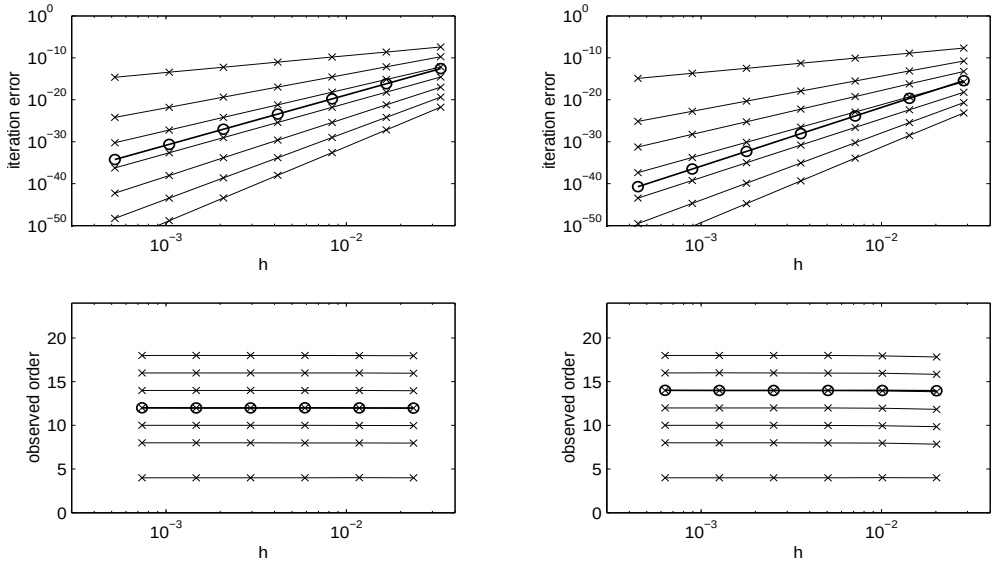

Figure 2.69: ISDeC, $m = 6$ and $m = 7$ Gaussian points, based on Yoshida for (2.6).

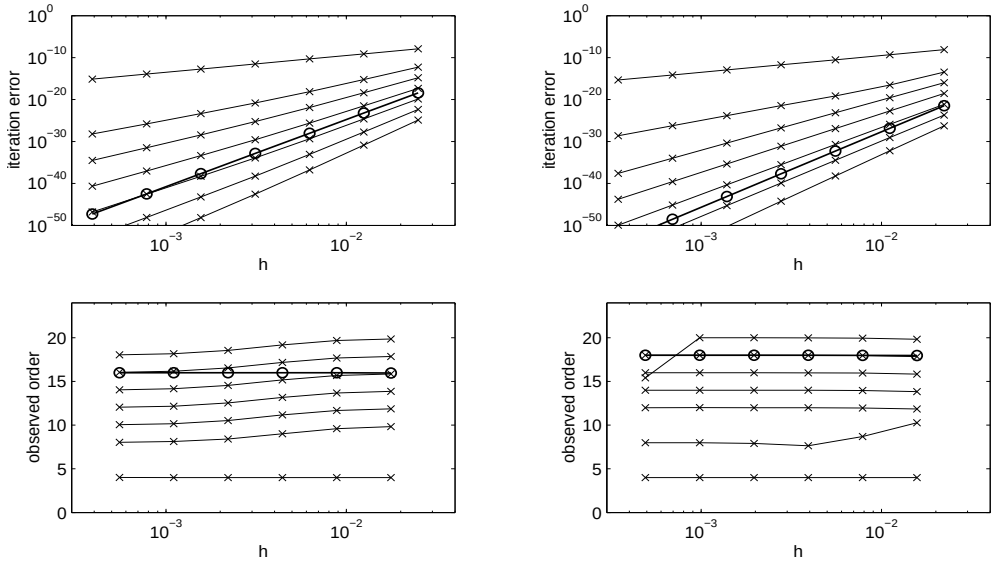

Figure 2.70: ISDeC, $m = 8$ and $m = 9$ Gaussian points, based on Yoshida for (2.6).

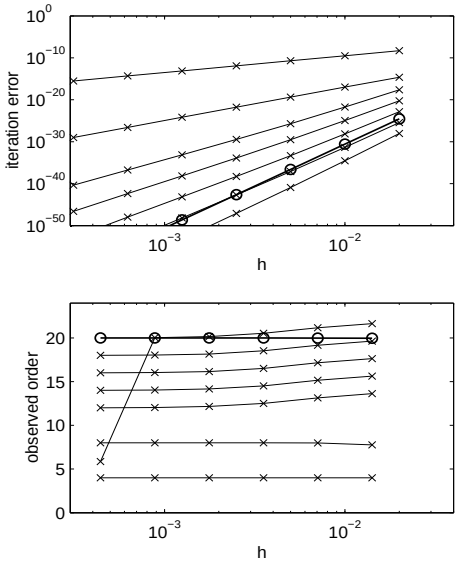

Figure 2.71: ISDeC, $m = 10$ Gaussian points, based on Yoshida for (2.6).

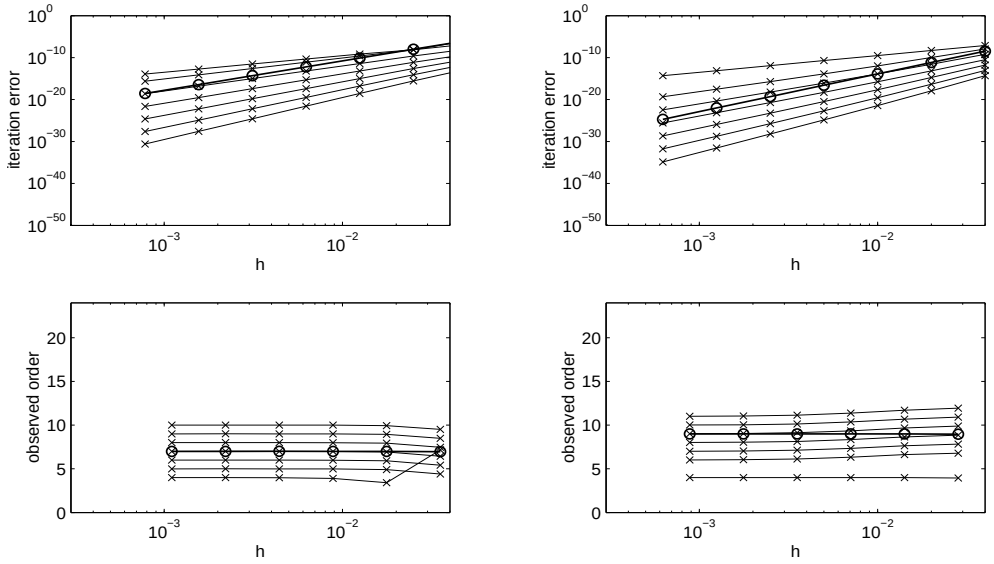

Figure 2.72: ISDeC, $m = 4$ and $m = 5$ Radau points, based on Yoshida for (2.6).

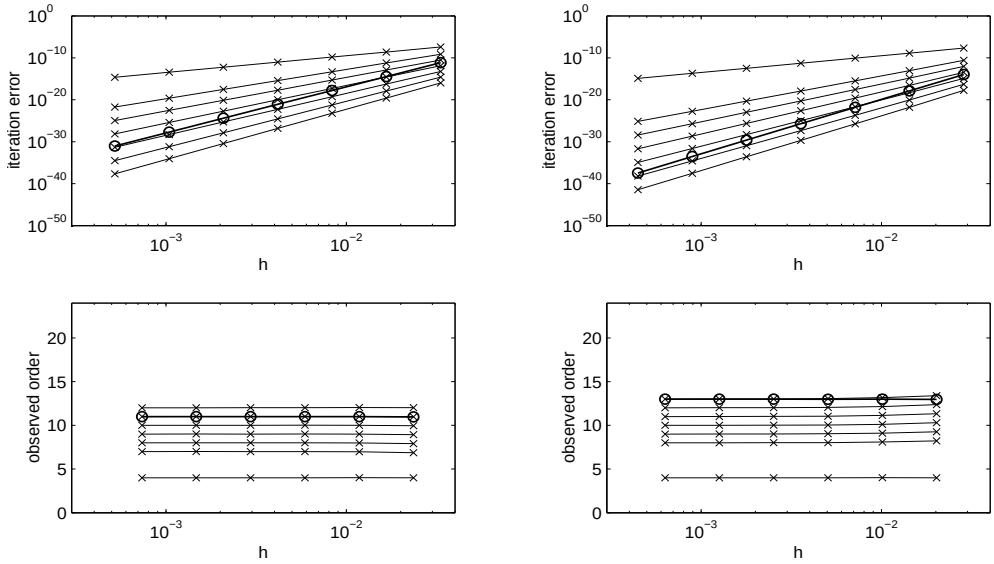

Figure 2.73: ISDeC, $m = 6$ and $m = 7$ Radau points, based on Yoshida for (2.6).

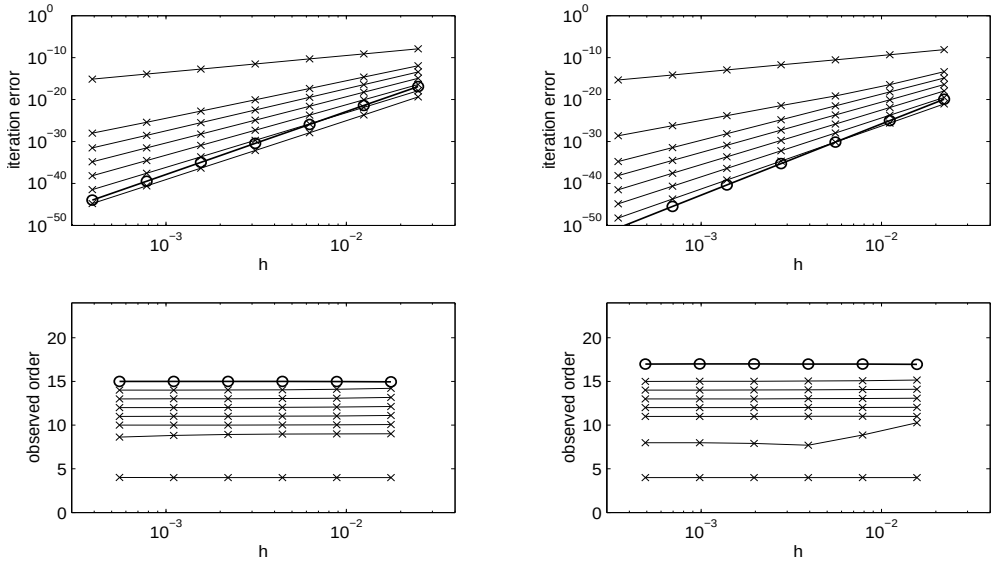

Figure 2.74: ISDeC, $m = 8$ and $m = 9$ Radau points, based on Yoshida for (2.6).

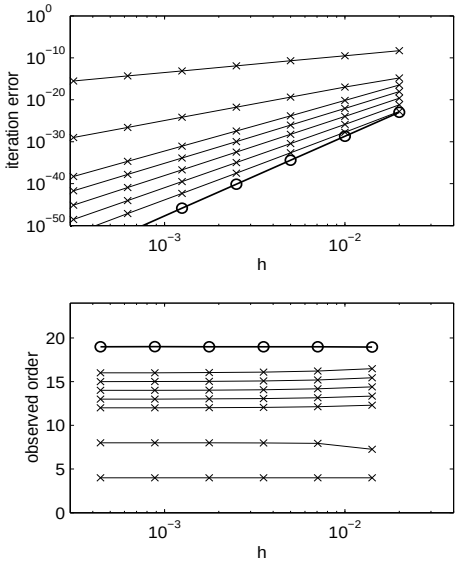

Figure 2.75: ISDeC, $m = 10$ Radau points, based on Yoshida for (2.6).

Finally, we give the errors in the norm of the numerical approximations. Table 2.6 shows that Suzuki's method based on the exponential midpoint rule preserves the norm exactly, thus reflecting an important property of the exact flow. The ISDeC iterates, however, only preserve the Euclidean norm up to terms of the order of the iteration error with respect to the fixed point, Gaussian collocation.

hm	Suzuki	ISDeC 1	ISDeC 2	ISDeC 3	ISDeC 4	ISDeC 5	ISDeC 6
1/5	0	$4.66 \cdot 10^{-11}$	$2.01 \cdot 10^{-13}$	$8.51 \cdot 10^{-16}$	$3.54 \cdot 10^{-18}$	$1.45 \cdot 10^{-20}$	$5.77 \cdot 10^{-23}$
1/10	0	$1.86 \cdot 10^{-13}$	$2.01 \cdot 10^{-16}$	$2.13 \cdot 10^{-19}$	$2.23 \cdot 10^{-22}$	$2.28 \cdot 10^{-25}$	$2.28 \cdot 10^{-28}$
1/20	0	$7.31 \cdot 10^{-16}$	$1.97 \cdot 10^{-19}$	$5.24 \cdot 10^{-23}$	$1.37 \cdot 10^{-26}$	$3.50 \cdot 10^{-30}$	$8.78 \cdot 10^{-34}$
1/40	0	$2.86 \cdot 10^{-18}$	$1.93 \cdot 10^{-22}$	$1.28 \cdot 10^{-26}$	$8.37 \cdot 10^{-31}$	$5.36 \cdot 10^{-35}$	$3.36 \cdot 10^{-39}$
1/80	0	$1.12 \cdot 10^{-20}$	$1.89 \cdot 10^{-25}$	$3.13 \cdot 10^{-30}$	$5.11 \cdot 10^{-35}$	$8.18 \cdot 10^{-40}$	$1.28 \cdot 10^{-44}$
1/160	0	$4.37 \cdot 10^{-23}$	$1.84 \cdot 10^{-28}$	$7.65 \cdot 10^{-34}$	$3.12 \cdot 10^{-39}$	$1.25 \cdot 10^{-44}$	$4.89 \cdot 10^{-50}$
1/320	0	$1.71 \cdot 10^{-25}$	$1.80 \cdot 10^{-31}$	$1.87 \cdot 10^{-37}$	$1.90 \cdot 10^{-43}$	$1.90 \cdot 10^{-49}$	$1.86 \cdot 10^{-55}$
1/5		7.97	9.97	11.96	13.95	15.96	17.95
1/10		7.99	9.99	11.99	13.99	15.99	17.99
1/20		8.00	10.00	12.00	14.00	15.99	18.00
1/40		8.00	10.00	12.00	14.00	16.00	18.00
1/80		8.00	10.00	12.00	14.00	16.00	18.00
1/160		8.00	10.00	12.00	14.00	16.01	18.00
1/320							

Table 2.6: Error in the norm for ISDeC based on Suzuki for (2.6), $m = 6$.

2.3 Exponential Integrators for Unsmooth Problems

In addition to geometric integration for Hamiltonian systems, one major motivation in our search for novel error estimation methods for differential equations with a special structure was the numerical solution of the Schrödinger equation. The characteristic feature of the ODEs related to the method of lines is a steep vector field resulting from the discretization of the unbounded Laplacian in the right-hand side [19]. Unfortunately, we found that defect correction does not work well for unsmooth problems of this type. In this last section, we want to give some examples illustrating that ISDeC works for these problems in principle, yet poses prohibitive restrictions on the step size for time integration.

2.3.1 The Test Equation

The simple test equation

$$\dot{y}(t) = \lambda y(t), \quad y(0) = 1, \tag{2.7}$$

where $\lambda \in \mathbb{C}$, demonstrates the behavior and the range of applicability of ISDeC which is also observed for more complicated equations like the Schrödinger

equation after space (semi-)discretization. The exact solution of (2.7) is

$$y(t) = \mathrm{e}^{\lambda t}.$$

To investigate the behavior of ISDeC, we can use a simplification which is possible due to the simplistic nature of the test equation. To exclude the effects of the choice of the basic method, we use *the exact flow*

$$\Phi_{t,h}(y) = \mathrm{e}^{h\lambda} y \tag{2.8}$$

as the basis for ISDeC. It turns out that even in this scenario, the modulus of λ determines the performance of ISDeC. Clearly, we may conclude from the observations made here, that we cannot expect a more favorable behavior if a numerical approximation is used as the basis for ISDeC. Particularly, if instead of the test equation (2.7) a more general linear system (2.4) is solved, where the system matrix A has large eigenvalues, we cannot hope to obtain better results than for (2.7) where λ is of the order of magnitude of the largest eigenvalues of A.

In Tables 2.7 to 2.9, we give the empirical convergence orders (with respect to the exact solution) of the ISDeC iterates computed at $t_{\text{end}} = 1$, when the exact flow (2.8) is used as the basic solution method and $m = 6$ Gaussian points $\tau_{i,j}$ are used to define (1.3). We compare the behavior for $\lambda = \mathrm{i}$, $\lambda = 100\mathrm{i}$ and $\lambda = 1000\mathrm{i}$. The reason for choosing purely imaginary eigenvalues is the presence of purely imaginary eigenvalues in the Hamiltonian operator in the time-dependent Schrödinger equation after space discretization [19], see also Section 2.3.2. Note however that the results are similar for λ real. We observe that for $\lambda = \mathrm{i}$, the ISDeC iterates indeed show increasing orders of convergence up to the theoretical limit defined by the fixed point of the iteration. Since we are – untypically – using the exact flow as the basic method, the first few iterates show a higher convergence order than should be expected in general, see Table 2.7. If in contrast we consider $\lambda = 100\mathrm{i}$, similar results are observed only when the step sizes are very small. For realistic h, the iteration does not seem to converge, while for very small h the expected behavior that was observed for smooth problems is restored, see Table 2.8. For $\lambda = 1000\mathrm{i}$, we do not observe proper asymptotics at all. In that case, the step size would have to be chosen prohibitively small.

2.3.2 Exponential Splitting for the Schrödinger Equation

As a last result, we demonstrate that the unfavorable behavior which we encountered for the test equation (2.7) for large modulus of λ is also observed for more general systems with large eigenvalues. To this end, we consider the *Schrödinger equation* for one degree of freedom in one space dimension,

$$\mathrm{i}\frac{\partial \psi(t,x)}{\partial t} = \Delta\psi(t,x) + V(x)\psi(t,x), \tag{2.9}$$

hm	exact	ISDeC 1	ISDeC 2	ISDeC 3	ISDeC 4	ISDeC 5	ISDeC 6
1	0	$1.05 \cdot 10^{-09}$	$6.50 \cdot 10^{-11}$	$4.59 \cdot 10^{-13}$	$1.68 \cdot 10^{-13}$	$1.70 \cdot 10^{-13}$	$1.70 \cdot 10^{-13}$
1/2	0	$4.16 \cdot 10^{-12}$	$2.61 \cdot 10^{-13}$	$3.36 \cdot 10^{-16}$	$3.89 \cdot 10^{-17}$	$4.22 \cdot 10^{-17}$	$4.22 \cdot 10^{-17}$
1/4	0	$1.63 \cdot 10^{-14}$	$1.03 \cdot 10^{-15}$	$3.00 \cdot 10^{-19}$	$6.84 \cdot 10^{-21}$	$1.03 \cdot 10^{-20}$	$1.03 \cdot 10^{-20}$
1/8	0	$6.38 \cdot 10^{-17}$	$4.02 \cdot 10^{-18}$	$2.86 \cdot 10^{-22}$	$9.66 \cdot 10^{-25}$	$2.53 \cdot 10^{-24}$	$2.53 \cdot 10^{-24}$
1/16	0	$2.49 \cdot 10^{-19}$	$1.57 \cdot 10^{-20}$	$2.78 \cdot 10^{-25}$	$2.81 \cdot 10^{-27}$	$6.17 \cdot 10^{-28}$	$6.17 \cdot 10^{-28}$
1/32	0	$9.74 \cdot 10^{-22}$	$6.14 \cdot 10^{-23}$	$2.71 \cdot 10^{-28}$	$3.20 \cdot 10^{-30}$	$1.51 \cdot 10^{-31}$	$1.51 \cdot 10^{-31}$
1/64	0	$3.81 \cdot 10^{-24}$	$2.40 \cdot 10^{-25}$	$2.64 \cdot 10^{-31}$	$3.24 \cdot 10^{-33}$	$3.68 \cdot 10^{-35}$	$3.68 \cdot 10^{-35}$
1							
1/2		7.98	7.96	10.42	12.08	11.98	11.98
1/4		8.00	7.99	10.13	12.47	12.00	12.00
1/8		8.00	8.00	10.03	12.79	11.99	11.99
1/16		8.00	8.00	10.01	8.43	12.00	12.00
1/32		8.00	8.00	10.00	9.78	12.00	12.00
1/64		8.00	8.00	10.00	9.95	12.00	12.00

Table 2.7: Convergence of ISDeC applied to (2.7) with $\lambda = \mathrm{i}$, $m = 6$ Gaussian points.

hm	exact	ISDeC 1	ISDeC 2	ISDeC 3	ISDeC 4	ISDeC 5	ISDeC 6
1	0	$9.38 \cdot 10^{+01}$	$4.47 \cdot 10^{+03}$	$1.74 \cdot 10^{+05}$	$6.29 \cdot 10^{+06}$	$2.23 \cdot 10^{+08}$	$7.89 \cdot 10^{+09}$
1/2	0	$5.86 \cdot 10^{+01}$	$1.72 \cdot 10^{+03}$	$3.53 \cdot 10^{+04}$	$5.92 \cdot 10^{+05}$	$8.77 \cdot 10^{+06}$	$1.20 \cdot 10^{+08}$
1/4	0	$1.38 \cdot 10^{+02}$	$9.58 \cdot 10^{+03}$	$4.47 \cdot 10^{+05}$	$1.60 \cdot 10^{+07}$	$4.75 \cdot 10^{+08}$	$1.22 \cdot 10^{+10}$
1/8	0	$2.49 \cdot 10^{+01}$	$3.10 \cdot 10^{+02}$	$2.67 \cdot 10^{+03}$	$1.86 \cdot 10^{+04}$	$1.12 \cdot 10^{+05}$	$6.08 \cdot 10^{+05}$
1/16	0	$5.94 \cdot 10^{-02}$	$2.56 \cdot 10^{-02}$	$2.70 \cdot 10^{-02}$	$2.78 \cdot 10^{-02}$	$2.77 \cdot 10^{-02}$	$2.77 \cdot 10^{-02}$
1/32	0	$7.74 \cdot 10^{-04}$	$5.21 \cdot 10^{-05}$	$1.38 \cdot 10^{-05}$	$1.25 \cdot 10^{-05}$	$1.24 \cdot 10^{-05}$	$1.24 \cdot 10^{-05}$
1/64	0	$3.61 \cdot 10^{-06}$	$2.20 \cdot 10^{-07}$	$5.81 \cdot 10^{-09}$	$3.51 \cdot 10^{-09}$	$3.51 \cdot 10^{-09}$	$3.51 \cdot 10^{-09}$
1							
1/2		0.68	1.38	2.30	3.41	4.67	6.04
1/4		-1.24	-2.48	-3.66	-4.76	-5.76	-6.67
1/8		2.47	4.95	7.39	9.75	12.05	14.29
1/16		8.71	13.56	16.59	19.35	21.95	24.39
1/32		6.26	8.94	10.93	11.12	11.13	11.13
1/64		7.74	7.89	11.21	11.80	11.79	11.79

Table 2.8: Convergence of ISDeC applied to (2.7) with $\lambda = 100\mathrm{i}$, $m = 6$ Gaussian points.

hm	exact	ISDeC 1	ISDeC 2	ISDeC 3	ISDeC 4	ISDeC 5	ISDeC 6
1/5	$5.18 \cdot 10^{-63}$	$8.20 \cdot 10^{+01}$	$1.76 \cdot 10^{+04}$	$2.45 \cdot 10^{+06}$	$3.51 \cdot 10^{+08}$	$5.13 \cdot 10^{+10}$	$7.50 \cdot 10^{+12}$
1/10	$1.91 \cdot 10^{-62}$	$8.84 \cdot 10^{+02}$	$3.91 \cdot 10^{+05}$	$1.16 \cdot 10^{+08}$	$2.62 \cdot 10^{+10}$	$4.86 \cdot 10^{+12}$	$7.78 \cdot 10^{+14}$
1/20	$1.37 \cdot 10^{-62}$	$7.58 \cdot 10^{+02}$	$2.88 \cdot 10^{+05}$	$7.49 \cdot 10^{+07}$	$1.52 \cdot 10^{+10}$	$2.61 \cdot 10^{+12}$	$3.95 \cdot 10^{+14}$
1/40	$1.78 \cdot 10^{-62}$	$7.69 \cdot 10^{+02}$	$2.96 \cdot 10^{+05}$	$7.59 \cdot 10^{+07}$	$1.47 \cdot 10^{+10}$	$2.29 \cdot 10^{+12}$	$3.01 \cdot 10^{+14}$
1/80	$1.55 \cdot 10^{-62}$	$1.04 \cdot 10^{+03}$	$5.40 \cdot 10^{+05}$	$1.87 \cdot 10^{+08}$	$4.87 \cdot 10^{+10}$	$1.02 \cdot 10^{+13}$	$1.77 \cdot 10^{+15}$
1/160	$1.34 \cdot 10^{-62}$	$1.15 \cdot 10^{+03}$	$6.56 \cdot 10^{+05}$	$2.51 \cdot 10^{+08}$	$7.18 \cdot 10^{+10}$	$1.65 \cdot 10^{+13}$	$3.14 \cdot 10^{+15}$
1/320	$1.22 \cdot 10^{-62}$	$6.58 \cdot 10^{+02}$	$2.16 \cdot 10^{+05}$	$4.74 \cdot 10^{+07}$	$7.80 \cdot 10^{+09}$	$1.03 \cdot 10^{+12}$	$1.13 \cdot 10^{+14}$
1/5							
1/10	-1.88	-3.43	-4.47	-5.57	-6.22	-6.57	-6.70
1/20	0.48	0.22	0.44	0.63	0.79	0.90	0.98
1/40	-0.38	-0.02	-0.04	-0.02	0.05	0.19	0.39
1/80	0.20	-0.44	-0.87	-1.30	-1.73	-2.16	-2.56
1/160	0.21	-0.16	-0.28	-0.42	-0.56	-0.69	-0.83
1/320	0.14	0.81	1.60	2.40	3.20	4.00	4.80

Table 2.9: Convergence of ISDeC applied to (2.7) with $\lambda = 1000\mathrm{i}$, $m = 6$ Gaussian points.

where Δ denotes the Laplacian, which for this simple case satisfies

$$\Delta\psi(t,x) = \frac{\partial^2\psi(t,x)}{\partial x^2},$$

and the potential V is chosen as

$$V(x) = 1 - \cos(x).$$

For space (semi-)discretization we use *pseudospectral methods* ([18], [19], [23]) with $N = 16$ and $N = 256$ spatial grid points in the interval $[-\pi, \pi]$, respectively. The size of the (purely imaginary) eigenvalues of the system matrix of the resulting system of ODEs depends critically on the step size used in the space discretization. Tables 2.10 and 2.11 give the results of our numerical tests. The tables give the convergence order of the global error at $t_{\text{end}} = 1$, where for both test runs we used the initial values $\hat{U}^0_{(2)}$ defined in [18] (with a different random vector, naturally). The basic numerical method is *exponential splitting*, a second order scheme which is introduced and analyzed in [18]. For the ISDeC iteration we use $m = 6$ Gaussian points in the interpolation. Table 2.10 demonstrates that ISDeC can be used successfully for the Schrödinger equation if the space discretization induces moderate eigenvalues of the system matrix in time integration. For sufficiently small step sizes the convergence order of the ISDeC iterates is enhanced up to the limit given by the fixed point similarly as in Table 2.7. If the number of spatial grid points increases, however, the results become unacceptable, the error of the ISDeC iterates even increases drastically in the course of the iteration. No significant improvement is observed for decreasing h.

hm	exact	ISDeC 1	ISDeC 2	ISDeC 3	ISDeC 4	ISDeC 5	ISDeC 6
1	$1.49 \cdot 10^{-02}$	$1.23 \cdot 10^{+01}$	$7.71 \cdot 10^{+02}$	$4.70 \cdot 10^{+04}$	$2.39 \cdot 10^{+06}$	$1.02 \cdot 10^{+08}$	$3.70 \cdot 10^{+09}$
1/2	$3.39 \cdot 10^{-03}$	$1.18 \cdot 10^{+01}$	$7.68 \cdot 10^{+02}$	$4.45 \cdot 10^{+04}$	$2.24 \cdot 10^{+06}$	$9.76 \cdot 10^{+07}$	$3.71 \cdot 10^{+09}$
1/4	$8.36 \cdot 10^{-04}$	$1.10 \cdot 10^{+01}$	$7.77 \cdot 10^{+02}$	$3.92 \cdot 10^{+04}$	$1.68 \cdot 10^{+06}$	$7.11 \cdot 10^{+07}$	$3.02 \cdot 10^{+09}$
1/8	$2.08 \cdot 10^{-04}$	$1.07 \cdot 10^{+01}$	$1.32 \cdot 10^{+03}$	$1.18 \cdot 10^{+05}$	$8.11 \cdot 10^{+06}$	$4.51 \cdot 10^{+08}$	$2.11 \cdot 10^{+10}$
1/16	$5.21 \cdot 10^{-05}$	$2.45 \cdot 10^{+00}$	$1.29 \cdot 10^{+02}$	$5.56 \cdot 10^{+03}$	$2.04 \cdot 10^{+05}$	$6.55 \cdot 10^{+06}$	$1.87 \cdot 10^{+08}$
1/32	$1.30 \cdot 10^{-05}$	$4.70 \cdot 10^{-03}$	$4.12 \cdot 10^{-03}$	$5.36 \cdot 10^{-03}$	$5.42 \cdot 10^{-03}$	$5.44 \cdot 10^{-03}$	$5.43 \cdot 10^{-03}$
1/64	$3.25 \cdot 10^{-06}$	$1.02 \cdot 10^{-04}$	$7.97 \cdot 10^{-06}$	$3.54 \cdot 10^{-06}$	$3.35 \cdot 10^{-06}$	$3.33 \cdot 10^{-06}$	$3.33 \cdot 10^{-06}$
1/128	$8.13 \cdot 10^{-07}$	$5.14 \cdot 10^{-07}$	$3.13 \cdot 10^{-08}$	$1.44 \cdot 10^{-09}$	$1.02 \cdot 10^{-09}$	$1.01 \cdot 10^{-09}$	$1.01 \cdot 10^{-09}$
1/256	$2.03 \cdot 10^{-07}$	$2.12 \cdot 10^{-09}$	$1.32 \cdot 10^{-10}$	$7.56 \cdot 10^{-13}$	$2.63 \cdot 10^{-13}$	$2.67 \cdot 10^{-13}$	$2.68 \cdot 10^{-13}$
1	2.14	0.06	0.01	0.08	0.09	0.06	-0.00
1/2	2.02	0.10	-0.02	0.18	0.42	0.46	0.30
1/4	2.01	0.04	-0.76	-1.59	-2.27	-2.67	-2.80
1/8	2.00	2.13	3.36	4.41	5.31	6.11	6.82
1/16	2.00	9.03	14.93	19.98	25.17	30.17	35.00
1/32	2.00	5.53	9.01	10.56	10.66	10.67	10.67
1/64	2.00	7.63	7.99	11.26	11.68	11.69	11.69
1/128	2.00	7.92	7.89	10.90	11.92	11.89	11.88
1/256							

Table 2.10: ISDeC, Schrödinger eqn. with $N = 16$ spatial grid points, $m = 6$ Gaussian points.

hm	exact	ISDeC 1	ISDeC 2	ISDeC 3	ISDeC 4	ISDeC 5	ISDeC 6
1	$7.20 \cdot 10^{-03}$	$1.89 \cdot 10^{+01}$	$2.67 \cdot 10^{+05}$	$4.22 \cdot 10^{+09}$	$5.83 \cdot 10^{+13}$	$7.48 \cdot 10^{+17}$	$1.01 \cdot 10^{+22}$
1/2	$1.94 \cdot 10^{-03}$	$1.84 \cdot 10^{+01}$	$2.58 \cdot 10^{+05}$	$3.99 \cdot 10^{+09}$	$5.28 \cdot 10^{+13}$	$6.06 \cdot 10^{+17}$	$6.18 \cdot 10^{+21}$
1/4	$4.58 \cdot 10^{-04}$	$1.84 \cdot 10^{+01}$	$2.64 \cdot 10^{+05}$	$4.10 \cdot 10^{+09}$	$5.30 \cdot 10^{+13}$	$5.77 \cdot 10^{+17}$	$5.42 \cdot 10^{+21}$
1/8	$1.37 \cdot 10^{-04}$	$1.85 \cdot 10^{+01}$	$2.58 \cdot 10^{+05}$	$3.91 \cdot 10^{+09}$	$5.02 \cdot 10^{+13}$	$5.46 \cdot 10^{+17}$	$5.12 \cdot 10^{+21}$
1/16	$2.43 \cdot 10^{-05}$	$1.84 \cdot 10^{+01}$	$2.62 \cdot 10^{+05}$	$4.09 \cdot 10^{+09}$	$5.39 \cdot 10^{+13}$	$6.04 \cdot 10^{+17}$	$5.84 \cdot 10^{+21}$
1/32	$6.05 \cdot 10^{-06}$	$1.82 \cdot 10^{+01}$	$2.60 \cdot 10^{+05}$	$4.03 \cdot 10^{+09}$	$5.30 \cdot 10^{+13}$	$5.94 \cdot 10^{+17}$	$5.75 \cdot 10^{+21}$
1/64	$1.51 \cdot 10^{-06}$	$1.79 \cdot 10^{+01}$	$2.59 \cdot 10^{+05}$	$4.04 \cdot 10^{+09}$	$5.34 \cdot 10^{+13}$	$5.97 \cdot 10^{+17}$	$5.76 \cdot 10^{+21}$
1/128	$3.78 \cdot 10^{-07}$	$1.78 \cdot 10^{+01}$	$2.55 \cdot 10^{+05}$	$3.81 \cdot 10^{+09}$	$4.81 \cdot 10^{+13}$	$5.15 \cdot 10^{+17}$	$4.78 \cdot 10^{+21}$
1/256	$9.44 \cdot 10^{-08}$	$1.68 \cdot 10^{+01}$	$2.55 \cdot 10^{+05}$	$3.75 \cdot 10^{+09}$	$4.64 \cdot 10^{+13}$	$4.85 \cdot 10^{+17}$	$4.38 \cdot 10^{+21}$
1	1.89	0.04	0.05	0.08	0.14	0.30	0.71
1/2	2.08	0.00	-0.03	-0.04	-0.01	0.07	0.19
1/4	1.74	-0.01	0.03	0.07	0.08	0.08	0.08
1/8	2.50	0.01	-0.02	-0.06	-0.10	-0.15	-0.19
1/16	2.01	0.02	0.01	0.02	0.02	0.02	0.02
1/32	2.00	0.02	0.01	-0.00	-0.01	-0.01	-0.00
1/64	2.00	0.01	0.02	0.08	0.15	0.21	0.27
1/128	2.00	0.08	0.00	0.02	0.05	0.09	0.13
1/256							

Table 2.11: ISDeC, Schrödinger eqn. with $N = 256$ spatial grid points, $m = 6$ Gaussian points.

Appendix A

Auxiliary Results

Lemma 2 *Let $y(t)$ be an $(m+2)$ times continuously differentiable function on $[t_0, t_0+mh]$. Let $p(t)$ be the interpolation polynomial of degree $\leq m$ which is defined by*

$$p(t_0+jh) = y(t_0+jh), \quad j = 0, \ldots, m, \tag{A.1}$$

and let $q(t)$ be any polynomial of degree $\leq m$ which satisfies

$$q'(t_0+\rho_j hm) = y'(t_0+\rho_j hm), \quad j = 1, \ldots, m. \tag{A.2}$$

If ρ_j satisfy

$$\sum_{j=1}^{m} \rho_j = \frac{m}{2}, \tag{A.3}$$

then for the m-th derivatives of $p(t) - q(t)$ we have

$$p^{(m)}(t) - q^{(m)}(t) = O(h^2). \tag{A.4}$$

Proof. Using the Lagrange interpolation formula with the Lagrange polynomials

$$L_j(\tau) = \prod_{\substack{i=0 \\ i\neq j}}^{m} \frac{\tau - i}{j - i}$$

and the Taylor expansions

$$y(t_0+jh) = \sum_{k=0}^{m+1} \frac{h^k j^k y^{(k)}(t_0)}{k!} + O(h^{m+2})$$

we obtain

$$\begin{aligned} p(t_0+\tau h) &= \sum_{j=0}^{m} y(t_0+jh) L_j(\tau) \\ &= \sum_{j=0}^{m}\sum_{k=0}^{m} \frac{h^k j^k y^{(k)}(t_0)}{k!} L_j(\tau) + \sum_{j=0}^{m} \frac{h^{m+1} j^{m+1} y^{(m+1)}(t_0)}{(m+1)!} L_j(\tau) + O(h^{m+2}) \\ &= \sum_{k=0}^{m} \frac{h^k \tau^k y^{(k)}(t_0)}{k!} + \frac{h^{m+1} y^{(m+1)}(t_0)}{(m+1)!} \left(\tau^{m+1} - \prod_{j=0}^{m} (\tau - j) \right) + O(h^{m+2}). \end{aligned}$$

In the last step we have used $\sum_{j=0}^{m} j^k L_j(\tau) = \tau^k$ and the fact that the interpolation polynomial $\sum_{j=0}^{m} j^{m+1} L_j(\tau)$ of τ^{m+1} at the nodes $0, \ldots, m$ is given by $\tau^{m+1} - \prod_{j=0}^{m}(\tau - j)$. Similarly, we obtain

$$q'(t_0+\tau h) = \sum_{k=0}^{m-1} \frac{h^k \tau^k y^{(k+1)}(t_0)}{k!} + \frac{h^m y^{(m+1)}(t_0)}{m!} \left(\tau^m - \prod_{j=1}^{m} (\tau - \rho_j m) \right) + O(h^{m+1})$$

and

$$\begin{aligned} q(t_0+\tau h) &= q(t_0) + \sum_{k=1}^{m} \frac{h^k \tau^k y^{(k)}(t_0)}{k!} + \\ &+ \frac{h^{m+1} y^{(m+1)}(t_0)}{(m+1)!} \left(\tau^{m+1} - (m+1) \int_{t_0}^{\tau} \prod_{j=0}^{m} (\sigma - \rho_j m) d\sigma \right) + O(h^{m+2}) \end{aligned}$$

by integration. Using

$$\frac{d^m}{d\tau^m} \prod_{j=0}^{m} (\tau - j) = (m+1)!\tau - m! \sum_{j=0}^{m} j = (m+1)!(\tau - \frac{m}{2})$$

and

$$(m+1) \frac{d^{m-1}}{d\tau^{m-1}} \prod_{j=0}^{m} (\tau - \rho_j m) = (m+1)! \left(\tau - \sum_{j=1}^{m} c_j \right),$$

and noting that the $O(h^{m+2})$ remainder terms from above are of the form $h^{m+2} R(\tau, h)$ with smooth functions $R(\tau, h)$ (which are actually polynomials in τ of degree $\leq m$, with $\frac{\partial^k}{\partial \tau^k} R(\tau, h) = O(h^{-k})$) we conclude

$$p^{(m)}(t_0+\tau h) - q^{(m)}(t_0+\tau h) = h y^{(m+1)}(t_0) \left(\frac{m}{2} - \sum_{j=1}^{m} \rho_j \right) + O(h^2),$$

from which the statement of the lemma follows. □

References

[1] U. Ascher, R. M. M. Mattheij, R. D. Russell: *Numerical Solution of Boundary Value Problems for Ordinary Differential Equations*. Prentice-Hall, Englewood Cliffs, NJ, 1988.

[2] W. Auzinger, R. Frank, H. Hofstätter, E. Weinmüller: *Defektkorrektur zur numerischen Lösung steifer Anfangswertprobleme*. Techn. Rep. No. 131/00, Inst. for Appl. Math. and Num. Anal., Vienna Univ. of Techn., 2000. Available at `http://www.math.tuwien.ac.at/~winfried`.

[3] W. Auzinger, O. Koch, S. Lammer, E. Weinmüller: *Variationen der Defektkorrektur zur effizienten numerischen Lösung gewöhnlicher Differentialgleichungen*. Techn. Rep. ANUM Preprint Nr. 8/02, Inst. for Appl. Math. and Numer. Anal., Vienna Univ. of Technology, Austria, 2002. Available at `http://www.math.tuwien.ac.at/~inst115/preprints.htm`.

[4] W. Auzinger, O. Koch, E. Weinmüller: *New Variants of Defect Correction for Boundary Value Problems in Ordinary Differential Equations*. In *Current Trends in Scientific Computing* (Z. Chen, R. Glowinski, K. Li, eds.), American Mathematical Society, Vol. 329 of *AMS Series in Contemporary Mathematics*, pp. 43–50.

[5] W. Auzinger, W. Kreuzer, H. Hofstätter, E. Weinmüller: *Modified Defect Correction Algorithms for ODEs. Part I: General Theory*. Numer. Algorithms 36 (2004), pp. 135–155.

[6] S. Blanes, F. Casas, J. Ros: *Extrapolation of Symplectic Integrators*. DAMTP 1999 NA09, Dept. of Appl. Math. and Theor. Physics, Univ. of Cambridge, England, 1999.

[7] K. Engø, A. Marthinsen, H. Munthe-Kaas: *DIFFMAN – an Object Oriented MATLAB Toolbox for Solving Differential Equations on Manifolds*. Report 164, Department of Informatics, University of Bergen, Norway, 1999.

[8] R. Frank: *The Method of Iterated Defect Correction and Its Application to Two-Point Boundary Value Problems, Part I*. Numer. Math. 25 (1976), pp. 409–419.

[9] R. Frank: *The Method of Iterated Defect Correction and Its Application to Two-Point Boundary Value Problems, Part II*. Numer. Math. 27 (1977), pp. 407–420.

[10] R. Frank, F. Macsek, C. Überhuber: *Iterated Defect Correction for Differential Equations, Part II: Numerical Experiments*. Computing 33 (1984), pp. 107–129.

[11] R. Frank, C. Überhuber: *Iterated Defect Correction for the Efficient Solution of Stiff Systems of Ordinary Differential Equations*. BIT 17 (1977), pp. 146–159.

[12] R. Frank, C. Überhuber: *Iterated Defect Correction for Differential Equations, Part I: Theoretical Results*. Computing 20 (1978), pp. 207–228.

[13] E. Hairer, C. Lubich, G. Wanner: *Geometric Numerical Integration*. Springer-Verlag, Berlin-Heidelberg-New York, 2002.

[14] E. Hairer, C. Lubich, G. Wanner: *Geometric numerical integration illustrated by the Störmer/Verlet method*. Acta Numerica (2003), pp. 1–51.

[15] E. Hairer, S. P. Nørsett, G. Wanner: *Solving Ordinary Differential Equations I*. Springer-Verlag, Berlin-Heidelberg-New York, 1987.

[16] F. B. Hildebrand: *Introduction to Numerical Analysis*, 2nd edn. McGraw-Hill, New York, 1974.

[17] H. Hofstätter, O. Koch: *Convergence Proof for Iterated Splitting Defect Correction*. AURORA TR-2004-XX, Inst. for Anal. and Sci. Comput., Vienna Univ. of Technology, Austria, 2004. Available at `http://www.vcpc.univie.ac.at/aurora/publications/`.

[18] T. Jahnke, C. Lubich: *Error bounds for exponential operator splittings*. BIT 40 (2000), pp. 735–744.

[19] O. Koch, W. Kreuzer, A. Scrinzi: *MCTDHF in Ultrafast Laser Dynamics*. AURORA TR-2003-29, Inst. for Appl. Math. and Numer. Anal., Vienna Univ. of Technology, Austria, 2003. Available at `http://www.vcpc.univie.ac.at/aurora/publications/`.

[20] O. Koch, E. Weinmüller: *Iterated Defect Correction for the Solution of Singular Initial Value Problems*. SIAM J. Numer. Anal. 38 (2001)(6), pp. 1784–1799.

[21] K. Schild: *Gaussian Collocation via Defect Correction*. Numer. Math. 58 (1990), pp. 369–386.

[22] H. J. Stetter: *The Defect Correction Principle and Discretization Methods*. Numer. Math. 29 (1978), pp. 425–443.

[23] L. Trefethen: *Spectral Methods in MATLAB*. SIAM, Philadelphia, 2000.

[24] P. E. Zadunaisky: *On the Estimation of Errors Propagated in the Numerical Integration of ODEs*. Numer. Math. 27 (1976), pp. 21–39.